



VRIJE  
UNIVERSITEIT  
BRUSSEL



Dissertation submitted in partial fulfillment of the requirements for the  
degree of Master of Science in Physics and Astronomy

# **QUANTUM INFORMATION, HOLOGRAPHY AND ENTWINEMENT: ORBIFOLDING TENSOR NETWORKS**

**JONAS VERHELLEN**  
**2016-2017**

Promotor: Prof. Dr. Ben Craps  
Co-Promotor: Dr. Gábor Sárosi  
Supervisor: Tim De Jonckheere  
Science & Bio-engineering Sciences

Jonas Verhellen  
Quantum information, Holography and Entwinement: Orbifolding Tensor Networks,  
2016-2017, Brussels





## ABSTRACT

---

Theoretical physics aims to construct abstract mathematical models that quantify, predict and eventually explain the nature of physical events. Two prime examples of such kind of models are general relativity (Einstein's theory of gravity) and quantum field theory (which describes fundamental particles and their interactions). To discover how gravity works at small scales (or high energies), general relativity and quantum field theory must be unified into a self-consistent theory of quantum gravity. Unfortunately, it has turned out that this unification is highly elusive.

An important reason for the difficulty of constructing self-consistent quantum gravity models is the holographic principle. This principle, which originates from the study of black hole thermodynamics, claims that in any realistic quantum gravity model all physical information is encoded in a lower dimensional quantum field theory. From string theory, a possible high-energy extension of gravity, it is known that quantum gravity in a negatively curved spacetime is equivalent to a (scale-invariant) quantum field theory that lives on the boundary of the spacetime. This mathematical realization of holography is known as the AdS/CFT correspondence. Unfortunately, our own universe is not negatively curved but there is hope that studying AdS/CFT might lead us to a model for positively curved spacetimes like our own.

Recent research has proposed that certain facets of the AdS/CFT correspondence can be described using quantum information techniques. For instance, it can be shown that the entanglement between a spatial section of the boundary theory and its boundary complement corresponds to the length of a minimal curve in the interior which begins and ends at the outer points of the boundary interval. Additionally, it is known that in certain spacetimes, extremal but non-minimal curves can be related to the entanglement between internal degrees of freedom of the boundary theory. In this dissertation these quantum information ideas were translated and further expanded into tensor networks, discrete quantum information models often used in condensed matter physics.

To advance beyond the current literature, in which it is known that minimal curves in the interior of the spacetime can be described by holographic tensor network models, it was discovered that the tensor networks needed to be folded up according to a specific symmetry pattern. Because tensor networks are discrete, some of the symmetries of the underlying spacetime are broken, which makes it harder to understand how to do origami with tensor networks. Using a mathematical device, called the Coxeter group, it can be determined which kind of folds are still allowed. By applying this procedure, this dissertation constructed many-layered tensor networks for massive but non-rotating three-dimensional black holes and certain "party hat"-shaped spacetimes called conical defects.

As a surprise extra, it was also discovered that these layered types of tensor networks provide a (conceptual) link between internal boundary entanglement and how the holography principle acts on small patches of spacetime. Specifically, layered tensor networks can help understand how quantum information on the boundary is related to quantum gravity in small regions of the interior where the curvature of the spacetime is no longer relevant, i.e. flat space. Obtaining a better understanding of how holography works in those regions, might lead to a successful model of holography for universes like our own.

## S A M E N V A T T I N G

---

Theoretische fysica streeft naar het opbouwen van abstracte wiskundige modellen die de aard van fysieke gebeurtenissen kwantificeren, voorspellen en uiteindelijk verklaren. De twee voornaamste voorbeelden van dergelijke modellen zijn algemene relativiteit (Einstiens zwaartekrachtstheorie) en kwantumveldentheorie (die fundamentele deeltjes en hun interacties beschrijft). Om te ontdekken hoe de (kwantum) theorie van zwaartekracht werkt op kleine schalen (of hoge energieën), moeten algemene relativiteit en kwantumveldentheorie verenigd worden in een zelf-consistente theorie van kwantum-zwaartekracht. Helaas blijkt dat deze vereniging uitzonderlijk moeilijk te bekomen is.

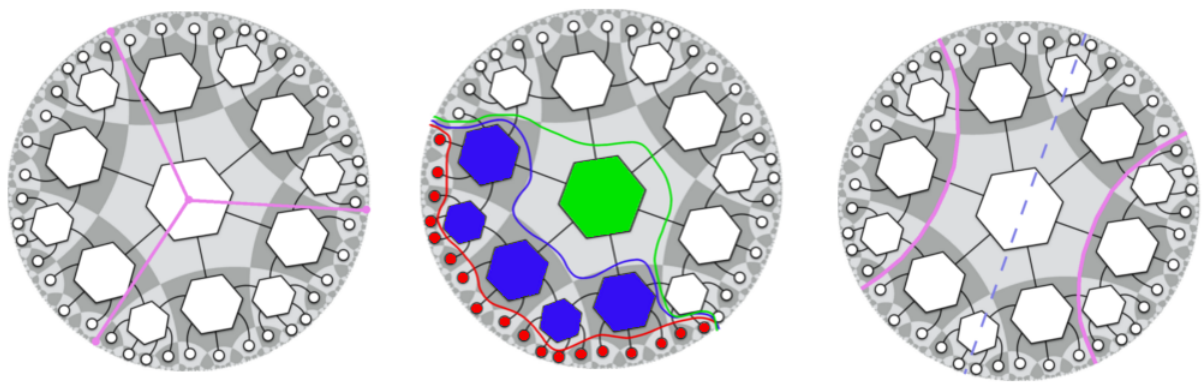
Een belangrijke oorzaak voor de moeilijkheid in het modeleren van kwantumzwaartekracht is het holografische principe. Dit principe, dat voortkomt uit de studie van zwart gaten, beweert dat in elk realistisch kwantumzwaartekracht-model alle fysische informatie wordt gecodeerd in een kwantumveldentheorie die leeft in een lager aantal dimensies. Uit snaartheorie, een mogelijke extensie van zwaartekracht, is bekend dat kwantum-zwaartekracht in een negatief gekromde ruimte-tijd equivalent is aan een (schaal-invariante) kwantumveldentheorie die leeft op de grens van de ruimtetijd. Deze wiskundige realisatie van holografie staat bekend als de AdS/CFT correspondentie. Helaas blijkt dat ons eigen universum geen negatieve kromming heeft, maar er is hoop dat het bestuderen van AdS/CFT ons kan leiden tot een model voor positief gekromde ruimtetijden zoals het onze.

Recent onderzoek heeft uitgewezen dat bepaalde facetten van de AdS/CFT correspondentie kunnen worden beschreven met behulp van kwantuminformatietechnieken. Zo kan worden aangetoond dat de kwantumverstrekking tussen een ruimtelijke sectie van de grenstheorie en zijn complement overeenkomt met de lengte van een minimale kromme in de bulk van de ruimtetijd zolang de kromme begint en eindigt op de eindpunten van het ruimtelijk interval op de grens. Bovendien is het bekend dat in bepaalde ruimtetijden, extreme maar niet-minimale curven kunnen worden gerelateerd met de kwantumverstrekking tussen interne vrijheidsgraden van de grenstheorie. In dit proefschrift werden deze ideeën uit kwantuminformatie vertaald en uitgebreid tot tensornetwerken, een set discrete kwantuminformatietechnieken die vaak in de fysica van gecondenseerde materie worden gebruikt.

Om verder te gaan dan de huidige literatuur, waarin bekend is dat minimale krommen in de ruimte-tijd kunnen worden beschreven door holografische tensornetwerkmodellen, werd ontdekt dat de tensor netwerken opgevouwen moesten worden volgens een specifiek symmetriepatroon. Omdat tensor netwerken discreet zijn, is het moeilijker te begrijpen hoe dit soort origami met tensornetwerken kan worden uitgevoerd. Met behulp van een wiskundig apparaat - de Coxeter

symmetriegroep - kan worden bepaald welk vouwen en plooien nog steeds zijn toegestaan. Door deze procedure toe te passen, was het mogelijk om gelaagde tensor netwerken voor massieve maar niet-roterende zwarte gaten in drie dimensies en enkele andere ruimtetijden te maken.

Bovendien werd ook ontdekt dat deze gelaagde tensor netwerken een (voornamelijk conceptueel) verband bieden tussen interne kwantumverstrekking en holografie voor vlakke ruimtes. Specifiek blijkt het dat gelaagde tensor netwerken helpen te begrijpen hoe kwantuminformatie in de kwantumveldentheorie verband houdt met kwantum-zwaartekracht in gebieden waar de kromming van de ruimtetijd niet meer relevant is. Verder onderzoek over hoe holografie in deze regio's werkt, kan leiden tot een succesvol model van holografie voor universum zoals het onze.



ARE WE HOLOGRAPHERS OR HOLOGRAPHISTS?  
TIM DE JONCKHEERE

This dissertation is dedicated, with love, to my grandmother, Maria D'haese.

## PREFACE

---

This dissertation on [Quantum Information and Holography](#) was completed as part of the two-year masters course in Physics and Astronomy at the Vrije Universiteit Brussel. The thesis and accompanying research, corresponding to 30 ECTS credits, were realized in a eight month period starting in October 2016 and ending in early June 2017. In July of 2017 an oral defense of this dissertation will take place.

Early on in September 2016, Prof. Dr. Ben Craps proposed to align this research thesis with the emerging international interest in the connection between holography and quantum information. Recently, a large collaboration between some of the leading institutes in both high-energy physics and quantum information has formed under the name [It from Qubit: Simons Collaboration on Quantum Fields, Gravity, and Information](#). The goal of the collaboration is to foster interaction between the two fields in the hope of yielding answers to some of the most fundamental questions in modern physics.

Against the backdrop of this international movement, Prof. Craps assembled a team consisting of Dr. Gábor Sárosi, Tim De Jonckheere, Marine De Clerck and myself to conduct research in this area. Dr. Sárosi is a postdoctoral researcher at the [Vrije Universiteit Brussel](#) and the co-promoter of this dissertation. Tim De Jonckheere is a doctoral student at the Vrije Universiteit Brussel. Marine De Clerck is a fellow second-year master student whose thesis work is strongly correlated with the research presented here.

Several members of this group have a close working relationship with Prof. Dr. [Vijay Balasubramian](#). Prof. Balasubramian is a full-time professor at the University of Pennsylvania and part-time professor at Vrije Universiteit Brussel. Prof. Balasubramian is also a principle investigator of the It from Qubit collaboration. The research in this dissertation is specifically supported by the [FWO project: Entanglement, space and time](#) of which both he and Prof. Craps are the promoters.

During March of 2017, Prof Craps hosted Prof. Dr. Erik Verlinde from the University of Amsterdam for a [Solvay Colloquium on the topic of Emergent Gravity](#). In the margin of this colloquium several discussions with Prof. Verlinde took place which turned the focus of this dissertation to the applications of our research to questions with regard to sub-AdS locality. Later on, discussions on these topics were held with other member of the [University of Amsterdam](#), most notably with Dr. Ben Freivogel and Prof. Dr. Jan de Boer.



## ACKNOWLEDGEMENTS

---

I am extraordinarily thankful to my promoter, [Ben Craps](#). Ben, for a second time, you were willing to lend me your full encouragement, guidance and support. I will not forget it. The bachelor's project of two years ago, in which you gave me so much freedom, has led me to some unexpected but wonder experiences. I can only start to imagine how the time spent during this masters dissertation will influence me in the coming years. My respect for you is both profound and singularly extensive.

[Gábor and Tim](#) have my deep gratitude for all the effort, enthusiasm and time they have put into the projects of this dissertation. The two of you were always there to answer questions, to come up with new ideas and to explore research options. It was a pleasure to be entangled in your conversations. Your comments on the final manuscript are simply invaluable. The lavish amount of time you spent on this dissertation is hereby fully acknowledged.

To [my fellow classmates](#) who have gone down other paths in physics and beyond, I will miss you and I thank you, deeply, for all the time, tea and friendship we have shared. Paul, Pablo, Matthias, Jonathan, Timmy and Pieter, I cannot start to list all the things you have done for me in the past five years. It has been a privilege. In the last couple of months you have all been reminding me that there is still some elegance, beauty and happiness to be found away from the blackboard. I'll try not to forget.

From my first physics campfire to – quite literally – the end of this dissertation I have had the luck to have two great mentors. It is only fitting that [Jeriek and Sophie](#) are thanked here, for all the laughs they brought me, for the copious amounts of advice they doled out so graciously and for lending me their powers in relativity (both the human and the general kind). I hope Scandinavia treats both of you at least as kindly as you deserve. [My family](#) is also thanked for all their support in the past five years. No physics can emerge without the right boundary conditions. I hope that you can appreciate the results.

Most of the research found in the pages of this dissertation was achieved in collaboration with [Marine](#). I would like to express my thanks to you, in ever-ascending order of gratitude, for being an amazingly helpful classmate, a kind desk-sharer, an exceptionally focused physicist and an outstandingly gentle and graceful friend. You are absolutely, unequivocally the best. Marine, may your life be filled with yellow sun-dresses, good pop-songs, endless pizza-nights and maybe the occasional surprise-gift of an abstract painting.



## AUTHOR'S DECLARATION

---

I hereby declare that the work in this dissertation was carried out in accordance with the regulations of the *Vrije Universiteit Brussel* and the master thesis agreement as signed on 14 October 2016. No part of the dissertation has been previously submitted for examination. Any views expressed in the dissertation are those of the author and do not necessarily represent those of the promoter, co-promoter, supervisor or the *Vrije Universiteit Brussel*. This dissertation has not been presented to any other university nor for any other degree.

---

Jonas Verhellen, Brussels,  
8th June 2017



## CONTENTS

---

<b>i</b>	<b>INTRODUCTION</b>	<b>1</b>
1	A GENTLE START	3
1.1	Motivation . . . . .	3
1.1.1	Why Holography? . . . . .	3
1.1.2	The Experimental Spoils of AdS/CFT . . . . .	5
1.1.3	It from Qubit . . . . .	6
1.2	Context . . . . .	7
1.2.1	Entwinement and Spacetime Origami . . . . .	8
1.2.2	Holographic Tensor Networks . . . . .	10
1.2.3	The Road to sub-AdS Locality . . . . .	11
1.3	Thesis Structure . . . . .	11
<b>ii</b>	<b>THE HOLOGRAPHIC CORRESPONDENCE OF ADS AND CFT</b>	<b>15</b>
2	A TALE OF TWO SUPER-THEORIES	17
2.1	Introduction . . . . .	17
2.2	Symmetries of a Physical Theory . . . . .	17
2.2.1	The Poincaré Group . . . . .	19
2.2.2	Yang-Mills Gauge Theory . . . . .	20
2.3	Supersymmetry . . . . .	21
2.3.1	The Supersymmetry Algebra . . . . .	22
2.3.2	$\mathcal{N} = 1$ Supersymmetric Yang-Mills Theory . . . . .	23
2.3.3	$\mathcal{N} = 4$ Supersymmetric Yang-Mills Theory . . . . .	23
2.4	Supergravity . . . . .	24
2.4.1	Briefly, General Relativity . . . . .	25
2.4.2	Introducing Frame Fields . . . . .	26
2.4.3	The Einstein-Hilbert Action . . . . .	27
2.4.4	Leveraging the Spin Connection . . . . .	27
2.4.5	The Rarita-Schwinger Field for Gravitinos . . . . .	28
2.4.6	Basic Supergravity . . . . .	29
2.4.7	Ten-dimensional Type IIB Supergravity . . . . .	29
2.4.8	Scalar fields in AdS . . . . .	31
2.5	Conclusion . . . . .	32
3	EXPLORATION OF THE ADS/CFT CORRESPONDENCE	33
3.1	Introduction . . . . .	33
3.2	A String Theoretical Perspective . . . . .	33
3.2.1	Constraints and Boundary Conditions . . . . .	35
3.2.2	Solutions and Supersymmetry . . . . .	36
3.2.3	Two-faced D-Branes . . . . .	36
3.2.4	A Correspondence, At Last! . . . . .	39

3.3	The Large N Expansion of Gauge Theories . . . . .	39
3.3.1	't Hooft Expansion of Gauge Theories . . . . .	40
3.3.2	Large N in AdS/CFT . . . . .	40
3.4	Fields, Operators and Sources . . . . .	41
3.5	Correlation Functions in AdS/CFT . . . . .	43
3.5.1	Functional Methods . . . . .	43
3.5.2	Correlation Functions of Conformal Operators . . . . .	44
3.5.3	Linear Response Theory . . . . .	45
3.5.4	Two-point Function for Scalar Fields . . . . .	47
3.6	AdS-Rindler Bulk Reconstruction . . . . .	47
3.7	Conclusion . . . . .	49
4	INCORPORATING QUANTUM INFORMATION	51
4.1	Introduction . . . . .	51
4.2	Quantum Information Theory . . . . .	52
4.2.1	Quantum Error Correction . . . . .	53
4.2.2	Density Matrices, Entanglement and Entropy . . . . .	54
4.3	Holographic Quantum Error Correction . . . . .	55
4.3.1	Non-equivalent Representations . . . . .	56
4.4	Ryu-Takayanagi: Entropy for a Holographic Universe . . . . .	58
4.4.1	Validity in $\text{AdS}_3/\text{CFT}_2$ . . . . .	58
4.4.2	Higher Dimensions, Heuristically . . . . .	59
4.5	Holographic Tensor Networks . . . . .	61
4.5.1	Perfect Tensors . . . . .	62
4.5.2	HaPPY Tensor Networks . . . . .	63
4.5.3	The Greedy Algorithm . . . . .	65
4.6	Conclusion . . . . .	66
iii	BLACK HOLES, ORBIFOLDS AND TENSOR NETWORKS	69
5	ENTWINEMENT: THE RICH MAN'S ENTANGLEMENT	71
5.1	Introduction . . . . .	71
5.2	$2+1$ -Dimensional Gravity . . . . .	71
5.2.1	Negatively Curved Gravity in Three Dimensions . . . . .	72
5.2.2	Gravity as a Topological Theory . . . . .	72
5.2.3	BTZ Black Holes . . . . .	73
5.2.4	Orbifolds . . . . .	74
5.3	Entwinement of Orbifolds . . . . .	75
5.3.1	Introducing Entwinement . . . . .	76
5.3.2	Winding around Conical Defects . . . . .	77
5.3.3	A Covering Space Picture for Massive BTZ's . . . . .	78
5.4	Entwinement of Discretely Gauged Theories . . . . .	82
5.4.1	Defining Entwinement . . . . .	82
5.5	A Lightning Introduction to the D1-D5 CFT . . . . .	85
5.5.1	Conical Defects, Once More . . . . .	86
5.5.2	Relationship with Entanglement Entropy . . . . .	86

5.5.3	Massless BTZ Black Holes . . . . .	86
5.6	Conclusion . . . . .	87
6	TANGIBLE HOLOGRAPHY: ENTWINEMENT ON TENSOR NETWORKS	89
6.1	Introduction . . . . .	89
6.2	Entanglement Shadows . . . . .	89
6.2.1	Why are there Shadows? . . . . .	89
6.2.2	A Tensor Network for the Conical Defect. . . . .	90
6.3	A Covering Space Picture for Tensor Networks . . . . .	94
6.3.1	A Tensor Network for a Massive BTZ black hole . . . . .	96
6.3.2	The Coxeter group . . . . .	97
6.4	The path to Sub-AdS Locality . . . . .	98
6.4.1	Matrix Degrees of Freedom . . . . .	98
6.4.2	Long Strings to the Rescue . . . . .	99
6.4.3	On Pluperfect Tensors and sub-AdS locality . . . . .	100
6.5	Conclusion . . . . .	101
iv	CONCLUSION AND OUTLOOK	103
7	THE STATE OF THE ART	105
7.1	Quantum Information, Holography and Entwinement . . . . .	105
7.2	Orbifolding Holographic Tensor Networks . . . . .	106
7.3	Sub-AdS Locality in Terms of Long Strings . . . . .	107
7.4	Outlook . . . . .	108
7.5	Further Reading . . . . .	109
7.6	One More Thing . . . . .	109
v	TECHNICAL APPENDICES	111
A	NOTATION, CONVENTIONS AND SOME DIFFERENTIAL GEOMETRY	113
A.1	Notation . . . . .	113
A.2	Conventions . . . . .	113
A.3	Differential Geometry . . . . .	114
B	THREE-DIMENSIONAL GRAVITY AS A CHERN-SIMONS THEORY	115
B.1	Chern-Simons Theories . . . . .	115
B.2	Negatively Curved Three-Dimensional Gravity . . . . .	115
C	TENSOR NETWORK CALCULATIONS	117
C.1	General Approach . . . . .	117
C.2	Case 1: $\mathbb{Z}_2$ . . . . .	118
C.3	Case 2: $\mathbb{Z}_3$ . . . . .	118
C.4	Case 3: $\mathbb{Z}_6$ . . . . .	118
D	CODE LISTING OF SELECTED GRAPHS	121
D.1	Figure 34 . . . . .	121
D.2	Figure 35 . . . . .	122

BIBLIOGRAPHY	127
INDEX	141

## ACRONYMS

---

- AdS anti-de-Sitter space  
BTZ Bañados, Teitelboim and Zanelli  
CFT Conformal Field Theory  
GR General Relativity  
HaPPY Harlow, Pastawski, Preskill and Yoshida  
MERA Multiscale Entanglement Renormalization Ansatz  
SUGRA Supergravity  
SUSY Supersymmetry  
SYM super-Yang-Mills  
QFT Quantum Field Theory  
RHIC Relativistic Heavy Ion Collider



|

## INTRODUCTION



## A GENTLE START

---

### 1.1 MOTIVATION

#### 1.1.1 Why Holography?

Physics, as the most exact of all sciences, is well-known for its cultivation of elegance through unrelenting unification of its subfields. Yet the two jewels of contemporary physics, general relativity and quantum field theory, are typically described by two inherently contrasting formalisms [1]. A natural and experimentally verifiable unification of both quantum physics and strong gravity, however elusive, has been the holy grail of theoretical physics for several decades. Holography is the primary exponent of the radical and powerful ideas born in this quest for the theory of quantum gravity.

Quantum gravity, once found, will be able (among other things) to model, predict and explain the peculiar behavior of black holes. The second law of thermodynamics [2] states clearly that no entropy can be lost. This fundamental statement forces black holes to obtain the entropy contained in objects crossing their event horizon. In an early attempt to reconcile this striking black hole property with general relativity, Hawking [3] and Bekenstein [4] discovered that entropy  $S$  of a black hole is proportional to the area of its event horizon,  $A_{BH}$ . In natural units, the exact relationship is given by

$$S = \frac{A_{BH}}{4G_N}, \quad (1)$$

where  $G_N$  is Newton's constant. Intuitively, one expects the entropy of an object to be proportional to its volume rather than to its area. The situation in black hole physics however, indicates that all the information in the interior of a black hole is represented, in its entirety, on its event horizon.

Later on, Hawking and Page showed [5] that similar properties are present at cosmological event horizons in general. In 1993, 't Hooft theorized [6] that this apparent property of entropy is a fundamental law of nature, generally present and strictly necessary for any realistic quantum gravity theory.

The declaration made by 't Hooft was soon supported [7] by Susskind and became known within the high-energy physics community as the "Holographic Principle". The principle states that for a quantum gravity theory of a certain spacetime, equivalent physics can be represented on the boundary of that spacetime using a theory without gravity. Entirely like in a classical hologram, the information of a volume (the bulk) is encoded on a lower-dimensional boundary area region.

Holography leaped into the limelight when it was realized [8, 9] that string theory, a possible theory of quantum gravity [10], provides an exact correspondence (a duality) between super-gravity, a high energy extension of general relativity, regarded in certain curved background spacetimes in  $d + 1$ -dimensions and a pure quantum field theory in  $d$ -dimensions. In the low-energy limit, supergravity reduces to some form of classical gravity and hence a powerful equivalence between general relativity and quantum field theory takes shape.

The most intensely studied (and celebrated) example of a holographic duality is the AdS/CFT correspondence [8, 11]. This correspondence postulates that a specific kind of string theory in asymptotically Anti-de-Sitter is precisely equivalent to a conformal field theory on the boundary of that spacetime.

The depth of the radial direction of the asymptotically Anti-de-Sitter can be shown [12, 13] to correspond (roughly) to the energy scale of the CFT. If one accepts the CFT as the fundamental description then the gravitational physics can be interpreted as emerging from the boundary. The ultraviolet regime of the CFT gives rise to the near-boundary region of AdS while the infrared behavior of the CFT corresponds to the deep interior of AdS.

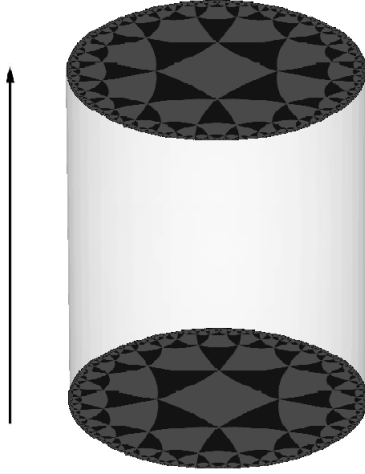


Figure 1: A typical representation of the AdS/CFT correspondence, adapted from Wikipedia Commons [14]. For three-dimensional AdS, a stack of tessellated hyperbolic disks is shown, where each disk represents the spatial configuration of the spacetime at a given time. The boundary represents the conformal field theory. In this picture time flows upwards, the radial direction of AdS is horizontal.

By now the reader will have noticed that the holographic principle is more than an elegant theoretical concept. The applications of the principle from black hole physics to string theory are profound and diverse. Using techniques from quantum information, holography will be shown to be even richer in variety. While this all makes studying holography more than worthwhile from a theoretical vantage point, AdS/CFT also adds considerable experimental motivation.

### 1.1.2 The Experimental Spoils of AdS/CFT

The AdS/CFT correspondence, being the prominent example of the holographic principle, has received a lot of attention. The correspondence was first postulated [8] by Maldacena in 1997 and as of the beginning of 2017 that original publication has received well over 12000 citations [15]. This remarkable amount of recognition is partially due to the applications of AdS/CFT in experimental nuclear physics and condensed matter physics.

The Relativistic Heavy Ion Collider [16] (RHIC) at Brookhaven National Laboratory reported [17, 18] in 2008 that quark-gluon plasma [19], an exotic state of matter that is formed when heavy ions are collided at high energies, was produced and that its sheer-viscosity  $\eta$  was so small that it was nearly negligible. Three years before this landmark experimental result, theorists [20] used AdS/CFT to (correctly) predict this behavior of quark-gluon plasma.

*RHIC [16] is a relativistic spin-polarized research collider using heavy ions and protons.*

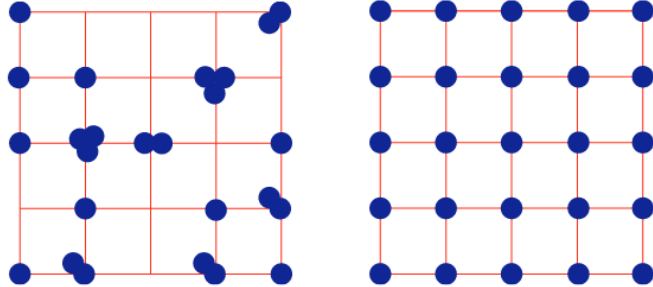


Figure 2: A graphical representation [21] of the transformation between superfluid (left) and insulator (right). The lattice in red can be interpreted as the crisscrossing laser beams. Clearly, information has to be shared between the individual atoms to go from one state to the other. This implies that the entanglement is significant [22–24] during the phase transition.

In condensed matter physics AdS/CFT has been shown [21, 25] to be useful to understand specific phase transitions. When a material undergoes a quantum phase transition however, entanglement becomes profound [22–24, 26], meaning that the system cannot be described by independent particles, and conventional condensed matter physics breaks down [25]. In these cases condensed matter physicists have turned to holographic ideas [21, 25].

An example of such phase transition is that of a superfluid into an insulator. Experimentally this can be achieved [25] by placing supercooled atoms into a web of crisscrossing lasers and increasing the intensity of the lasers. At first the atoms move around frictionless, as expected from a superfluid [27], but then the atoms stop moving and form an insulator. Remarkably, the properties of the transition are dependent on quantum parameters and can be explained [21, 25, 28] by use of AdS/CFT.

*Quantum phase transitions are instigated via variation of an (external) parameter at zero temperature.*

### 1.1.3 It from Qubit

All of the previous examples of holography (black holes, quark-gluon plasma and phase transitions) have some connection to information theory. Sheer-viscosity is a measure [29] of how easily signals are propagated through a system. Entanglement is related [30] to the amount of information shared within a system and the entire mathematical theory of information [31] itself is deeply rooted in the properties of thermodynamic entropy. It is hence to be expected that holography has deep links to information theory.

In 1990 John Wheeler famously postulated [32] that information might not only be fundamental to (holographic) physics but that it might be the cornerstone of all reality. He expressed this idea in his "It from Bit" philosophy: "It from Bit symbolizes the idea that every item of the physical world has at bottom — a very deep bottom, in most instances — an immaterial source and explanation; that which we call reality arises in the last analysis from the posing of yes-or-no questions and the registering of equipment-evoked responses; in short, that all things physical are information-theoretic in origin[.]"

Within AdS/CFT, the entanglement entropy (the quantum informational measure for entanglement) of a spatial region of the boundary theory  $A$  is related to the area of a bulk minimal surface  $\gamma_A$  spanned by the edges of the regarded boundary region by

$$S = \frac{\text{Area}(\gamma_A)}{4G_N}. \quad (2)$$

The analogy with the Hawking-Bekenstein entropy is obvious. This remarkable result [33] by Ryu and Takayanagi provides an intriguing link between the geometry of asymptotically AdS spacetime and quantum information theory on the boundary.

Hence, the physics community started to wonder whether "it" (the physical world) originates from a quantum bit or "qubit" rather than some form of classical information (the bit). Recently, an international research program [35] which aims to expand the "It from Bit" idea to quantum information has emerged under the unsurprising moniker "It from Qubit". Specifically, this collaboration wants to foster the interchange of ideas between quantum information theory and high-energy physics.

Promising preliminary research [36–38] indicates that entanglement entropy (and thus quantum information) plays a significant role in the emergence of gravity in AdS/CFT. From the Ryu-Takayanagi formula it was realized [39] that the field theory on the boundary region  $A$  can be used to reconstruct the (quantum) gravitational physics within the bulk region demarcated by the minimal surface  $\gamma_A$ . An example of this kind of geometry is shown in figure 3.

From the perspective of the boundary theory, this reconstruction of the bulk physics implies unexpected and highly non-trivial locality properties in the radial direction of the asymptotically AdS spacetime. In some cases [41] the minimal

*By definition [31]  
a bit, the basic  
unit of  
information, is in  
either of two  
possible states.*

*Contrastingly, a  
qubit [34] can be  
in a superposition  
of both states of  
the bit.*

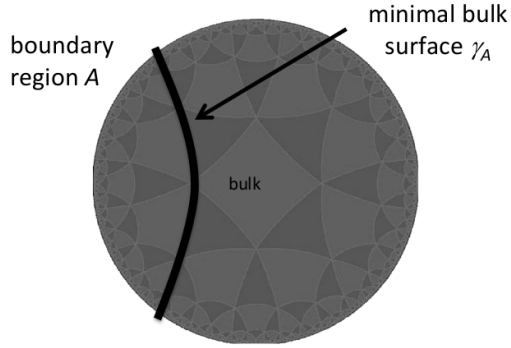


Figure 3: A graphical interpretation of the Ryu-Takayanagi formula, adapted from the 'Quantum Information and Spacetime' slides at QIP 2017 [40]. A time-slice of AdS is shown including a geodesic (the minimal surface on a time-slice)  $\gamma_A$ . According to Ryu-Takayanagi the length of the geodesic corresponds to the entanglement entropy of the boundary region  $A$ . The physics inside the spacetime region between  $A$  and  $\gamma_A$  can be reconstructed by the information on the boundary region  $A$ .

surface cannot penetrate into the middle of the spacetime. Therefore it is an important research question [42, 43] whether or not the entanglement entropy of a boundary region can contain sufficient information to reconstruct the entirety of the bulk geometry.

Another active research topic is based on the discovery [45] of natural quantum error-correction properties in the reconstruction of bulk physics. Consider for instance a set of disjoint intervals on the boundary. When their corresponding minimal surfaces overlap, the boundary information used to extract the bulk physics is partly redundant [44, 45] and hence the emergence of gravitational physics is safeguarded against erasures of part of the boundary.

During the autumn of 2016 many of these ideas caught the eye of the general public through Erik Verlinde's paper [46] on 'Emergent Gravity and the Dark Universe'. This paper strongly suggested that spacetime itself could be a manifestation of entanglement and that a correct implementation of emergent gravity in this setting might potentially replace the need for dark matter in astrophysics.

The work presented in that paper assumes an extension of holography to de-Sitter spacetime. Open questions [47] with regard to this generalization and some challenges in the phenomenological aspects of the theory provide a unique motivation for a deeper understanding of holographic bulk reconstruction from boundary entanglement entropy.

*Quantum  
error-correction  
protocols  
originated [44]  
from quantum  
computing to  
protect quantum  
information.*

## 1.2 CONTEXT

To expand the current knowledge on holography with respect to bulk reconstruction and emergent physics, it would be useful to gain understanding of the value of boundary quantum information in some more complicated spacetimes than

AdS itself. As mentioned earlier, research has shown that it is not always certain that in these cases, the entanglement entropy will suffice to describe the entirety of the spacetime. In this dissertation these ideas will be expanded to the framework of tensor networks, a set of quantum information tools at the cutting-edge of contemporary holographic research. At the end, conceptual links to questions regarding sub-AdS scale locality will be made.

### 1.2.1 Entwinement and Spacetime Origami

As specified previously, entanglement entropy is a measure of information shared between spatially separated regions of the same physical system. Spatial entanglement entropy quantifies [34] exactly how much information is available about a spatially distinct part of a system without accessing that particular region. It is however not difficult to imagine a distinction between the different parts of a system which is not (purely) spatial.

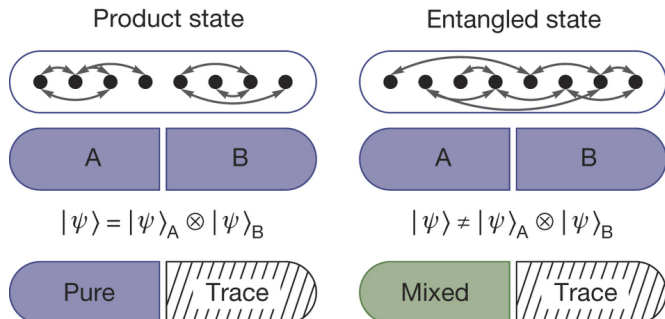


Figure 4: A graphical representation [26] of entanglement entropy. Generically, a quantum many-body system contains (quantum) correlations, here shown as arrows, between its different constituents. When the system is divided into two sub-systems  $A$  and  $B$ , they are either entangled (on the right) or not (on the left). The trace over spatial region  $B$ , i.e. ignoring all information about region  $B$ , yields either a pure or a mixed state, depending on its entanglement.

To be precise, recall from elementary quantum mechanics [48] that a quantum system in a mixed state, i.e. a quantum statistical ensemble, is described by a density matrix  $\rho$ . Accordingly, the quantum mechanical extension of classical entropy, the Von Neumann entropy [34], of a system is defined as

$$S = -\text{tr}(\rho \ln \rho). \quad (3)$$

The Von Neumann entropy of a reduced density matrix of a spatial component of the mixed state, like the one in question, is known as the entanglement entropy [33, 40, 43]. Similarly, an entanglement entropy quantity computed as the Von Neumann entropy of the reduced density matrix of a non-spatial subsystem can be defined. For example [43, 49], the entanglement entropy between the high and low momentum modes of a generic Hilbert space for an interacting field theory can be calculated.

As explained earlier, spatial entanglement entropy can be holographically interpreted via the Ryu-Takayanagi formula. Application of a quantum informational quantity, based on a non-spatial separation of degrees of freedom, to holography would be scientifically valuable. Several options are available to make non-spatial separations in a system, but the challenge is to develop one that has sufficient meaning in a holography setting. One proposal in this regard is entwinement [42, 43].



Figure 5: A graphical representation of the long string model, adapted from the original paper [43]. The intervals are indicated in blue. On the left the same interval is used on each level of the string so that the entwinement reduces to standard entanglement entropy. On the right the interval shows a non-spatial separation of the system indicating the usefulness of entwinement to discern between internal degrees of freedom.

Consider for a moment the following "long string"-model [43], not to be confused with string theory, that consists of long closed strings or spin chains which are wound multiple times around a spatial circle. The resulting situation clearly has more than one "internal" degree of freedom, more than one spin, per spatial position on the circle. Shared information between these internal degrees of freedom, can be interpreted holographically in the setting of 2+1-dimensional gravity [50, 51], and is quantified by a concept called entwinement [42, 43].

Spacetime solutions of 2+1-dimensional gravity with a negative cosmological constant [52], are all asymptotically AdS and hence perfectly suitable for AdS/CFT. Each of these solutions can be obtained by identification [51, 53] of the spacetime-points of AdS under (subgroups of) the isometries of AdS and due the geometric properties of AdS, boundary points are mapped to other boundary points. The boundary of AdS is therefore essentially a closed long string which is wound by the isometric identifications.

One way to make a separation in this model [43] is to distinguish between the different layers of the wound string. Another option would be to regard different intervals on different levels of the string. Both these examples bring a non-trivial entwinement interpretation to the boundary of 2+1-dimensional gravity solutions. If the intervals on different levels are the same, the entwinement reduces [43] to the entanglement entropy of a boundary interval. In this thesis a more concrete understanding of entwinement is sought through the use of tensor network techniques.

*2+1-dimensional gravity has two spatial dimensions and one temporal dimension.*

### 1.2.2 Holographic Tensor Networks

Entanglement plays, as indicated before, an important role in condensed matter physics. Numerical models of large-scale entanglement, known as tensor networks [54], have led to significant progress in the simulation of emergent condensed matter phenomena of quantum many-body states [55, 56]. These networks employ [57] a graphic representation of entanglement at different length scales by using a hierarchical pattern of discrete units (tensors) to achieve an exactly solvable model of (strongly coupled) systems. Recently, tensor networks have successfully been introduced [57–59] to holography.

Emergent phenomena essentially arise [60] due to interacting microscopic entities which combined produce an effect on a macroscopic level. It is immediately clear that the entanglement structure leading to emergent holographic phenomena is suitable for interpretation in tensor networks but the true motivation for the use of tensor networks in holography and quantum information is found in the fact that tensor networks capture a much subtler range [57, 59] of aspects of holography. Tensor networks can be constructed that explicitly include the quantum error correction properties of holography [45] and even a discrete, algorithmic version of the Ryu-Takayanagi formula has been found [57] for tensor networks.

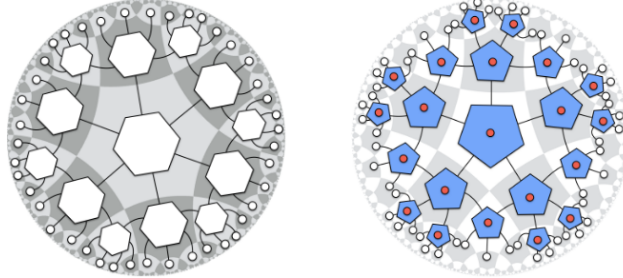


Figure 6: A graphical representation [57] of two types of holographic tensor networks. The tensors are connected by legs or links which indicate entanglement. Notice that each single tensor fits on a single patch of the tessellation of an AdS time-slice. The size of each of these patches is of order of the AdS scale. This property of these specific holographic tensor networks will be paramount to this dissertation.

Concerning emergent gravity and dark matter, one hypothesis [36, 46, 58] is that spacetime itself emerges from an underlying entangled structure. Because each link between two tensors represents entanglement, it is not unthinkable that tensor networks are a discrete toy-model of spacetime itself. A more conservative approach interprets a tensor network solely as a discrete representative of holographic physics. Whether or not to regard spacetime as an emergent holographic entity is currently subject of much debate but has no practical implications for the work presented in this thesis.

Questions remain about where the exact limitations of the different currently known holographic tensor networks lie. Recently a few attempts [61, 62] have been made to explore the nearly uncharted domain of tensor networks on space-times that are not strictly AdS, like 2+1-dimensional gravity solutions. The work presented in this thesis will go beyond the current literature by the use of layers of holographic tensor networks. This layered approach also introduces the use of entwinement to tensor networks.

### 1.2.3 The Road to sub-AdS Locality

Somewhat surprisingly, the results in this dissertation are conceptually linked to an old question in AdS/CFT. The correspondence contains [12, 13] a peculiar inversion of energy scales known as the UV/IR correspondence. Practically, this inversion implies that an ultraviolet cut-off in the boundary theory corresponds to a radial cut-off in the bulk. To some extent, this boils down to the idea [63] that a point in the boundary CFT corresponds to a region of AdS-scale  $R_{AdS}$  in the bulk.

To see this, one could divide [13] the field theory into discrete cells so that each of these cells contains one degree of freedom (per field). The sphere in AdS corresponding [13, 63] to this, according to the radial cut-off, has a radius of order  $R_{AdS}$ . Taking into account the number of degrees of freedom in a  $SU(N)$  field theory, Susskind and Witten [13] concluded that it takes  $N^2$  degrees of freedom to describe the bulk physics within a sphere of AdS-scale.

Later on it was shown [47] that such an AdS-scale region is indeed described by a system of square matrices of dimension  $N$ . The question of how these  $N^2$  matrix degrees of freedom encrypt all the physical information inside an AdS-scale region remains unsolved and is known as the sub-AdS locality problem [13, 47, 63].

If the entanglement of the internal structure of the bulk is ever understood, especially considering the corresponding entanglement in the boundary CFT, this might explain, at least conceptually, how physical information can be encoded in  $N^2$  degrees of freedom. Because tensor networks, which essentially model entanglement, are in general exactly solvable, it is worthwhile to consider them in this context. By combining entwinement with the notion of layered holographic tensor networks and the long string model, a novel conceptual link between sub-AdS locality and tensor networks is formulated in this dissertation.

## 1.3 THESIS STRUCTURE

In five parts, seven chapters (and several appendices) this thesis makes its way from this gentle start to the state of the art in holography and quantum information. The first part is the introduction. The second part presents a literature study of relevant subjects in the research field. The third part deals with current developments and original research. The fourth part covers the conclusion and

outlook. The fifth and final part bundles the appendices, most of which are technical in nature. At the end of the dissertation, the bibliography and index can be found.

- **Chapter One:** The first chapter, which you are currently reading, starts by providing motivation for a study of holography and quantum information. The second section of this chapter sketches the context of the specific research presented in this dissertation in view of holography, quantum information and theoretical high-energy physics. Finally, this chapter contains an overview of the contents of the different chapters.
- **Chapter Two:** The path to AdS/CFT is paved with supertheories. The second chapter tells the tale of supersymmetry and supergravity. In addition to briefly reiterating some of the important points of quantum field theory and general relativity, this chapter develops both of the super-theories in a minimalistic fashion. The cardinal objective of this chapter is to bridge the gap between the compulsory master courses and the specific needs of this dissertation. A secondary point made here is that the AdS/CFT correspondence is not obvious ab initio but also not entirely unexpected due to symmetry arguments.
- **Chapter Three:** The third chapter focuses on the relevant pre- "quantum information" aspects of AdS/CFT. As the correspondence is a stringy manifestation of holography, string theory will be introduced (albeit sparsely) to elucidate the origins of the AdS/CFT correspondence. Furthermore, the large N expansion of gauge fields, the properties of conformal field theories, correlation functions and the reconstruction of operators will be discussed in a holographic context.
- **Chapter Four:** Having sufficiently developed a range of aspects in high-energy physics throughout the previous chapters, this chapter incorporates some crucial facets of quantum information theory into the dissertation. Entanglement entropy, the Ryu-Takayanagi formulation of AdS/CFT, quantum error correction and some specific holographic tensor networks are all discussed in depth.
- **Chapter Five:** The entirety of the fifth chapter deals with entwinement in holography. As part of this venture, 2+1 dimensional gravity and the D1-D5 CFT are discussed, leaning heavily on the material developed in the earlier chapters on high-energy physics. On top of synthesizing some of the literature's most recent concepts in the field of holography and quantum information, this chapter also provides the reader with a hitherto unknown covering space picture of entwinement for massive, non-rotating BTZ black holes.
- **Chapter Six:** The final corpus chapter deals with the implementation of entwinement in tensor networks. Up to now no work had been published on

the application of entwinement to tensor networks. In this chapter the latest developments in holographic tensor networks for non-trivial spacetimes are augmented with entwinement concepts. The results of this method, including the link to sub-AdS locality, are discussed in detail in this chapter.

- **Chapter Seven:** The concluding chapter contains an extensive discussion of the results obtained in this dissertation and an overview of the new challenges that have come to light during the development of the research. Comments on the general state and evolution of holography and quantum information are included, especially concerning research directions tangent to those in this dissertation.

On many of the pages of this thesis, the reader can find small pieces of text in the margin. These margin notes contain supplementary comments, additional clarifications and complementary context. The objective of these notes is to provide support and amusement for a wide range of readers with different backgrounds without disrupting the logical flow of the main text. Technical calculations, code listings and remarks on conventions can be found in the appendices which are collected in the final part of this dissertation.



II

## THE HOLOGRAPHIC CORRESPONDENCE OF ADS AND CFT



# 2

## A TALE OF TWO SUPER-THEORIES

---

### 2.1 INTRODUCTION

Maldecena proposed [8, 11] (but did not explicitly prove) that the holographic principle has a concrete realization in the so-called AdS/CFT correspondence. In the low-energy regime, which is of interest in this dissertation, the correspondence reduces to a duality between two theories, a four-dimensional supersymmetric field theory and a five-dimensional supergravity, that do not, *ab initio* seem to describe the same physics. The aim of this chapter is to familiarize readers with these super-theories, highlight the relevant differences between them and to show them that even though the proposed duality is not obvious it is also not entirely unexpected.

For instance, the symmetries of the theories on both sides of the duality will turn out to match. In physics, symmetries are ubiquitous and shape theories by limiting the different possible states and interactions which a physical system can exhibit. In the case of the two theories regarded here, the matching of the symmetries indicates that there should at least be some similarity between supergravity in five-dimensional AdS and the four-dimensional supersymmetric QFT living on its boundary. To properly set the stage for a discussion on this symmetry matching and to facilitate the rest of this dissertation, a few basic facts about symmetries, gauge theories and spacetime transformations are recapitulated at the beginning of this chapter.

### 2.2 SYMMETRIES OF A PHYSICAL THEORY

Consider for a moment, a set of scalar fields  $\phi_i(x)$  propagating [64–66] through a flat spacetime whose metric tensor is

$$\eta_{\mu\nu} = \eta^{\mu\nu} = \text{diag}(+, -, -, -, \dots), \quad (4)$$

which corresponds to Minkowski spacetime in Cartesian coordinates  $x^\mu$ . This simple set-up suffices to briefly repeat much of the basic machinery of quantum field theory. For instance, these scalar fields can then be used to describe an action of a physical theory,

$$S[\phi_i] = \int d^Dx \mathcal{L}(\phi_i), \quad (5)$$

where  $\mathcal{L}$  is a Lagrangian density. The infinitesimal symmetry variation of these scalar fields is given by,

$$\delta\phi_i(x) = \epsilon^A \Delta_A \phi_i(x) \quad (6)$$

where  $\epsilon^A$  is a symmetry parameter and where  $\Delta_A$  is a matrix or linear differential operator applied to  $\phi_i(x)$ . Finally, using this notation, the Euler-Lagrange equations, which yield the equations of motion, are

$$\frac{\partial}{\partial x^\mu} \frac{\delta \mathcal{L}}{\delta \partial_\mu \phi_i(x)} - \frac{\delta \mathcal{L}}{\delta \phi_i(x)} = 0. \quad (7)$$

Speaking a bit more formally [28, 64], a symmetry transformation of the theory is a mapping  $\phi_i(x) \rightarrow \phi'_i(x)$  that leaves the action invariant, i.e.  $S[\phi_i(x)] = S[\phi'_i(x)]$ . Expansion of this definition and previous notions to other types of fields, e.g. spinor fields, is straightforward. It is also worth noting that most common field theories, like those used in the standard model of particle physics [65, 67], contain both symmetries of spacetime components, i.e. spacetime symmetries, and internal symmetries.

The importance of symmetries [64–66] to physics can hardly be overstated. Primarily, Noether's theorem [68, 69] relates the symmetry properties of a physical system to its conservation laws. If the variation in equation (6) is a symmetry of the theory, then [64] the Lagrangian density is an explicit total derivative so that,

$$\delta \mathcal{L} = \epsilon^A \left[ \frac{\delta \mathcal{L}}{\delta \partial_\mu \phi^i(x)} \partial_\mu \Delta_A \phi^i(x) + \frac{\delta \mathcal{L}}{\delta \phi^i(x)} \Delta_A \phi^i(x) \right] \dot{=} \epsilon^A \partial_\mu K_A^\mu, \quad (8)$$

which can be made to read  $\partial_\mu J_A^\mu = 0$  with the Noether current  $J_A^\mu$  defined by

$$J_A^\mu = - \frac{\delta \mathcal{L}}{\delta \partial_\mu \phi^i(x)} \Delta_A \phi^i(x) + K_A^\mu. \quad (9)$$

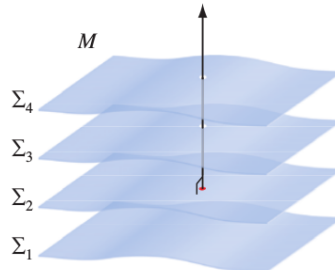


Figure 7: A graphical representation [70] of space-like hypersurfaces. The integral of the Noether current over surfaces like these gives Noether charges. For more information on integrating in a differential geometric setting see the appendices.

Any Noether current is conserved [64, 65] for all solutions of the equations of motions. For each Noether current  $J_A^\mu$ , an integrated Noether charge  $Q_A$  exists. To obtain a Noether charge [64] regard a space-like  $(D-1)$ -surface  $\Sigma$ , then

$$Q_A = \int d\Sigma_\mu J_A^\mu(x). \quad (10)$$

*The defining property [71] of space-like hypersurfaces is that they exclusively contain space-like curves.*

This system of Noether charges and currents is valid for both spacetime symmetries and internal symmetries. Both types of symmetries have different kinds of applications and peculiarities, these will be addressed one-by-one in the upcoming sections. First up, spacetime symmetries.

### 2.2.1 The Poincaré Group

The spacetime symmetries of relativistic quantum field theory form a symmetry group, known as the Poincaré group [28, 64]. All elementary particles fit into representations of this group. To define [28] the Poincaré group, it is necessary to regard the infinitesimal length  $ds$  of a space-time interval. In Minkowski spacetime, the infinitesimal space-time interval is defined by

$$ds^2 = \eta_{\mu\nu} dx^\mu dx^\nu. \quad (11)$$

The elements of the Poincaré group [64] are symmetry transformations defined so that they leave  $ds^2$  invariant. The resulting group consists of two distinct parts [28, 64], namely the Lorentz transformations and the translations of a point  $x^\mu$  by a vector  $a^\mu$ . Lorentz transformations are characterized [28] by a matrix  $\Lambda$  obeying

$$\Lambda^\mu{}_\rho \Lambda^\nu{}_\sigma \eta_{\mu\nu} = \eta_{\rho\sigma}, \quad (12)$$

while spacetime translations are characterized [28] by the vector  $a^\mu$ . Consequently, the symmetry transformations of the Poincaré group are denoted by the pairs  $(\Lambda, a)$ . Each of these pairs dictates a transformation on a spacetime point  $x$  according to

$$x'^\mu = \Lambda^\mu{}_\nu x^\nu + a^\mu. \quad (13)$$

The group multiplication of the elements of the Poincaré group is defined [28] as

$$(\Lambda_1, a_1) \circ (\Lambda_2, a_2) = (\Lambda_1 \Lambda_2, a_1 + \Lambda_1 a_2). \quad (14)$$

The infinitesimal Poincaré transformations give [64] the following variation,

$$\delta\phi^i(x) = \epsilon^A \Delta_A \phi^i(x) = [a^\mu \partial_\mu - \lambda^{\rho\sigma} (x_\rho \partial_\sigma - x_\sigma \partial_\rho)] \phi^i(x) \quad (15)$$

where the first part represents the translation with parameter  $a$  and where the second part denotes the Lorentz transformation with parameter  $\lambda^{\rho\sigma}$ . Assuming a Lagrangian density with standard (i.e. of the form  $-\frac{1}{2}\partial_\mu\phi^i\partial^\mu\phi_i$ ) kinetic terms, the Noether current for spacetime translations and Lorentz transformations are respectively given [64, 66] by

$$T^\mu{}_\nu = \partial^\mu \phi(x)^i \partial_\nu \phi(x)_i + \delta^\mu_\nu \mathcal{L} \quad \& \quad M^\mu{}_{\rho\sigma} = -x_\rho T^\mu{}_\sigma + x_\sigma T^\mu{}_\rho. \quad (16)$$

Poincaré group representations are usually labeled [28, 64] by (the square of) the four-momentum of each particle and a series of discrete quantum numbers.

The charges corresponding to these currents are denoted [64] as  $P_\mu$  and  $M_{\rho\sigma}$  and are vital to the development of supersymmetry. More in-depth analysis of the Poincaré transformations and derivations of the above results can be found in the literature [28, 64, 66]. Finally, it is important to note that strict adherence to invariance under Lorentz transformations is an experimental constraint on many theories.

### 2.2.2 Yang-Mills Gauge Theory

If a symmetry of a theory does not involve spacetime components, then this symmetry is called an internal symmetry [64]. Local internal symmetries of a quantum field theory are known as gauge symmetries [64, 67, 72]. These symmetries have an extraordinarily profound effect on physical reality because they govern the possible interactions between particles and fundamental forces in a quantum field theory.

Usually [64, 65], internal symmetries form a compact Lie algebra which has a linear representation in the form of  $n \times n$  matrices  $t_A$ . The infinitesimal transformation of the internal symmetry is therefore given by

$$\delta\phi^i(x) = \epsilon^A \Delta_A \phi^i(x) = -\theta^A(x) (t_A)^i{}_j \phi^j(x), \quad (17)$$

where  $\theta^A(x)$  is the (gauge) symmetry parameter. The corresponding conserved current [64] is

$$J^\mu{}_A = -\partial^\mu \phi_i(x) (t_A)^i{}_j \phi^j(x). \quad (18)$$

The conserved charge related to this current is denoted by  $Q_A$ . With this notation, the commutation relations of the algebra are given [64] by

$$[t_A, t_B] = f_{AB}{}^C t_C, \quad (19)$$

where the different factors  $f_{AB}{}^C$  (as defined by the above equation) are known as the structure constants [65, 72] of the corresponding Lie algebra.

As an example of internal symmetries in quantum field theories, a generic Yang–Mills theory with coupling strength  $g_{YM}$  is featured here. The Lagrangian density [65, 72] for this kind of theory is

$$\mathcal{L} = -\frac{1}{4g_{YM}} F_{\mu\nu}(x) F^{\mu\nu}(x), \quad (20)$$

where the field strength of the gauge field  $A_\mu(x)$  of the internal symmetry group is given by

$$F_{\mu\nu}^C(x) = \partial_\mu A_\nu^C(x) - \partial_\nu A_\mu^C(x) + g_{YM} f_{AB}{}^C A_\mu^A(x) A_\nu^B(x). \quad (21)$$

Notice that the symmetry indices here, are (exceptionally) unsuppressed. The use of the structure constants is allowed here, because the gauge field transforms in the adjoint representation of the symmetry group.

Notice [65, 72] that the Yang-Mills Lagrangian density is invariant under gauge transformations,

$$\phi_i(x) \rightarrow e^{-\theta^A(x)t_A} \phi_i(x) \quad \& \quad A_\mu(x) \rightarrow \theta^A(x) [t_A, A_\mu(x)] + \partial_\mu (\theta^A(x)t_A). \quad (22)$$

and to obtain a derivative that is also invariant under these gauge transformations, the covariant derivative is defined as

$$D_\mu = \partial_\mu - ig_{YM} A_\mu(x). \quad (23)$$

For the purposes of this dissertation is sufficient to say that the introduction of the covariant derivative [72, 73] is needed for equation (22) to hold. Due to the covariant derivative  $D_\mu$ , non-linear terms will appear in the equations of motion for this theory. In perturbation theory, these non-linear terms are understood [65, 72] as interaction terms.

The Yang-Mills gauge theory as briefly presented here is at the core of the unification of the electromagnetic and weak forces in the standard model of elementary particle physics [65, 72]. In that setting the gauge group is chosen to be  $U_Y(1) \times SU_W(2) \times SU_C(3)$  so that the theory becomes applicable to electromagnetic, weak and strong nuclear forces. The success of this theory strongly accentuates the importance of internal  $SU(N)$  symmetries to physics.

### 2.3 SUPERSYMMETRY

Unfortunately, the standard model of particle physics has its limitations [74, 75]. For instance, higher-order loop corrections to the mass of scalar field particles, like the Brout-Englert-Higgs particle [76–78], cause divergences. One possible solution to this problem is to cut-off [65, 72] the theory at an energy scale at which new physics should occur. Besides being ad-hoc, this solution is prone to fine-tuning [75] issues. An alternative, more elegant, solution is the introduction of supersymmetry.

The central idea of supersymmetry [75, 79] is that every fermionic particle has a bosonic partner and the other way around. Supersymmetry solves the above described divergence problem, because fermion and boson loops, which are now in balance, add corrections with opposite signs [65, 72]. The divergences of both kind of loops cancel [74, 75] each others divergence out and the calculation of the scalar particle masses is no longer problematic.

Further motivation for supersymmetry can be found on purely theoretical grounds. As argued previously, the symmetries of a theory (either spacetime or internal) are crucial to the kind of physics the theory can contain. Hence, it is worthwhile contemplating which kind of symmetry groups are, in general, allowed in a quantum field theory. Coleman and Mandula [80] developed a framework in which to answer this question which allowed Haag, Łopuszański and Sohnius [79]

*Technically, the opposite signs are due to the fact that fermions are Grassmann variables [64, 72] while bosons are not.*

to show that supersymmetries can, generically, be present. Based on Gell-Mann's totalitarian principle [81, 82] which states that everything that is not forbidden is compulsory, it might be expected that supersymmetry is indeed a fundamental symmetry of reality.

### 2.3.1 The Supersymmetry Algebra

In a supersymmetric theory (SUSY), the internal symmetry groups of theory are extended to include supersymmetries [75, 83–85]. The generators  $Q_\alpha^i$  of the supersymmetric transformations are spinors (as indicated with a spinor index  $\alpha$ ). Regarding terminology, it is worth remarking that the supersymmetry generators are known as supercharges and that the amount of different supersymmetries in a theory is denoted by  $\mathcal{N}$  so that in the above definition of the supercharges, the index  $i$  can run from 1 to  $\mathcal{N}$ .

*Recall that classical conserved charges correspond to generators of symmetries in quantum physics.*

In AdS/CFT, supersymmetry is important because both sides of the correspondence make use of theories that are supersymmetric. As will be shown shortly, the CFT side will have global supersymmetries while the AdS side is governed by a local theory of supersymmetry. To gain a somewhat deeper understanding of supersymmetries, its advantageous to take a look at their algebra; the superalgebra. To define this algebra it is convenient to start from the Poincaré algebra [64] defined by,

$$\left\{ \begin{array}{l} [P^\mu, P^\nu] = 0, \\ [M^{\mu\nu}, P^\lambda] = i(\eta^{\mu\lambda}P^\nu - \eta^{\nu\lambda}P^\mu), \\ [M^{\mu\nu}, M^{\rho\sigma}] = i(\eta^{\nu\rho}M^{\sigma\mu} + \eta^{\mu\sigma}M^{\rho\nu} - \eta^{\mu\rho}M^{\sigma\nu} - \eta^{\nu\sigma}M^{\rho\mu}), \end{array} \right. \quad (24)$$

where, as indicated earlier,  $P^\nu$  is the conserved charge of the translations and where  $M^{\rho\sigma}$  is the conserved charge of the Lorentz transformations. The extension [64] of the Poincaré algebra to the superalgebra, which contains the generators of the supersymmetry, is

$$\left\{ \begin{array}{l} [P_\mu, Q_\alpha] = 0, \\ [M^{\mu\nu}, Q_\alpha] = -\frac{1}{2}(\gamma_{\mu\nu})_\alpha^\beta Q_\beta, \\ \{Q_\alpha, Q^{+\beta}\} = -\frac{1}{2}(\gamma_\mu)_\alpha^\beta P^\mu, \end{array} \right. \quad (25)$$

where the gamma-matrices  $\gamma_{\mu\nu} = \frac{1}{2}[\gamma_\mu, \gamma_\nu]$  are a specific case of the general higher rank gamma matrices defined by  $\gamma_{\mu\dots\nu} \doteq \gamma_{[\mu}\dots\gamma_{\nu]}$ . Representations of the superalgebras are used to build up Lagrangian densities for supersymmetric theories. An additional benefit of using supersymmetric multiplets is that they always [64, 75] contain an equal number of bosonic and fermionic degrees of freedom.

### 2.3.2 $\mathcal{N} = 1$ Supersymmetric Yang-Mills Theory

Reprising the  $SU(N)$  field theories that were discussed earlier, and adding in supersymmetry leads to the study of supersymmetric Yang-Mills (SYM) theories [28, 64]. To obtain the Lagrangian density of the  $\mathcal{N} = 1$  supersymmetric Yang-Mills theory, consider a supersymmetric multiplet consisting of a vector gauge boson  $A_\mu(x)$  and its SUSY partner a spin- $1/2$  particle known as the gaugino,  $\lambda(x)$ . Taking inspiration from the standard massless Yang-Mills theory, equation (20), the obvious candidate for the action of a gauge theory with this content with field strength  $F^{\mu\nu}$  and covariant derivative  $D_\mu$  is

$$S = \int \left[ -\frac{1}{4g_{YM}} F^{\mu\nu}(x) F_{\mu\nu}(x) - \frac{i}{2} \bar{\lambda}(x) \gamma^\mu D_\mu \lambda(x) \right] d^4x. \quad (26)$$

It can be shown, although this is significantly non-trivial [64], that this action is indeed invariant under supersymmetric variations. Notice that the action includes a Dirac term which contains the fermionic fields  $\lambda(x)$  that were introduced to the theory by the supersymmetry.

### 2.3.3 $\mathcal{N} = 4$ Supersymmetric Yang-Mills Theory

In a vein similar to the  $\mathcal{N} = 1$  case, a  $\mathcal{N} = 4$  supersymmetric Yang-Mills theory [28, 64] can be constructed. An extra subtlety [64, 86] is that the four supercharges  $Q_\alpha^i$  of this theory can be rotated into each other using an  $SU(4)$  symmetry. For later use, note the Lie algebra isomorphism  $SU(4) \approx SO(6)$  of this symmetry group.

Several equivalent forms for the Lagrangian density for the  $\mathcal{N} = 4$  supersymmetric Yang-Mills theory exist in the literature [28, 64]. The exact expression of the Lagrangian density is fairly complicated and is unnecessary for this dissertation. It is however worthwhile to note that the  $\mathcal{N} = 4$  SYM theory is obtained as a special case [64] from  $\mathcal{N} = 1$  SYM, which illustrates [28] the close relationship between the two theories.

The field content [64] of the  $\mathcal{N} = 4$  SYM theory will be particularly beneficial to grasping the structure of the AdS/CFT correspondence. The theory contains a vector gauge potential, four chiral fermion fields (and associated chiral conjugates) and six real scalars. In the next chapter this field content is interpreted in terms of string theory degrees of freedom.

The single most important reason that  $\mathcal{N} = 4$  SYM, and hence this whole foray into global supersymmetry, is relevant for AdS/CFT is that this Yang-Mills theory is exactly scale invariant [28], i.e. scale invariant on both the classical and the quantum level. Scale invariance is the critical indicator of the presence of conformal symmetry in a theory. Conformal transformations are defined [71] as those coordinate transformations that leave the metric  $g_{\mu\nu}$  invariant up to a locally arbitrary positive scale factor. The scale factor is often chosen to be the

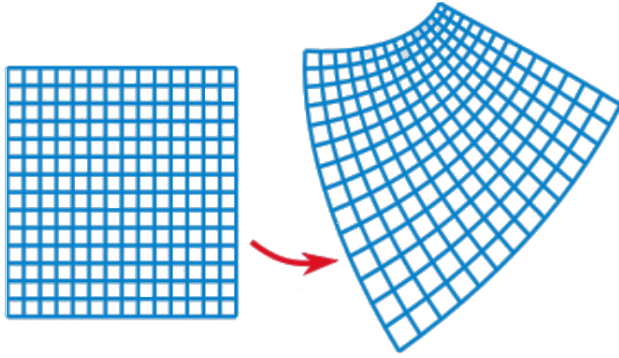


Figure 8: A graphical representation adapted from wikipedia commons [87] of conformal transformations. Observe that a conformal map is a function that locally preserves angles, pairs of lines intersecting perpendicularly are mapped to pairs of curves still intersecting perpendicularly.

so-called Weyl scale factor  $e^{2\sigma(x)}$  so that conformal transformations take the form,

$$g_{\mu\nu} \rightarrow g'_{\mu\nu} = e^{2\sigma(x)} g_{\mu\nu}. \quad (27)$$

This coordinate transformation equation implies [71] that the angles are locally invariant under conformal transformations and that conformal transformations preserve causal structure. The length of an infinitesimal spacetime interval  $ds$  is however modulated by the scale factor, in this case  $e^{2\sigma(x)}$ .

As conformal theories cannot have any preferred kind of length scale, their field content is prohibited from being massive [88] because mass inherently correspond to a length-scale. The particles of quantum field theory are approximately massless in the high-energy limit and hence one could imagine that CFT's like  $\mathcal{N} = 4$  SYM describe features of physics at high energies. In chapter 3, it is shown conclusively that  $\mathcal{N} = 4$  SYM is the conformal field theory in the AdS/CFT duality, the remaining question is how supersymmetry shows up on the gravitational side of the correspondence.

#### 2.4 SUPERGRAVITY

While supersymmetry is global in the CFT, the gravitational side of the conjectured AdS/CFT correspondence adheres to the laws of a local theory of supersymmetry, called supergravity [64]. In supergravity, the principles of supersymmetry and general relativity mix to form a gravitational theory that gauges supersymmetry. In AdS/CFT, a specific ten-dimensional extension of supergravity will be used. As supergravity is a local theory, the symmetry parameter of supersymmetry, the constant spinor  $\epsilon_\alpha$ , is turned into a spacetime dependent spinor  $\epsilon_\alpha(x)$ . This makes supergravity specifically suited for the description of fermions in curved spacetimes.

The challenge in supergravity is to find an appropriate gravitational action that is invariant under these local supersymmetries. By the requirements of supersymmetry, a vector-spinor field is needed to describe the gravitons fermionic superpartner [75], the gravitino. The fields for the graviton and the gravitino will be discussed in the upcoming sections on supergravity but first, general relativity is succinctly recapitulated.

#### 2.4.1 Briefly, General Relativity

The concept of Einstein's theory of general relativity is elegant and profound [89, 90]: matter (or energy) tells spacetime how to bend and a curved spacetime tells matter how to move. In general relativity, spacetime is regarded as a (smooth) manifold upon which a test-particle can move according to the local curvature. The resulting theory, which expands the principles of special relativity, is most conveniently expressed in the language of differential geometry and is able to describe gravity far beyond the Newtonian regime.

For the purposes of this dissertation, all geometrical properties of a smooth manifold are given by its metric [71]. Mathematically speaking, a metric on a manifold is a (non-degenerate) symmetric bilinear map [64] from the tangent space to real numbers which contains geometric information on the manifold. This map is specified by a local second rank tensor  $g_{\mu\nu}$  but an explicit distinction between the tensor and the map is usually not made.

The path of a free-falling test-particle  $x^\mu(\tau)$  in a curved spacetime is given [71, 89] by the geodesic equation

$$\frac{d^2x^\mu}{d\tau^2} + \Gamma_{\nu\rho}^\mu \frac{dx^\nu}{d\tau} \frac{dx^\rho}{d\tau} = 0, \quad (28)$$

where  $\tau$  is the eigentime (the time as measured by the test-particle) and where the  $\Gamma_{\rho\sigma}^\mu$  are the Christoffel symbols. The Christoffel symbols, which are not tensors, are defined by

$$\Gamma_{\nu\rho}^\mu = \frac{1}{2} g^{\mu\sigma} (\partial_\nu g_{\rho\sigma} + \partial_\rho g_{\nu\sigma} - \partial_\sigma g_{\nu\rho}). \quad (29)$$

Christoffel symbols relate [89–91] local vector spaces (tangent spaces) to the local curvature of the manifold. The Christoffel symbols are also used to express the covariant derivative  $\nabla_\mu$  of general relativity.

The relationship between the matter in a spacetime and its curvature is given by a set of coupled non-linear differential equations [89, 90], the Einsteins equations,

$$G_{\mu\nu} = \kappa^2 T_{\mu\nu}, \quad (30)$$

where  $G_{\mu\nu} = R_{\mu\nu} - \frac{1}{2}g_{\mu\nu}R$  is generally known as the Einstein tensor,  $\kappa^2 = 8\pi G$  is the gravitational coupling constant. The energy-momentum tensor  $T_{\mu\nu}$  represents

For a (tangent) vector  $V^\rho$  the covariant derivative is  
 $\nabla_\mu V^\rho = \partial_\mu V^\rho + \Gamma_{\mu\sigma}^\rho V^\sigma$ .

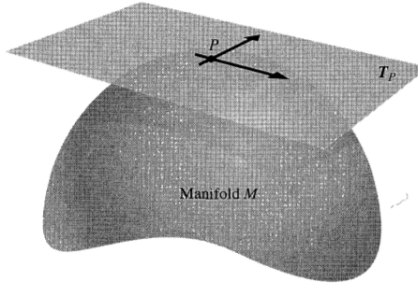


Figure 9: A graphical representation [71] of a tangent space of a smooth manifold. A tangent space is a local generalization of a vector space.

all the matter and energy in a spacetime. The Einstein tensor consists respectively of the metric tensor  $g_{\mu\nu}$ , the Ricci scalar  $R = g^{\mu\nu}R_{\mu\nu}$  and the Ricci tensor  $R_{\mu\nu}$ .

The Ricci tensor is obtained by contraction from the Riemann curvature tensor  $R^\rho_{\mu\sigma\nu}$ . The Riemann curvature tensor embodies [89, 90] all the information on the curvature of a generic spacetime and is directly related to the Christoffel symbols by

$$R^\rho_{\mu\sigma\nu} = \partial_\sigma\Gamma^\rho_{\nu\mu} - \partial_\nu\Gamma^\rho_{\sigma\mu} + \Gamma^\rho_{\sigma\lambda}\Gamma^\lambda_{\nu\mu} - \Gamma^\rho_{\nu\lambda}\Gamma^\lambda_{\sigma\mu}, \quad (31)$$

as discussed extensively in most textbooks [89, 90] on general relativity.

Maximally symmetric spacetime solutions of general relativity are classified [71] on the basis of their curvature. The flat solution is Minkowski space, the positively curved one is the de Sitter (dS) spacetime and the negatively curved solution is Anti-de Sitter (AdS) space. In AdS/CFT, the gravitational side of the duality consists of higher-dimensional supergravity in some kind of augmentation of Anti-de Sitter spacetime. Other less symmetric but important solutions [71] of general relativity are the Schwarzschild solution for black holes and the Robertson-Walker Friedmann metric for cosmology.

#### 2.4.2 Introducing Frame Fields

To include fermions in gravity, an alternative way to deal with a metric has to be introduced [64, 89]. Additionally, this new approach provides a field, known as the frame field, which represents the graviton in supergravity. First, notice that the metric (tensor) can be diagonalized by an orthogonal transformation  $O^a_\mu$ ,

$$g_{\mu\nu} = O^a_\mu K_{ab} O^b_\nu. \quad (32)$$

The resulting diagonalized metric matrix  $K_{ab}$  has  $D$  ordered eigenvalues,  $\lambda^a$ , where  $D$ , as usual, denotes the spacetime dimension. The diagonalisation of the metric allows for the definition of the frame field

$$e_\mu^a(x) \doteq \sqrt{\lambda^a(x)} O^a_\mu(x), \quad (33)$$

which in four dimensions is commonly known as the "vierbein". In general, a transformation between the frame field  $e_\mu^a(x)$  and the metric  $g_{\mu\nu}$  is of the form

$$g_{\mu\nu}(x) = e_\mu^a(x) \eta_{ab} e_\nu^b(x). \quad (34)$$

A local Lorentz transformation can be used to construct a different frame field, which will also adhere to equation (34). Therefore, in this dissertation, the different choices in frame fields due to local Lorentz transformations are regarded as equivalent and will not be distinguished.

It can be shown [64] that the frame fields  $e_a^\mu$  form an orthonormal basis in each tangent space. The frame fields  $e_a^\mu$  and  $e_\mu^a$  can hence be used to transform any tensor from a coordinate basis (coordinate indices  $a, b, c, \dots$ ) to a local Lorentz basis (frame field indices  $\mu, \nu, \rho, \dots$ ). Note that a local Lorentz transformation only acts on the frame field indices and not on coordinate indices.

An inverse frame field  $e_a^\mu$  can also be defined with the usual properties,  $e_a^\mu e_\mu^b = \delta_a^b$  and  $e_a^\mu e_\nu^a = \delta_\nu^\mu$ .

Clearly, a gauged (and thus local) theory of supersymmetry, i.e. supergravity, will need a local treatment of Lorentz transformations, therefore general relativity must be reformulated [64] using frame fields. It is convenient to introduce the use of frame fields in general relativity via an action principle. Conveniently, this will also allow for the introduction of interactions of fermions, like the gravitino, with gravity.

### 2.4.3 The Einstein-Hilbert Action

To understand general relativity with frame fields, it is useful to start from an action principle for gravity [90]. The action for general relativity is

$$S = \int d^D x \sqrt{|\det(g)|} \left( \frac{1}{2\kappa^2} g^{\mu\nu} R_{\mu\nu} \right) = \int d^D x \sqrt{|\det(g)|} \left( \frac{1}{2\kappa^2} R \right), \quad (35)$$

where  $\kappa^2$  is again the gravitational coupling constant and  $R = g^{\mu\nu} R_{\mu\nu}$  the Ricci scalar for a torsion-free connection. The origin of the  $\sqrt{|\det(g)|}$  in the volume element of curved spacetime is due to some subtleties [71, 91] in the calculus of  $p$ -forms [91] which are discussed in the appendices.

Technically speaking, this action needs an extra term [92] to compensate for non-vanishing surface terms.

After varying the action (35) with respect to the metric and assuming (incorrectly) a vanishing surface term, one can obtain the Einstein equations. This action for general relativity was published [93] by Hilbert and is therefore known as the Einstein-Hilbert action. To rephrase this action in terms of frame fields, the connection one-form  $\omega^{ab} \doteq \omega_\mu^{ab}(x) dx^\mu$ , is needed. The components  $\omega_\mu^{ab}(x)$  of this one-form are known as the spin connection [64, 94] because they relate spinors, specifically fermions, to the gravity action.

### 2.4.4 Leveraging the Spin Connection

Within general relativity, the spin connection plays the role of the gauge field. For a torsion-free manifold, the spin connection is given [64] by

$$\omega_\nu^{ab} = 2e^\nu{}^{[a} \partial_{[\mu} e_\nu{}^{b]} - e^\nu{}^{[a} e^{b]\sigma} e_{\mu\sigma} \partial_\nu e_\nu{}^c. \quad (36)$$

The spin connection is intimately connected to the torsion of a spacetime via the Cartan structure equations [95].

This spin connection  $\omega_\mu{}^{ab}$  transforms under coordinate transformations as a Yang-Mills potential would under a gauge transformation for an  $O(D - 1, 1)$  group. Therefore [64], the spin connection behaves as a gauge field of Lorentz transformations so that the spin connection defines a covariant derivative,

$$\psi(x) \rightarrow \psi'(x) = e^{-\frac{1}{4}\lambda^{ab}\gamma_{ab}}\psi(x) \quad \& \quad D_\mu\psi(x) = \left(\partial_\mu + \frac{1}{4}\omega_{\mu ab}\gamma^{ab}\right)\psi(x). \quad (37)$$

Correspondingly [64] the field strength of this gauge like theory is

$$R_{\mu\nu ab} = \partial_\mu\omega_{\nu ab} - \partial_\nu\omega_{\mu ab} + \omega_{\mu ac}\omega_{\nu}{}^c{}_b - \omega_{\nu ac}\omega_{\mu}{}^c{}_b, \quad (38)$$

which is readily recognized as the frame field equivalent of the Riemann curvature tensor, conform equation (31). The Einstein-Hilbert action can be fully rewritten [64, 94] in function of frame fields by use of this new expression for the Riemann tensor,

$$S = \int d^Dx |\det(e)| \left( \frac{1}{2\kappa^2} e_a^\mu e_b^\nu R_{\mu\nu}{}^{ab} \right). \quad (39)$$

Fermions  $\psi$  can now readily be included [64] by extending the Einstein-Hilbert action to

$$S = \int d^Dx |\det(e)| \left( \frac{1}{2\kappa^2} e_a^\mu e_b^\nu R_{\mu\nu}{}^{ab} - \frac{1}{2}\bar{\psi}\gamma^\mu D_\mu\psi + \frac{1}{2}\bar{\psi}\overleftrightarrow{D}_\mu\gamma^\mu\psi \right). \quad (40)$$

#### 2.4.5 The Rarita–Schwinger Field for Gravitinos

The final missing part of supergravity is the appropriate vector-spinor field for the superpartner of the graviton; the gravitino [75]. Peculiarly, the gravitino field  $\psi_\mu$  is exactly the gauge field of local supersymmetry transformations [64]. The field for the gravitino is named the Rarita–Schwinger field [96] after its inventors and its own gauge transformation is

$$\psi_\mu(x) \rightarrow \psi_\mu(x) + \partial_\mu\epsilon(x), \quad (41)$$

where the symmetry parameter  $\epsilon(x)$  is, as expected, a spacetime dependent spinor.

From general principles [64, 96] it is inferred that the action for the Rarita–Schwinger field, must be Lorentz invariant, first order in spacetime derivatives, Hermitian and invariant under the supersymmetric gauge transformation postulated in equation (41). The appropriate action fulfilling [96] all these requirements is given by the Lagrangian density

$$\mathcal{L} = \bar{\psi}_\mu\gamma^{\mu\nu\rho}\partial_\nu\psi_\rho. \quad (42)$$

The corresponding equation of motion is

$$\gamma^{\mu\nu\rho}\partial_\nu\psi_\rho = 0. \quad (43)$$

To obtain supergravity, which essentially is a gravitational gauge theory of supersymmetry, the Rarita–Schwinger field must be aptly combined with a frame field formulation of gravity. The resulting theory then predicts how the above equation of motion and Einstein’s equation are modified to fit each other.

#### 2.4.6 Basic Supergravity

Any version of supergravity [64, 84] must at the very least contain a supersymmetric multiplet consisting of a frame field, that describes the graviton, and  $\mathcal{N}$  vector-spinors that describe the corresponding gravitinos. The action for the simplest case of supergravity, which is minimal  $\mathcal{N} = 1$  supergravity [64], is

$$S = \frac{1}{2} \int d^D x |\det(e_\mu^a)| \frac{1}{2\kappa^2} [e^{a\mu} e^{av} R_{\mu vab} - \bar{\psi}_\mu \gamma^{\mu\nu\rho} D_\nu \psi_\rho] , \quad (44)$$

where the covariant derivative is taken with respect to local Lorentz transformations,

$$D_\mu = \partial_\mu + \frac{1}{4} \omega_{\mu ab} \gamma^{ab} . \quad (45)$$

To conceptually understand the origin of this action, note that the first part of the action is simply the Hilbert-Einstein action, equation (35), while the second part can easily be identified as a natural extension of the action of the Rarita–Schwinger field, equation (41). The transformation rules for the different elements of the Lagrangian density are

$$e_\mu^a(x) \rightarrow e_\mu^a(x) + \frac{1}{2} \bar{\epsilon}(x) \gamma^a \psi_\mu(x) \quad \& \quad \psi_\mu(x) \rightarrow \psi_\mu(x) + D_\mu \epsilon(x) . \quad (46)$$

The proof of invariance of the supergravity action, equation (44), under these transformation rules is highly involved [64], even in  $D = 4$ , and will not be covered in this dissertation. The result [64] however is that variation of the action with regard to the Rarita–Schwinger field yields an equation of motion for the gravitino that is the dynamical extension ( $\partial_\mu \rightarrow D_\nu$ ) of the free field equation, equation (43),

$$\gamma^{\mu\nu\rho} D_\nu \psi_\rho = 0 . \quad (47)$$

Einstein’s equations are obtained from the supergravity action via variation with respect to the frame field but they are adapted so that the energy-momentum tensor now includes the contributions of the gravitino. Therefore, the supergravitational action as shown here, describes a self-consistent gravitational gauge theory of supersymmetry.

#### 2.4.7 Ten-dimensional Type IIB Supergravity

A (low-energy) treatment of the AdS/CFT correspondence requires [28, 86], as mentioned before, a ten-dimensional extended version of supergravity. When considering extended supergravity ( $\mathcal{N} > 1$ ) in higher dimensions, i.e.  $4 < D \leq 11$ ,

*Additionally, matter multiplets [64, 84] that adhere to global supersymmetry may be present.*

the supersymmetry algebra determines [64] the different possible types of supergravity. In ten dimensions, there are three options: the theory either has one chiral supercharge  $Q_\alpha$ , two chiral supercharges of the opposite chirality or two chiral of the same chirality. The first option is known as Type I, the second and third options are respectively known as Type IIA and Type IIB. Due to string theoretical reasons, Type IIB supergravity is of relevance for the AdS/CFT correspondence.

Certain non-perturbative solutions [64, 86] of type IIB supergravity, called *D*3-branes, are paramount [28, 97] to the postulation of the AdS/CFT correspondence in string theory. Here it will be shown that in their near-horizon limit, which is essentially their low-energy regime, *D*3-branes reduce to an  $AdS_5 \times S^5$  spacetime which provides the AdS spacetime after which AdS/CFT is named. For the present discussion of *D*3-branes, only the bosonic field content of Type IIB supergravity is relevant. Under this restriction, the entire ten-dimensional type IIB supergravity action reverts to [64]

$$S_{IIB} = \int dx^{10} \sqrt{|g_{10}|} \left( \frac{1}{2} R_{10} - \frac{F_{\alpha\beta\gamma\sigma\theta} F^{\alpha\beta\gamma\sigma\theta}}{2 \times 5!} - \frac{1}{2} \partial_\alpha \phi \partial^\alpha \phi \right), \quad (48)$$

where  $g_{10}$  and  $R_{10}$  respectively represent the determinant of the ten-dimensional metric and the ten-dimensional Ricci scalar. The other symbols represent a 5-form field strength  $F$  and a scalar field  $\phi$ , both of which have their origin in string theory [28]. The indices  $\alpha, \beta, \gamma, \sigma, \theta$  are chosen [64] so that they first run through  $x^\mu$ , the Cartesian coordinates of Minkowski space, and then through  $y^a$  which are the coordinates of flat Euclidean space. This peculiar choice of coordinates is motivated by the use of *D*3-branes in string theory.

The resulting line-element of a *D*3-brane [64] is

$$ds_{10}^2 = \frac{\eta_{\nu\mu} dx^\nu dx^\mu}{\sqrt{H(y^a)}} + \sqrt{H(y^a)} \delta_{ab} dy^a dy^b, \quad (49)$$

where  $H(y^a)$  is a harmonic function. For the applications of *D*3-branes in the string theory postulation of AdS/CFT, it is necessary to regard a stack of  $N$  coincident *D*3-branes [86, 97], which can be constructed by choosing [64] the harmonic function  $H(y^a)$  so that

$$H(y^a) = 1 + \frac{L^4}{r^4}, \quad (50)$$

where  $r = \sqrt{\delta_{ab} y^a y^b}$  is a specific radial coordinate and where  $L^4 = 4\pi\alpha'^2 g_s N$  is the radius of the AdS space that will be obtained from these *D*3-branes. For now, the reader may simply regard  $\alpha'$  and  $g_s$  as nondescript real positive constants, later on (in a string theory discussion) they will be given a specific meaning.

The line-element of the stack of  $N$  *D*3-branes, as shown in equation (49), can be rewritten to manifestly express [64, 86] the presence of a  $S^5$  line-element,

$$ds_{10}^2 = \frac{\eta_{\nu\mu} dx^\nu dx^\mu}{\sqrt{H(y^a)}} + \sqrt{H(y^a)} (dr^2 + r^2 d\Omega_5^2), \quad (51)$$

*The five-form  $F^{\alpha\beta\gamma\sigma\theta}$  must be self-dual in this action.*

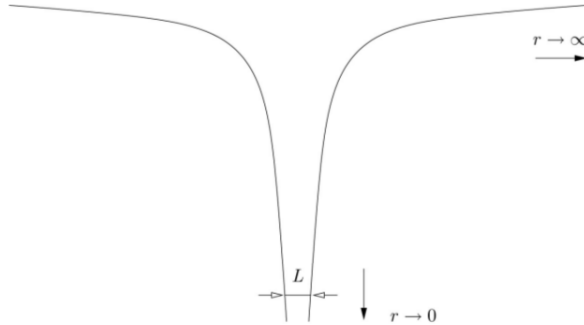


Figure 10: A graphical representation [98] of the geometry of (a stack of)  $D3$ -branes.

The throat of the  $D3$ -branes is in the  $r \rightarrow 0$  region where the metric has a horizon due to the specific form of  $H(y^a)$ . Away from the throat, the geometry is asymptotically flat. Taking red-shifting into account, it is clear to see that low-energy degrees of freedom of supergravity reside in the throat.

where  $d\Omega_5^2$  is the standard metric on the unit 5-circle  $S^5$ . The corresponding metric is asymptotically flat for  $r \rightarrow \infty$ . In the  $r \rightarrow 0$  limit however, the spacetime has a horizon. The near-horizon limit is called the "throat" and is characterized by  $H(y^a) \approx L^4/r^4$ , so that the line-element is given by

$$ds_{10}^2 = \frac{r^2}{L^2} \eta_{\mu\nu} dx^\mu dx^\nu + \frac{L^2 dr^2}{r^2} + L^2 d\Omega_5^2. \quad (52)$$

This expression can be brought into a highly suggestive form after the introduction [64, 86] of a new radial coordinate  $z \doteq L^2/r$ ,

$$ds_{10}^2 = \frac{L^2}{z^2} [dz^2 + \eta_{\mu\nu} dx^\mu dx^\nu] + L^2 d\Omega_5^2. \quad (53)$$

The first part of this line-element corresponds to a coordinate system of  $AdS_5$ , which is generally known as the Poincaré patch [97], so that the near-horizon limit of  $D3$ -branes is indeed an  $AdS_5 \times S^5$  spacetime.

*It can be seen here, that  $L$  determines the  $AdS$  radius.*

#### 2.4.8 Scalar fields in $AdS$

For holography, the  $S^5$  part of  $AdS_5 \times S^5$  is generally seen as an internal part can be compactified [28, 86]. In essence this comes down to applying the Kaluza-Klein method [99]. This technique consists of writing the part of the equation of motions that deals with  $S^5$ -components as a harmonic expansion [86]. The result is that massless fields of IIB supergravity on  $AdS_5 \times S^5$  are observed in  $AdS_5$  as infinite towers of massive particles.

Indeed [64, 86], starting from the ten-dimensional Klein-Gordon equation for a massless scalar field  $\phi$  in  $AdS_5 \times S^5$ ,

$$\nabla_{AdS_5}^2 \phi + \nabla_{S^5}^2 \phi = 0, \quad (54)$$

*Dimensional compactification originated from the need [28] to explain unseen extra dimensions as physically real.*

and setting

$$\phi = \sum_l \phi_l Y^l, \quad (55)$$

with  $Y^l$  the spherical harmonics of  $S^5$ , reduces the equation to

$$\nabla_{AdS_5}^2 \phi_l = m_l^2 \phi_l \quad , \quad m_l^2 = \frac{l(l+4)}{L^2}. \quad (56)$$

The values for the scalar masses  $m_l$  are due to the eigenvalue equation [64, 86],

$$\nabla_{S^5}^2 Y^l = -\frac{l(l+4)}{L^2} Y^l. \quad (57)$$

## 2.5 CONCLUSION

Expanding on an elementary discussion on the use of symmetries in physics, supersymmetry and supergravity have been discussed in this chapter. Motivation for this discussion is found in the conjecture that each of these theories represent a side of an important duality; the AdS/CFT correspondence. The conformal field side is proposed to be governed by an  $\mathcal{N} = 4$  Supersymmetric Yang-Mills theory while the AdS-side would be governed by dimensionally reduced ( $10 \rightarrow 5$ ) supergravity on a stack of  $D3$ -branes. As shown in this chapter, these two super-theories differ significantly in nature (global  $\leftrightarrow$  local) and application (flat space  $\leftrightarrow$  curved space) and hence the proposed correspondence is neither trivial nor obvious.

Yet, even in this early chapter there are some strong but subtle indications [28, 64, 86] that there is indeed an equivalence between the two theories. For instance, the  $AdS_5 \times S^5$  background obtained from the stack of  $D3$ -branes has, as shown in this chapter, a  $SO(6)$  spherical rotational symmetry which corresponds to the global  $SU(4)$  symmetry of the  $\mathcal{N} = 4$  supersymmetric Yang-Mills theory. In addition, the supersymmetric Yang-Mills theory also contains six scalars which transform as directions along the 5-sphere in  $AdS_5 \times S^5$  do. It is truly remarkable, especially in light of the importance of symmetries that was discussed here, that the two theories of supersymmetry and supergravity have matching symmetries. The next chapter will strongly motivate this surprising equivalence between AdS and CFT based on string theoretical arguments.

### 3.1 INTRODUCTION

As mentioned in the introduction, holography can most tractably be studied using the AdS/CFT correspondence [8, 9] (or a variant thereof). The AdS/CFT conjecture can be defined [64] as the proposal of a “one-to-one correspondence between the local fields in an  $\text{AdS}_{D+1}$  (super)gravity theory and the (gauge invariant, composite) operators in a  $D$ -dimensional conformal, quantum field theory”. The goal of this chapter is to explore, clarify and solidify this proposition.

The previous chapter already alluded to the fact that  $D3$ -branes, solitonic solutions of supergravity, are involved in the origin of the correspondence. Here, in this chapter,  $D3$ -branes will be reinterpreted as string theory objects [100] and coaxed into providing considerable confidence [28] in the existence of a holographic correspondence between AdS and CFT.

To showcase its versatility and to foster additional confidence in the conjecture, a series of specific aspects of the AdS/CFT correspondence are discussed in this chapter. These topics include, but are not limited to, the large  $N$  expansion of gauge theories, CFT correlators and AdS-Rindler bulk reconstruction. Given this summary of AdS/CFT, the comparative impact of a quantum informational perspective on holography can be analyzed in the following chapters.

### 3.2 A STRING THEORETICAL PERSPECTIVE

String theory [28, 64, 100] is an extraordinarily rich subject that can obviously, but regrettably, not be treated in full (mathematical) detail in this dissertation. Therefore, this dissertation aims to provide just the right amount of background knowledge on string theory to elucidate the origin of the AdS/CFT correspondence. Interested readers can learn more on string theory from several excellent sources [100–102].

The main idea of string theory is to use extended objects to describe physics. Instead of using point particles, the fundamental objects in quantum field theory, string theory employs the concept of extended strings. While a point particle sweeps out a worldline [86] through spacetime, a string [100], in contrast, sweeps out a  $1+1$  dimensional worldsheet  $\Sigma$ . Such a worldsheet is embedded in a background spacetime and can be parametrized [100] by two coordinates; the proper time  $\tau$  and a string extent parameter  $\sigma$ .

The motivation for this kind of parametrization for the worldsheet can be found in the fact that the worldline of a particle is generally parametrized by

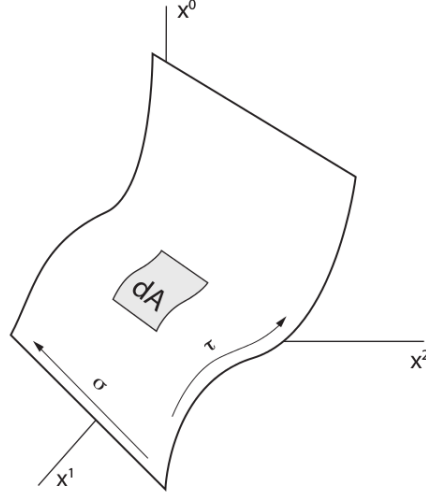


Figure 11: A graphical representation [86] of a worldsheet. This graphic contains the essential idea of string theory that fundamental physics is best described using extended objects instead of pointlike particles.

the eigentime  $\tau$ . It is hence natural to retain this coordinate for strings. Recall that the action [86] for a particle with mass  $m$  moving along a worldline with coordinates  $x^\mu(\tau)$  is

$$S = -m \int ds = -m \int d\tau \sqrt{g_{\mu\nu} \partial_\tau x^\mu(\tau) \partial_\tau x^\nu(\tau)}, \quad (58)$$

where  $g_{\mu\nu}$  is the metric of the background spacetime. A string moving along a worldsheet with coordinates  $X^\mu(\tau, \sigma)$  can similarly be described by the Nambu-Goto action [28, 100],

$$S_{NG} = -T \int dA = -T \int \sqrt{\det(g_{\mu\nu} \partial_\alpha X^\mu \partial_\beta X^\nu)} d\tau d\sigma, \quad (59)$$

where  $T$  is the tension of the string. The tension is defined [28] by

$$T = \frac{1}{2\pi\alpha'} \quad (60)$$

with  $\alpha'$  a fundamental string theory parameter known as the Regge slope [28, 100]. The length  $l_s$  and mass  $m_s$  of the string are also defined [28] in function of that parameter,

$$l_s = \sqrt{\alpha'} = \frac{1}{m_s}. \quad (61)$$

Because the Nambu-Goto action is manifestly non-linear in  $X^\mu(\tau, \sigma)$ , the resulting equations of motions will also be non-linear. To smoothen away this unpleasant property of the Nambu-Goto action, a worldsheet metric  $h_{\alpha\beta}$  must be

introduced as an auxiliary field. The resulting action for the string is the Polyakov action [28, 86],

$$S_P = -T \int \sqrt{\det(h_{\alpha\beta})} h^{\alpha\beta} g_{\mu\nu} \partial_\alpha X^\mu \partial_\beta X^\nu d\tau d\sigma. \quad (62)$$

The Polyakov action has an expansive set of symmetries [28]. Both Lorentz transformations and spacetime translations of the embedding spacetime leave this action invariant and re-parameterizations of the worldsheet are also symmetries of the theory. This last fact implies that the choice of parametrization  $(\tau, \sigma)$  does not contain any physical information.

### 3.2.1 Constraints and Boundary Conditions

As a consequence of the equations of motions resulting from the Polyakov action, the energy-momentum tensor  $T_{\alpha\beta}$  of the worldsheet has to vanish [28]. This puts constraints on the  $X^\nu(\tau, \sigma)$  fields, which are widely known as the Virasoro constraints [28, 100]. In addition to these constraints, the solutions of the Polyakov equations of motions must also adhere to boundary conditions.

The spatial extension of the string is either periodic [100], which indicates a closed string, or it has explicit boundary conditions which indicates that a string is open. For open strings, the boundary conditions are either Dirichlet boundary conditions,

$$\delta X^\mu(\tau, \sigma)|_{\text{boundary}} = 0, \quad (63)$$

or Neumann boundary conditions,

$$\partial_\sigma X^\mu(\tau, \sigma)|_{\text{boundary}} = 0. \quad (64)$$

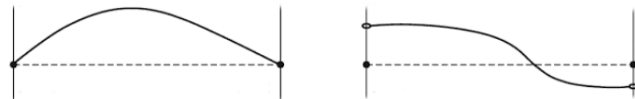


Figure 12: A graphical representation of the boundary conditions for open strings adapted from "A First Course in String Theory" [103]. The left side of the figure represents the Dirichlet boundary conditions while the right side represents Neumann boundary conditions.

The choice of boundary conditions has an effect [28, 100, 103] on the momentum flow of a string. In the closed case, momentum just keeps flowing through the string and hence it is conserved. Conservation of momentum is also valid for a string with Neumann conditions. In the case of Dirichlet conditions however, translational invariance is manifestly broken and therefore momentum is not conserved. As a consequence, the hypersurfaces defined by the collection of string endings with Dirichlet conditions become dynamical objects [28, 100, 103], which are unerendipitously called  $D$ -branes.

### 3.2.2 Solutions and Supersymmetry

To find solutions [28, 100] for the equations of motions of this Polyakov action, the fields  $X^\mu(\tau, \sigma)$  are Fourier expanded. Just like in field theories, the terms of the expansion can be interpreted as oscillations, which in this case are vibrations of the string. After quantization [28, 100] the different boundary conditions determine the different types of particle that each kind of vibrating string can produce.

Interactions [28, 86] between strings are modeled by worldsheets with non-trivial topologies. The topology of the non-interacting strings that have been described up to now were either that of a cylinder (for a closed string) or that of a strip (for an open string). The topology of an interaction between strings is essentially obtained [86] by the splitting and joining of the worldsheet of the strings.

In general this splitting and joining causes [28] either worldsheet ruptures or the formation of additional handles on the worldsheet. Each kind of topology resulting from these string interactions, can be interpreted [28, 86] as a term in a perturbative expansion where the power of the term, expressed in function of the string coupling constant  $g_s$ , is determined by the genus of the corresponding worldsheet.

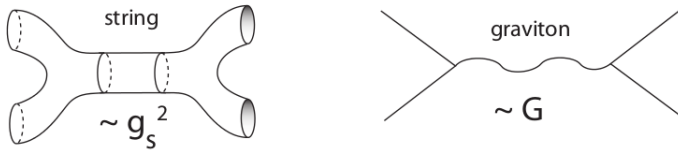


Figure 13: A graphical representation [86] of an interacting graviton in string theory, at tree-level. Higher order diagrams will have a different topology and hence contribute to a different power of  $g_s$ .

The theory as discussed up to now, only describes bosonic degrees of freedom [101]. To introduce fermionic degrees of freedom to the theory, supersymmetry is called upon once more [102]. From symmetry arguments it can be concluded that superstring theory is most natural [28] in ten dimensions. This is essentially the reason why ten is the amount of dimensions used in the supergravity theory in AdS/CFT. That supergravity, which inherently possesses fermions, follows from the low-energy limit [28, 64] of superstring theory is one of the more alluring aspects of superstring theory.

### 3.2.3 Two-faced D-Branes

In (super)string theory, *D*-branes are a class of extended objects [28, 86, 100] that serve as the endpoints of strings with Dirichlet conditions. D-branes are classified by their spatial dimension and the type of a brane is indicated [28] by a number:

a  $D0$ -brane is a point particle, a  $D1$ -brane is a (kind of) string and a  $Dp$ -brane is a  $p + 1$ -dimensional hyperplane where  $D$  denotes the dimension of the embedding spacetime. For the purpose of motivating the AdS/CFT correspondence, a stack of  $N$  coincident  $D3$ -branes in ten-dimensional flat Minkowski space is considered.

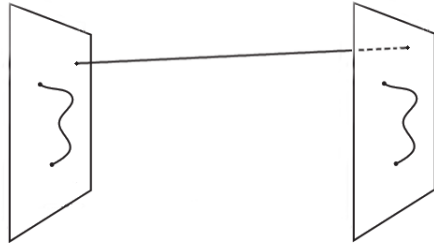


Figure 14: An adapted graphical representation [28] of the ways in which open strings can end on a  $D$ -brane. A string with two Dirichlet boundary conditions can either begin and end on the same  $D$ -brane or start one  $D$ -brane and end on another.

To support Maldacena's proposal [8] of the AdS/CFT correspondence, this  $D3$ -brane setup is considered in the low-energy limit of type IIB string theory. It turns out [28, 86, 104] that there are two different perspectives in which to contemplate this; one perspective for open strings and one for closed strings. Which perspective is the right one depends on the value of the effective string coupling for the stack of branes, i.e.  $g_s N$ .

In the so-called open string perspective [28, 104], which is valid for  $g_s N \ll 1$ , the stack of  $D3$ -branes can be described as an extended object [28, 64] upon which open strings end. Because of the chosen parameter regime, these open strings act as perturbative effects [28] upon the brane. When neglecting massive string excitations, which is allowed in the low-energy regime, the open string dynamics can be described [28, 86] as a  $\mathcal{N} = 4$  SYM theory, with  $SU(N)$  as gauge group, living in the (four-dimensional) world-volume of the stack of  $D3$ -branes.

From this perspective,  $D3$ -branes are seen to have two classes of excitations [28, 86] which correspond to the six scalar fields and the one gauge field of four-dimensional  $\mathcal{N} = 4$  SYM, respectively. The first class of excitations [28, 64, 86] of the  $D3$ -brane describes its rigid motions and deformations, which can be parameterized by the six coordinates, i.e. six scalars, or alternatively as open string perturbations, transverse to the  $D3$ -brane worldvolume. The other class of  $D3$ -brane excitations are internal perturbations [28, 64, 86] which can be identified as the gauge field  $A^\mu$  of the  $\mathcal{N} = 4$  SYM theory.

So in the low-energy limit, the open string perspective contains the gauge theory belonging to the open string perturbations but there are still closed strings around. Because the open string perspective is in the weak-coupling regime, the closed strings do not interfere with the stack of  $D3$ -branes. The closed strings that

live in ten-dimensional Minkowski thus simply form a flat supergravity theory there. In total, the open string perspective thus consists of a four-dimensional  $\mathcal{N} = 4$  SYM and supergravity in ten-dimensional Minkowski space.

In the closed string perspective [28, 104], valid for the strong coupling regime  $g_s N \gg 1$ , the stack of coincident  $D3$ -branes is regarded as a source in the low-energy limit of superstring theory, i.e. supergravity. With this as a background, the closed strings are seen as the propagating part of the type IIB string theory. The spacetime curved by the  $D3$ -branes is a solitonic solution of supergravity which has a near-horizon limit, a.k.a. the throat, as seen in the previous chapter, namely  $AdS_5 \times S^5$ . Due to red-shifting in the throat, all of the string theory physics there appears to be low in energy.

The characteristic length scale of the throat,  $L = 4\pi\alpha'^2 g_s N$ , is large [64, 86] in the closed string perspective. This implies that the curvature of the spacetime is weak so that stringy effects can be ignored and that approximation of superstring theory by supergravity is validated. Away from the throat [28, 104], this closed string perspective also looks like supergravity in ten-dimensional Minkowski space.

These two perspectives on stacks of  $D3$ -branes provide a different description of the same situation in a low-energetic type IIB superstring theory in flat ten-dimensional Minkowski space. This indicates that two perspectives should [28, 104], in some sense at least, be dual to one another. Both perspectives contain a decoupled supergravity sector in ten-dimensional Minkowski space. Both supergravities are promptly identified [28] with each other. The remaining parts of both perspectives should thus also correspond. The type IIB supergravity on  $AdS_5 \times S^5$  is therefore expected to be (dynamically) equivalent with a  $\mathcal{N} = 4$  SYM on a flat four-dimensional spacetime. This is exactly what the AdS/CFT correspondence proposes!

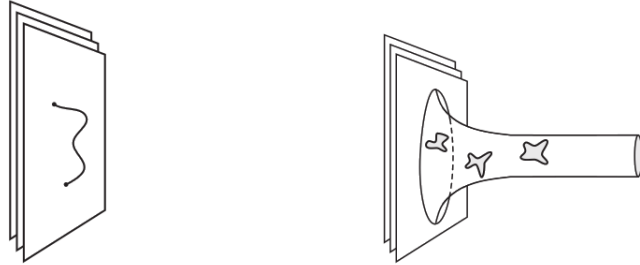


Figure 15: A graphical representation [28] of a stack of coincident  $D$ -branes. The left open string perspective is shown on the left, the closed string perspective is shown on the right. Notice the formation of a "throat" in the picture on the right.

### 3.2.4 A Correspondence, At Last!

Forgetting this whole string theory story for a moment, the theories on both sides of the AdS/CFT correspondence look very different. Yet, the AdS/CFT correspondence states [8, 9] that the two theories are dual to another. This is certainly a strong statement. Therefore it is befitting the current situation to exercise some caution. Certainly in light of the fact that no proof for the conjecture has yet been found, even though the literature contains an extensive range of persuasive arguments in favor of the correspondence [28, 97, 104–106]. To deal with this somewhat ambiguous state of things, language for the different gradations in the range of validity for the proposed correspondence has been developed.

Typically, three forms (the weak, the strong and the strongest) of the correspondence are discerned. In its weakest form [97, 104, 107], the AdS/CFT correspondence states that the two theories are dual to each other when gravity is weakly coupled and the CFT is strongly coupled. In its strongest version [97, 104, 107], the conjecture claims that the two theories are equivalent for all values of  $g_s$  and  $N$ . The strong version of the AdS/CFT conjecture, which proposes its validity for all values of  $g_s N$  with large  $N$ , will be used and assumed throughout the remainder of this dissertation. Some motivation for choosing  $N \gg 1$  is provided in the upcoming section.

*In its strongest form, the conjecture places no restrictions on  $N$ .*

## 3.3 THE LARGE N EXPANSION OF GAUGE THEORIES

As was just shown, a stack of  $N$  coincident  $D3$ -branes in string theory corresponds to an  $\mathcal{N} = 4$  SYM with an  $SU(N)$  internal symmetry. In this section it will be argued that AdS/CFT can be used with reasonable confidence if  $N \gg 1$ . Motivated [86, 104] by statistical mechanics, 't Hooft [108] pointed out that non-abelian  $SU(N)$  gauge theories simplify significantly in the limit  $N \rightarrow \infty$ . In a particle physics language [67], this parameter region would correspond to a gauge theory with a large number of colors.

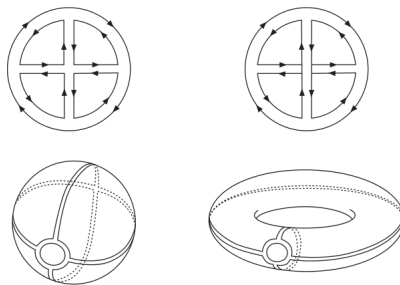


Figure 16: A graphical representation [86] of the difference between a planar diagram (left) and a non-planar diagram (right). Notice that the edges of diagrams have been glued together. A planar diagram can triangulate a sphere while the non-planar diagram must draw on a torus. Planar diagrams are dominant in the 't Hooft expansion.

The large  $N$  limit is interesting because it allows for a rearrangement [86] of the perturbation terms in a quantum field theory so that they correspond to a topological expansion [28, 86], similar to that for string theory, with coupling  $g_s \propto 1/N$ . This strongly suggests [86] that non-abelian gauge theories at large  $N$  are equivalent to (super)string theories, which in their low-energy limit reduce to supergravity. This kind of relationship between gauge theories and supergravity is principally a rudimentary version of the AdS/CFT correspondence.

### 3.3.1 't Hooft Expansion of Gauge Theories

From the previous chapter, it is known that an  $SU(N)$  Yang-Mills theory is prime example of a non-abelian gauge theory. For convenience, the Yang-Mills Lagrangian density, equation (20), is repeated here,

$$\mathcal{L} = -\frac{1}{4g_{YM}^2} F_{\mu\nu}(x) F^{\mu\nu}(x). \quad (65)$$

It can easily be seen [86] that this equation can be rephrased by the introduction of the 't Hooft coupling  $\lambda = g_{YM}^2 N$ ,

$$\mathcal{L} = -\frac{N}{4\lambda} F_{\mu\nu}(x) F^{\mu\nu}(x). \quad (66)$$

In the 't Hooft expansion [108],  $\lambda$  is kept fixed and the expansion is performed in powers of  $1/N$ . Different powers of  $N$  correspond in different topologies of the Feynman diagram, in a way similar (but inversely) to the expansion in  $g_s$  in string theory. The clearest way to see this, is to replace [28, 86] each line in a Feynman diagram by an oriented double line and gluing together the endpoints. From topology [86], it follows that diagrams have an  $N^{2-2h}$  dependency, where  $h$  is the number of handles of the surface associated to the double-lined diagram. Because  $\lambda$  is kept constant and  $N \gg 1$ , planar diagrams (those that have no handles) are dominant [28, 86] in the large  $N$  expansion.

### 3.3.2 Large $N$ in AdS/CFT

The question remains how the condition  $N \gg 1$  has an influence on AdS/CFT. From general string theoretical arguments [86], it can be shown that

$$\frac{L^4}{\alpha'^2} = N g_{YM}^2. \quad (67)$$

Using the definition of the 't Hooft coupling [108] this expression can be rewritten to read

$$\frac{\alpha'}{L^2} = \frac{1}{\sqrt{\lambda}}. \quad (68)$$

Two equivalent definitions [86] of the ten-dimensional Newton's constant  $G = l_p^8$ , where  $l_p$  is the Plank length, and  $G = \frac{\pi^4}{2} g^4 \alpha'^4$  show that the previous expression can be reformed to give

$$\left(\frac{l_p}{L}\right)^8 = \frac{\pi^4}{2N^2}. \quad (69)$$

As discussed above, the length scale  $L$  has to be large to legitimize the use of supergravity and therefore  $l_p/L \ll 1$  is required, or equivalently  $N \gg 1$ . The string theory derivation of the AdS/CFT correspondence thus suggests [28, 86, 104, 107] that the  $SU(N)$  group of  $\mathcal{N} = 4$  SYM has a large  $N$ .

### 3.4 FIELDS, OPERATORS AND SOURCES

To grasp how the gravitational side of AdS/CFT emerges from the boundary field theory, it is worthwhile to consider, for a moment, the following condensed matter physics toy model [86]. The toy model consists of a discrete lattice system with spacing  $a$  and a simple Hamiltonian,

$$H = \sum_{x,i} J_i(x, a) O^i(x), \quad (70)$$

where  $i$  labels the different operators  $O^i(x)$  which are coupled to different sources (a.k.a. coupling constants)  $J_i(x, a)$ . In these expressions,  $x$  denotes the lattice positions.

The lattice spacing of this toy model determines [86] the explicit values of the sources  $J_i(x, a)$ . The evolution of the sources with regard to a varying lattice spacing is governed by some kind of renormalization flow [28]. The sources can be written as  $J_i(x, u)$  given that  $u = (a, 2a, 4a, \dots)$  is defined as the length scale at which the system is observed. Essentially, the lattice spacing variation parameter  $u$  can be regarded as an extra dimension.

In this new higher-dimensional space, the evolution of the sources is governed by some kind of (field) dynamics that represents the renormalization group equations. In AdS/CFT a similar process happens [28, 36, 86], there the new dimension is the radial direction of AdS and the dynamics of the sources is subject to (super)gravity. This motivates the idea that in holography, gravity emerges via renormalization group flow from a boundary theory (where the UV sources live).

In AdS/CFT, the sources, which act as gravitational fields in the bulk, have dual conformal field operators in the boundary theory. To see how this works explicitly [28, 64, 86], write a scalar field  $\phi$  in AdS as a Fourier transform with  $z$  the coordinate of the emergent (radial) direction and  $x$  the collection of other coordinates,

$$\phi(z, x) = \int \frac{d^d k}{(2\pi)^d} e^{ik \cdot x} f_k(z), \quad (71)$$

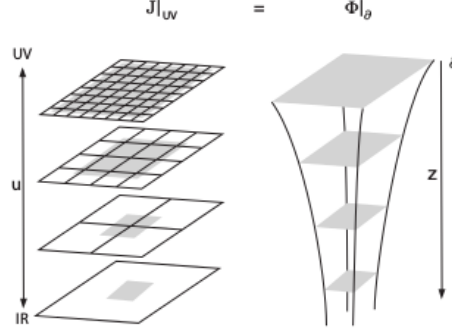


Figure 17: A graphical representation [86] of the comparison between the discrete lattice toy model and the situation in AdS/CFT. From this visual, it can be understood that gravity emerges from  $UV$  sources that live at the conformal boundary, denoted by  $\partial$ . Notice the orientation of the axis of the radial coordinate.

and look for the resulting boundary source term  $\phi_{(0)}(x)$ . In terms of this Fourier transform, the equation of motion for the scalar field of mass  $m$  in AdS reads

$$z^{d+1} \partial_z \left( z^{1-d} \partial_z f_k \right) - k^2 z^2 f_k - m^2 L^2 f_k = 0, \quad (72)$$

where  $L$  is, as usual, the AdS radius. From near-boundary analysis [86] it is known that the function  $f_k(z)$  behaves as

$$f_k(z) = A(k) z^{D-\Delta} + B(k) z^\Delta, \quad (73)$$

near  $z \approx 0$ . In addition, it can be shown that  $\Delta$  is

$$\Delta = \frac{D}{2} + \sqrt{\left(\frac{D}{2}\right)^2 + m^2 L^2}. \quad (74)$$

A more systematic approach for this kind of holographic renormalisation exists [28, 64].

Neglecting the sub-dominant term in  $f_k(z)$ , the field  $\phi(z, x)$  at the boundary at  $z = \epsilon$  becomes

$$\phi(\epsilon, x) \approx \epsilon^{D-\Delta} A(x). \quad (75)$$

To identify a boundary source  $\phi_{(0)}(x)$  with the corresponding scalar field  $\phi(\epsilon, x)$ , any divergent term from  $\phi(\epsilon, x)$  has to be removed [28, 86]. This can easily be done by identifying  $A(x)$  with  $\phi_{(0)}(x)$  and setting,

$$\phi_{(0)}(x) = \lim_{z \rightarrow 0} z^{\Delta-D} \phi(z, x). \quad (76)$$

This explicitly and self-consistently shows that a boundary source is the near-boundary limit of a gravitational field in the bulk, so that a field in the bulk corresponds to a specific boundary operator. A deeper analysis [28, 86] of scalar fields combines this calculation with the Kaluza-Klein reduction discussed in the

previous chapter and shows that the Kaluza-Klein tower of scalar fields corresponds to the operators in the  $\mathcal{N} = 4$  SYM theory. The same approach has successfully [86] been applied to other fields, further bolstering trust in the AdS/CFT correspondence.

### 3.5 CORRELATION FUNCTIONS IN ADS/CFT

As mentioned before, it is known that a dictionary exists between field operators  $O(x)$  on the CFT and gravitational fields  $\phi(z, x)$  in AdS. The boundary value of such field has just been implied to act as the source for a corresponding (conformal) field operator and combined with the motivation from string theory, this suggests that the dynamics on both sides of the duality should match. To considerable extent, this statement will be made concrete in this section. To do this however some concepts from both conformal field theory and functional field theory methods are necessary.

#### 3.5.1 Functional Methods

The functional alternative to the canonical quantization of quantum fields is to use the path-integral formalism [28, 66, 109]. In essence, this elegant formalism is built on an abstract action principle over the infinitely many quantum-mechanically allowed paths of particles. In quantum field theory, the path integral formalism translates to an action principle over all possible field configurations. One advantage of the path-integral formalism that there is a strong link with statistical mechanics, a downside is that it has a less well-defined mathematical foundation than canonical methods.

For the purposes of this dissertation, it suffices to note that the transition probability amplitude in this formalism is given [28] by,

$$\langle \phi_f, +\infty | \phi_i, -\infty \rangle = C \int \mathcal{D}\phi e^{iS[\phi]}, \quad (77)$$

where the integration measure  $\mathcal{D}\phi$  is formally defined as the integrand over all possible quantum field configurations that satisfy the boundary conditions  $\phi_f, \phi_i$  at  $t = \pm\infty$ . The action of the theory is denoted, as usual, with  $S[\phi] = \int_{-\infty}^{+\infty} dt \int d^{D-1}x \mathcal{L}(\phi, \partial\phi)$  and  $C$  is a normalization parameter defined so that the vacuum transition amplitude  $\langle 0 | 0 \rangle = 1$ .

Another notion of interest is the correlation function [65] a.k.a. Green's function  $G(\dots)$ , defined as the expectation values of the form

$$G(x, y, z, \dots) = \langle 0 | \phi(x) \dots \phi(y) \dots \phi(z) | 0 \rangle \doteq \langle \phi(x) \dots \phi(y) \dots \phi(z) \rangle, \quad (78)$$

where the time-ordering over  $\phi$ -fields is implicit. As discussed in the appendices, all physical information of a theory is incorporated into these correlation func-

*In the case of interacting theories, this kind of integral can typically not be solved exactly and perturbation techniques become necessary.*

*Generating functionals originate from statistical mechanics and are hence calculated in Euclidean time [65, 111].*

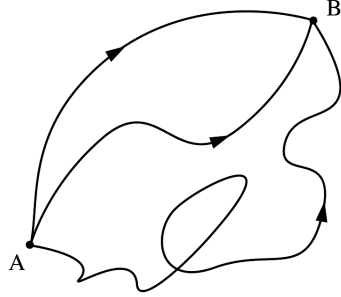


Figure 18: A graphical representation [110] of the concept of path integrals. In quantum mechanics, observable quantities can be expressed as a weighted average over all possible paths the involved particles can take. Quantum statistical physics is best described by a Euclidean version of this.

tions in a way equivalent to Feynman diagrams. Correlation functions like this are related [65] to the path integral formalism by

$$G(x, y, z, \dots) = \int \mathcal{D}\phi [\phi(x) \dots \phi(y) \dots \phi(z)] e^{iS[\phi]}. \quad (79)$$

In order to calculate correlation functions using path integrals, it is convenient to introduce another functional concept, namely the generating functional  $Z_0[J]$  which is defined [28] by

$$Z_0[J_i] = \langle 0 | e^{\int d^D x J_i(x) O^i(x)} | 0 \rangle, \quad (80)$$

where  $J_i(x)$  is the source of the operator  $O^i(x)$ . Interest in generating functionals is due to the property [28] that (Euclidean) correlation functions can be obtained from them via functional variation,

$$\langle O(x) \dots O(y) \dots O(z) \rangle = \left[ \frac{1}{Z_0[J]} \frac{\delta^n Z_0[J]}{\delta J(x) \dots \delta J(y) \dots \delta J(z)} \right] \Big|_{J_i=0} \quad (81)$$

where  $n$  is the amount of fields considered in the correlation function.

### 3.5.2 Correlation Functions of Conformal Operators

The Euclidean correlation functions regarded here [28, 64], are those of composite operators  $O(x)$  on the boundary conformal field theory. The behavior [64] of these kind of operators under scale transformations of the form  $x \rightarrow x' = \rho^{-1}x$  is

$$O(x) \rightarrow O'(x') = \rho^\Delta O(x), \quad (82)$$

where  $\Delta$ , the scale dimension, is a real number which determines [64] the form of a two-point correlation function of two of this kind of operators,

$$\langle O(x) O(y) \rangle \sim \frac{1}{(x-y)^{2\Delta}}. \quad (83)$$

The choice to call the scale dimension  $\Delta$  is deliberate. It can be shown [28, 86] that, in AdS/CFT, gravitational fields with asymptotics as defined in equation (73), act as the sources for operators with scale dimension equal to  $\Delta$  as defined in equation (74). To prove this, the above described functional field techniques need to be discussed in a holographic setting.

The gravitational side of the AdS/CFT duality is described by a supergravity action  $S_{SUGRA}[\phi]$ , where the fields  $\phi$  are dimensionally reduced from  $AdS_5 \times S^5$  to  $AdS_5$  by Kaluza-Klein compactification as discussed in the previous chapter. According [28, 86, 104] to the conjectured AdS/CFT correspondence, the generating functional  $Z_0[\phi_{(0)}]$  of the composite operator  $O$  that is sourced by the emergent fields  $\phi(z, x)$  is exactly

$$\log(Z_0[\phi_{(0)}]) = S_{SUGRA}[\phi] \Big|_{\lim_{z \rightarrow 0} z^{\Delta-D} \phi(z, x) = \phi_{(0)}(x)}, \quad (84)$$

which implies that the logarithm of the generating functional of the boundary conformal field theory is identified with the (renormalized) supergravity action, evaluated at the boundary, for the corresponding bulk fields, subject to the appropriate asymptotic boundary conditions.

The map between the generating functionals on each side of the duality can be made more explicit, conform equation (81), by regarding [28, 86] the relationship between the correlation function of all composite conformal field operators  $O_i(x)$  and the generating functional  $Z_0[\phi^i]$  of all corresponding sources  $\phi^i(x)$  evaluated at the boundary,

$$\langle O_1(x_1) \dots O_n(x_n) \rangle = - \left[ \frac{1}{Z_0[\phi_{(0)}]} \frac{\delta^n Z_0[\phi_{(0)}]}{\delta \phi_{(0)}^1(x_1) \dots \delta \phi_{(0)}^n(x_n)} \right] \Big|_{\phi_{(0)}=0}. \quad (85)$$

Via this relationship, the AdS/CFT correspondence allows for an algorithmic [28] calculation of correlation functions of field operators  $O_i(x)$  in function of the fields  $\phi(z, x)$ .

In the algorithm [28], the bulk fields corresponding to the operators in correlation function are determined first. Then, via equation (84), the generating functional for the gravitational fields of interest is calculated. Finally the functional derivative with respect to the boundary values of these gravitational fields is taken in equation (85), the result is the correlation function of the conformal field operators. The following sections two applications [86] of this algorithm in action will be shown.

### 3.5.3 Linear Response Theory

By use of the AdS/CFT correspondence, it is possible [28, 64, 86, 104] to calculate the one-point correlation function  $\langle O(x) \rangle$  in the presence of a source  $\phi_0 \neq 0$ ,

$$\langle O(x) \rangle_{\phi_0} = \frac{\delta S_{SUGRA}[\phi]}{\delta \phi_0}. \quad (86)$$

*This is only valid for the on-shell action obtained via the equations of motion with the denoted boundary conditions.*

This expression can easily be rewritten in function of the gravitational fields

$$\langle O(x) \rangle_{\phi_0} = \lim_{z \rightarrow 0} z^{D-\Delta} \frac{\delta S_{SUGRA}[\phi]}{\delta \phi(z, x)}. \quad (87)$$

Taking inspiration from the Hamilton-Jacobi formalism [112–114] allows for the definition of the (renormalized) canonical momentum,

$$\Pi(z, x) = \frac{\delta S_{SUGRA}[\phi]}{\delta \dot{\phi}(z, x)}, \quad (88)$$

where the SUGRA action is on-shell and the derivative is taken with respect to the appropriate boundary conditions so that

$$\langle O(x) \rangle_{\phi_0} = \lim_{z \rightarrow 0} z^{D-\Delta} \Pi(z, x). \quad (89)$$

This one-point correlation function with a single source can be rewritten as an expansion [86], a power series to be more precise, in function of the source  $\phi_0$

$$\langle O(x) \rangle_{\phi_0} = \langle O(x) \rangle_{\phi_0=0} + \int d^D y \langle O(x) O(y) \rangle \phi_0(y) + \dots, \quad (90)$$

which after truncation, and a small change in notation, becomes

$$\langle O(x) \rangle_{\phi_0} = \langle O(x) \rangle_{\phi_0=0} + \int d^D y G(x, y) \phi_0(y). \quad (91)$$

For operators with a vacuum expectation value  $\langle O(x) \rangle_{\phi_0=0} = 0$  the above expression reduces to

$$\langle O(x) \rangle_{\phi_0} = \int d^D y G(x, y) \phi_0(y). \quad (92)$$

The one-point correlation function with source as defined here, measures [28, 86] fluctuations of the observables of the theory due to external perturbations. Due to the truncation earlier in this derivation, this expression is essentially a description of the linear response of the system. In momentum space the relationship between a one-point and the two-point correlation function simplifies, under the assumption that  $G(x, y)$  is translationally invariant, [86] to

$$\langle O(k) \rangle_{\phi_0} = G(k) \phi_0(k). \quad (93)$$

By virtue of the equations (76) and (89), reinterpreted in momentum space, the whole above expression can be written in function of gravitational quantities,

$$G(k) = \lim_{z \rightarrow 0} z^{2(D-\Delta)} \frac{\Pi(z, k)}{\phi(z, k)}. \quad (94)$$

### 3.5.4 Two-point Function for Scalar Fields

The machinery from linear response theory developed for AdS/CFT in the previous sections can be applied [28, 86] to a system with a source that is a scalar field  $\phi(z, x)$ . The (renormalized) canonical momentum [64, 86] for the relevant action of scalar field in AdS is

$$\Pi(z, x) = \eta \sqrt{|\det(g)|} g^{zz} \partial_z \phi(z, x), \quad (95)$$

where  $\eta$  is a nondescript normalization factor and where  $g^{\mu\nu} = \text{diag}(L/z, 1, 1, 1)$ , is the metric for Euclidean Poincaré patch of AdS. The (rather technical) result [86] of the linear response procedure applied on this setup, which is obtained via equation (94), is that the two point function in momentum space is given by

$$G(k) = (2\Delta - D)\eta L^{D-1} \frac{\Gamma(D/2 - \Delta)}{\Gamma(\Delta - D/2)} \left(\frac{k}{2}\right)^{2\Delta-D}. \quad (96)$$

In position space, this two-point correlation function reverts [86] to

$$G(x, 0) = \langle O(x)O(0) \rangle = \frac{(2\Delta - D)\eta L^{D-1}}{\pi^{\frac{D}{2}}} \frac{\Gamma(\Delta)}{\Gamma(-\Delta + D/2)} \frac{1}{|x|^{2\Delta}}. \quad (97)$$

In light of equation (83), this final expression shows that  $\Delta$ , as defined in equation (74), is indeed the scaling dimension of the operator  $O(x)$ . As expected, the  $UV$  sources that live at the conformal boundary match with the CFT operators there. So in the spirit of the condensed matter toy model, the radial direction and the physics in it, can be seen as emergent. This idea has been made significantly more concrete by the introduction of quantum information theory to the study of AdS/CFT. Before diving into the how and why of emergence, one more aspect of the AdS/CFT has to be examined, that of AdS-Rindler bulk reconstruction.

## 3.6 ADS-RINDLER BULK RECONSTRUCTION

Even though the AdS/CFT correspondence is generally a well-understood example of a theory of quantum gravity, some intriguing puzzles remain. One of the aspects of AdS/CFT that remains obscure is the emergence of approximate bulk locality [45]. The relationship between sources and operators, as discussed in the previous paragraphs, manifestly respects locality [45, 115] in the  $x$  directions because the conformal field theory does.

The story [45] of bulk locality in the emergent radial dimension  $z$  is, however, significantly more subtle than in the  $x$  directions. The properties of bulk locality in the  $z$  direction will turn out to be a crucial gateway to the later discussion on quantum information and holography. To understand bulk locality in the  $z$  direction it is important to know that, assuming all bulk interactions are suppressed, a bulk field  $\phi(z, x)$  can be represented on the CFT-side via

$$\phi(z, x) = \int dx K(z, x) O(x), \quad (98)$$

where the integral runs over the conformal boundary coordinates  $x$  and where the function  $K(z, x)$  is known as the "smearing function" [115–117]. An important comment is that the smearing function  $K(z, x)$  obeys the bulk wave equations [45] as would be expected from its  $z$ -dependence. Additionally, it is worth noting [45, 115, 116] that given this representation of  $\phi(z, x)$  in function of CFT operators, the boundary Hamiltonian can be utilized to rewrite all CFT operators in terms of a Heisenberg picture of a single CFT Cauchy surface.

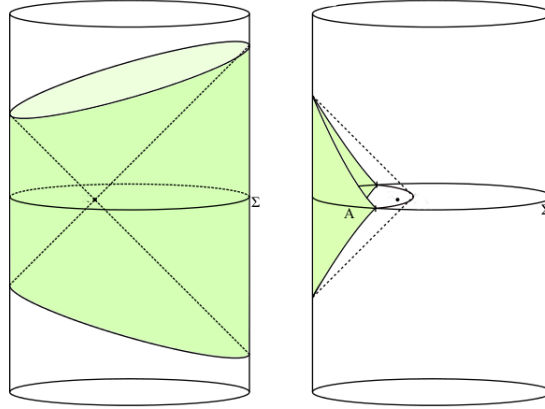


Figure 19: A graphical representation [45] of bulk reconstruction in global  $AdS_3$  (left) and in the AdS-Rindler wedge (right). The Cauchy surface  $\Sigma$  is indicated on the surface of the cylinder, i.e. the conformal boundary.  $D[A]$  is shaded green and  $\mathcal{W}_C[A]$  lies between the green area and the surface demarcated by the dashed lines. The location of the bulk operator is marked by a solid black point.

This approach does, however, have the unfortunate property [45] that when  $\phi(z, x)$  is taken close to the boundary (but not on it), the CFT representation still depends on operators with support on the whole of the Cauchy surface. It would be more natural to have a CFT representation whose support on the boundary falls off with the decrease of  $z$ . The AdS-Rindler representation fulfills this desire. [45].

To obtain the AdS-Rindler representation [45], consider a subsection  $A$  of the CFT Cauchy surface. The region of the boundary defined [45] so that inextensible causal curves that pass through this region also intersect with  $A$  is called the domain of dependence,  $D[A]$ . The intersection [39] of the bulk causal future and past of such a domain of dependence, i.e. the bulk within future and past horizon of the region, is known as the causal wedge  $\mathcal{W}_C[A]$  of the CFT boundary region  $A$ .

If the chosen CFT Cauchy surface is the  $t = 0$  slice of the boundary and if  $A$  is one hemisphere of this slice,  $\mathcal{W}_C[A]$  forms the so-called AdS-Rindler wedge [45]. To obtain a smaller region  $A$ , conformal transformations must be used. This situation is shown in figure 19. Using the metric of this AdS-Rindler wedge, the

*Causal curves  
have tangent  
vectors which are  
never space-like.*

CFT representations of bulk fields can be fully implemented [116] within the causal wedge, showing local boundary dependency. The only real subtlety [45] involved in this is that the smearing function  $K(z, x)$  no longer classifies as a function and must be treated as a distribution against conformal field theory expectation values [118, 119].

### 3.7 CONCLUSION

In this chapter, the conjecture of an AdS/CFT correspondence was studied as an explicit realization of the holographic principle. By looking at two different perspectives on  $D3$ -branes, where one yielded ten-dimensional supergravity and one provided a four-dimensional supersymmetric conformal field theory, the conjectured AdS/CFT correspondence was concretely motivated. The large  $N$  expansion of 't Hooft, was also discussed to provide a better understanding of the parameter region in which the strong version of the correspondence is proposed to be valid.

The second half of this chapter focused on how (scalar) fields in AdS act as sources for the CFT operators. Using functional techniques from quantum field theory, the exact relationship between boundary physics and asymptotic bulk behavior was examined. At the end, a discussion on the AdS-Rindler representation of bulk physics was provided. In addition to being another fascinating aspect of the duality, the AdS-Rindler reconstruction will turn out to be central to questions regarding locality in AdS/CFT. In the next chapter, this question will be re-interpreted in the language of quantum-error correcting protocols, transitioning this dissertation into the study of quantum information theory and its connection to holography.



# 4

## INCORPORATING QUANTUM INFORMATION

---

### 4.1 INTRODUCTION

Recently, it has been shown that quantum information is a tool useful [36–39, 41, 43, 46] for high-energy theoretical physics, especially holography. Even though the theory of quantum information [34] has a long and rich history, the treatment of the subject in dissertation will focus solely on its applications in AdS/CFT. Specifically, problems in the context of AdS-Rindler reconstruction, which turn out to be sensitive to description by certain quantum error correcting protocols, will be studied.

Quantum information is, in itself, a worthy research topic but here a pick-and-choose approach to its contents will be used. It would however be a disservice to the reader not to briefly mention the history and main concepts of classical information theory. In 1948, Claude Shannon wrote a seminal paper called "A Mathematical Theory of Communication" [31] which kick-started the study and use of mathematics in communication. Nowadays this field of study, or what it has grow into, is known as information theory [120–122].

Shannon's own concept of "information" [31, 122] consisted of a set of possible messages, send over a noisy communication channel, with as goal to have the receiving party reconstruct the messages with a known (or at least upper-bound) error-probability. To make this all quantifiable, he defined [31, 122] the "bit", the basic element of information, as a (classical) state being either zero (0) or one (1). He also refined [31, 34, 122] the idea of informational entropy  $H$ ,

$$H = - \sum_i p_i \log_2(p_i), \quad (99)$$

where  $p_i$  is the probability of one of the messages of the set being send. This definition is remarkably similar [31, 122, 124, 125] to the Gibbs-Boltzmann entropy  $S$  of statistical mechanics [2],

$$S = -k_B \sum_i p_i \ln(p_i), \quad (100)$$

where  $p_i$  is the probability of a micro-state choice from an ensemble. The conversion between the two formula is of the form [2, 31, 122],

$$S = k_B \ln(2) N h, \quad (101)$$

where  $N$  is the number of micro-states and where  $h$  is the intensive equivalent to the quantum informational entropy  $H$ . Landauer's principle [123–125], which has

*Landauer's principle [123] provides a theoretical lower limit on the energy consumption of a computation.*

been confirmed experimentally [126, 127] up to the individual bit [128] of data, further supports the link between information theory and thermodynamics.

The discussion on black hole entropy [3, 4] in the introduction of this dissertation already implicitly combined thermodynamics and information theory. In light of the concrete link between micro-states and informational entropy as discussed here, the origin story of the holographic principle in black hole thermodynamics advocates (adamantly) that (quantum) information theory is relevant to holography. In AdS/CFT this suspicion can be made concrete via the Ryu-Takayanagi formula [33, 129]. Before discussing this formula however, a few quantum information concepts have to be summarized.

#### 4.2 QUANTUM INFORMATION THEORY

The simplest of quantum information systems is the quantum bit [34, 130] or "qubit". A qubit is a two-level quantum system, e.g. the spin of an electron [131], which generally [34] is in an arbitrary superposition of the states of the bit, defined by  $0 \rightarrow |0\rangle$  and  $1 \rightarrow |1\rangle$ . Even though the physical realization of these kinds of systems is highly interesting [131, 132], this chapter will focus on the conceptual aspects. The  $d$ -level generalization of qubit [34, 130] is known as the "qudit" and in this dissertation a lot of attention will be given to the  $d = 3$  version, the "qutrit".

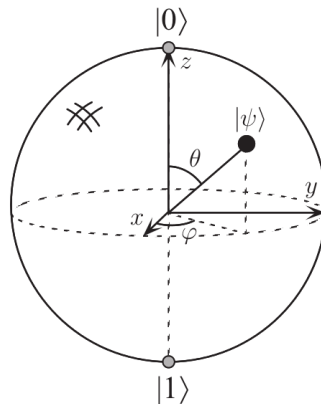


Figure 20: A graphical representation [34] of a Bloch sphere. This sphere geometrically represents the pure state space of a two-level quantum system, i.e. a qubit. The sphere has a unit radius and antipodal points correspond to orthogonal states. The basisvectors  $|0\rangle$  and  $|1\rangle$  are shown. A generic pure state in this system is easily written [34] as  $|\psi\rangle = \cos(\theta)|0\rangle + e^{i\varphi}\sin(\theta)|1\rangle$  as shown on the figure.

Going back to the original question that Shannon asked himself, i.e. how can information be communicated correctly, and placing it in a quantum mechanical setting, yields the following situation [31, 34, 122]. Alice and Bob, the archetypal

fictional characters [133, 134] in (quantum) information theory, want to communicate with each other using qutrits. Specifically, Alice wants to send Bob a message  $k$  qutrits long, but she is worried that some might get lost or altered on the way to Bob.

#### 4.2.1 Quantum Error Correction

To soothe Alice's worries, she and Bob may apply quantum error correcting protocols [34, 44, 122] to their communication. For instance, Alice can embed her  $k$  qutrits message into more than  $k$  qutrits, in a specific way so that even if some qutrits are lost or altered, Bob can still recover them. For later purposes in holography [45, 46, 57], it is sufficient to describe a system that only corrects for erasures of qutrits, not for their alteration. Say that Alice wants to send a message in the form of a state,

$$|\psi\rangle = \sum_{i=0}^2 a_i |i\rangle , \quad (102)$$

where  $|i\rangle \in |0\rangle, |1\rangle, |2\rangle$  and  $a_i \in \mathbb{C}$ . Then the idea of quantum error correction is to use a different state with more qutrits than the original one. For example [45], take the new state

$$|\bar{\psi}\rangle = \sum_{i=0}^2 a_i |\bar{i}\rangle , \quad (103)$$

which encrypts the original message with some redundancy. The states  $|\bar{i}\rangle$  are

$$|\bar{0}\rangle = \frac{1}{\sqrt{3}} (|000\rangle + |111\rangle + |222\rangle) , \quad (104)$$

$$|\bar{1}\rangle = \frac{1}{\sqrt{3}} (|012\rangle + |201\rangle + |120\rangle) , \quad (105)$$

$$|\bar{2}\rangle = \frac{1}{\sqrt{3}} (|021\rangle + |102\rangle + |210\rangle) . \quad (106)$$

and are chosen [45, 57] so that no single qutrit contains enough information to reconstruct the state  $|\bar{\psi}\rangle$ . More importantly, any two of these qutrits suffice for Bob to fully reconstruct the state. Assume, for example, that Bob only received the first two qutrits. Then he can make use of the existence [45, 137] of a unitary transformation  $U_{12}$  on those two first qutrits, that implements

$$(U_{12} \otimes I_3) |\bar{i}\rangle = |i\rangle \otimes \frac{1}{\sqrt{3}} (|00\rangle + |11\rangle + |22\rangle) , \quad (107)$$

where indices on operators indicate on which qutrit that operator acts. It is then obvious that this operator allows Bob to recover the original state (or message)  $|\psi\rangle$ , by

$$(U_{12} \otimes I_3) |\bar{\psi}\rangle = |\psi\rangle \otimes \frac{1}{\sqrt{3}} (|00\rangle + |11\rangle + |22\rangle) . \quad (108)$$

*On a practical level, quantum error correction protocols can be implemented via quantum circuits [34] and syndrome measurements [135] so that the no-cloning theorem [136] is not an issue.*

A similar protocol is also possible [45] if Bob can only access the second and third qutrits, or the first and third qutrit. Thus the communication between Alice and Bob is protected against the loss, also known as erasure, of any single qutrit.

In quantum information science, the subspace defined in equations (104), (105) and (106) is called the code subspace [45, 57]. From more advanced arguments [34, 45, 135, 137], it is known that the states in such a code subspace have to be entangled. This is not surprising, as reconstructing a state requires some information of that state to be available to the states used in the reconstruction.

#### 4.2.2 Density Matrices, Entanglement and Entropy

To define entanglement [34], the sharing of quantum information within a system, in a strict mathematical sense, consider two non-interacting (sub)systems  $A$  and  $B$ , held respectively by Alice and Bob, with Hilbert spaces  $H_A$  and  $H_B$ . Also consider a composite Hilbert space  $H = H_A \otimes H_B$ . Then regard, for instance, the state [138, 139]

$$|\varphi\rangle = \frac{1}{\sqrt{2}} (|0\rangle_A |1\rangle_B - |1\rangle_A |0\rangle_B) \doteq \frac{1}{\sqrt{2}} (|01\rangle - |10\rangle), \quad (109)$$

and notice that there is no way to rewrite it as a product state of pure states from either  $H_A$  or  $H_B$ . Neither Alice nor Bob has the full information of the system. Therefore, the composite system can only be described as a whole and its constituents are (what is known as) entangled.

Recall from the introduction that this kind of states [26, 30, 48] can be described by a density matrix  $\rho = |\varphi\rangle \langle \varphi|$ , which in this case is

$$\rho = \frac{1}{2} (|01\rangle \langle 01| - |01\rangle \langle 10| - |10\rangle \langle 01| + |10\rangle \langle 10|). \quad (110)$$

*In this kind of calculation,  
0 log(0) = 0 is  
typically assumed  
implicitly.*

The density matrix allows for the calculation [34] of the Von Neumann entropy,

$$S = -\text{tr}(\rho \ln(\rho)) = -\sum_i \lambda_i \ln(\lambda_i) = 0, \quad (111)$$

where  $\lambda_i$  are the eigenvalues of the density matrix and where the trace is taken over the whole system. The reduced density matrix [48] for the  $A$  subsystem,  $\rho_A$  is

$$\rho_A \doteq \text{tr}_B(\rho) = \frac{1}{2} (|0\rangle_A \langle 0|_A + |1\rangle_A \langle 1|_A), \quad (112)$$

where the trace is over the subsystem  $B$  and the corresponding Von Neumann entropy is

$$S_A = -\text{tr}(\rho_A \ln(\rho_A)) = -\ln\left(\frac{1}{2}\right) = \ln(2). \quad (113)$$

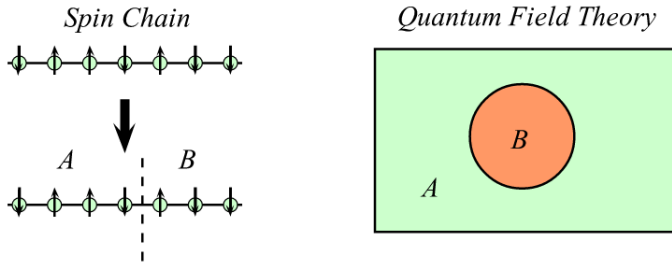


Figure 21: A graphical representation [129] of two of the situations where entanglement entropy can be calculated. Both systems, the spin-chain and the quantum field theory, are separated into two spatial regions  $A$  and  $B$ . A spin chain consists of a series interacting quantum states, called spins. At least conceptually, each spin can be considered to be a qudit.

So for the composite system the state  $|\varphi\rangle$  is pure but for its constituent subsystems, the state is not pure. This means that the systems  $A$  and  $B$  are entangled with one another.

The entanglement entropy [34], which measures the entanglement between these two subsystems is exactly defined as the Von Neumann entropy of the reduced density matrix as calculated above. In the holography community, the expression "entanglement entropy" is typically reserved for subsystems that are spatially separated but one could in principle think of more general kinds of separation. The holography community has an interest in these properties because in the AdS/CFT correspondence both quantum error correction and entanglement entropy show up in a surprisingly natural fashion.

#### 4.3 HOLOGRAPHIC QUANTUM ERROR CORRECTION

In the previous chapter, the AdS-Rindler reconstruction of bulk fields was discussed. To obtain local support of bulk fields in terms of conformal boundary operators, causal wedges were introduced. One peculiar property of this method is that a bulk field (operator)  $\phi(z, x)$  lies in several different causal wedges, and can thus be represented, via the smearing function, on more than one distinct boundary region. The existence of these overlapping wedges has some rather non-trivial consequences that can be linked to quantum information theory.

Consider for instance, a situation [45] with two overlapping wedges  $W_C[A]$  and  $W_C[B]$ , as shown in figure 22, which both contain the point  $(z, x)$ . For an operator at that point to have support on  $A$  and on  $B$  it must really only have support on  $A \cap B$  but the point  $(z, x)$  does not (necessarily) lie in  $W_C[A \cap B]$  and so the operator cannot be reconstructed from that boundary region. The solution to this conundrum is simple, it turns out [45, 57] that the representations of  $\phi(z, x)$  in different wedges are not the same CFT operator.

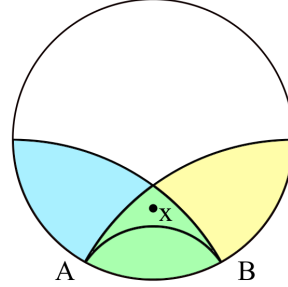


Figure 22: A graphical representation [45] of the situation with two overlapping causal wedges on an  $\text{AdS}_3$  time-slice. The operator can be reconstructed in  $A$  and in  $B$  but not in  $A \cap B$ . This is paradoxical.

#### 4.3.1 Non-equivalent Representations

This difference in the CFT representations of bulk fields is even more clear in a situation [45] where a bulk field  $\phi(z, x)$  lies outside the causal wedges  $W_C[A]$ ,  $W_C[B]$  and  $W_C[C]$  as is shown in figure 23. The bulk field can be reconstructed, from any one of the regions  $A \cup B$ ,  $B \cup C$  and  $A \cup C$  but not from  $A$ ,  $B$  or  $C$  individually. These regions  $A \cup B$ ,  $B \cup C$  and  $A \cup C$  have a mutual intersection of three single points, but by including infinitesimally displaced copies of these region, a set of six possible reconstructions regions whose mutual intersection is completely empty, can be formed. There is manifestly no way in which the bulk field can yield the same operator representation in all these regions.

This situation can be understood from the quantum error correcting code [34, 135] that was discussed in the previous section if it is rephrased in the language of operators rather than that of the recovery of messages. To see this, define [45, 57] an operator  $Q$  that acts on single qutrits as

$$Q |i\rangle = \sum_j Q_{ji} |j\rangle . \quad (114)$$

For such an operator  $Q$ , there exist three-qutrit operators  $\bar{Q}$ , called logical operations [135, 137] which implement the same action as  $Q$ , on the code subspace, i.e.

$$\bar{Q} |\bar{i}\rangle = \sum_j Q_{ji} |\bar{j}\rangle . \quad (115)$$

For the three-qutrit code subspace discussed here [45], it can be seen that

$$Q_{12} \doteq U_{12}^\dagger Q U_{12}, \quad (116)$$

where  $Q$ , which only acts on the first qutrit according to equation (114), operates as

$$Q_{12} |\bar{i}\rangle = \sum_j Q_{ji} |\bar{j}\rangle . \quad (117)$$

This last equation implies that  $Q_{12}$  is a logical operation with support limited to the first two qutrits. Likewise  $Q_{23}$  and  $Q_{13}$  can be constructed [45] so that a set of operators with non-trivial and varying support over the three different qutrits is formed. Notice that these different operators have the same effect on the code subspace. This situation is evocatively similar to overlapping wedges in the AdS-Rindler bulk reconstruction.

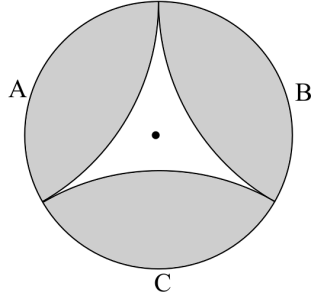


Figure 23: A graphical representation [45] of the situation with three causal wedges. The operator can only be reconstructed in any non-trivial union of  $A$ ,  $B$  and  $C$ . This indicates that the reconstruction is different in each disjunct region. The black dot denotes the point  $(z, x)$ .

In AdS-Rindler reconstruction [45, 115, 116] the field in the center of figure 23, can be represented either as an operator with support on  $A \cup B$ , an operator with support on  $B \cup C$  or an operator with support on  $C \cup A$ . Obviously, this is comparable to the situation with  $Q_{12}$ ,  $Q_{23}$  and  $Q_{13}$ . It has been proposed [45, 46] that quantum error correction properties like these are integral to bulk emergence from the boundary theory.

For instance [45, 57], local bulk fields can be seen as logical operators on a code subspace, which becomes increasingly protected against boundary erasure as the bulk field moves away from the boundary. The code subspace [45] itself is found by applying local bulk fields, as represented on the CFT via the global reconstruction, onto the vacuum state. Any causal wedge  $W_C[A]$  contains exactly [45] those local bulk fields that are needed to form the code subspace that protects against erasure of the complement of  $A$ .

Every time the code subspace is made bigger, i.e. each time a local bulk field is applied to the vacuum state, the energy of the new state increases [45]. At some point, the approximation of a fixed background geometry breaks down [45, 90, 140] and the whole discussion on quantum error correcting properties as presented here, becomes void. In essence, this means [45, 57] that the different CFT operators only need to have the same action on a low energy subspace which explains the peculiar behavior of the AdS-Rindler reconstruction.

#### 4.4 RYU-TAKAYANAGI: ENTROPY FOR A HOLOGRAPHIC UNIVERSE

In addition to quantum error-correcting protocols, an other element of quantum information theory, entanglement entropy, can also be interpreted in holography. Think about the Bekenstein-Hawking entropy formula for a black hole [3, 4] once more,

$$S = \frac{A_{BH}}{4G_N}. \quad (118)$$

Here, it can be seen that all information inside the black hole "lives" on the surface of its boundary. The question remains however, how and even if this kind of holographic statement about thermodynamical entropy can be related to entanglement entropy. On a conceptual level, entanglement entropy measures the how much information about a system can be obtained if a part of the system is inaccessible, just as [33, 141] the inside of a black hole is unavailable for an outside observer. It is hence not entirely unthinkable that these two descriptions of entropy show up together in AdS/CFT. In early and groundbreaking work, Shinsei Ryu and Tadashi Takayanagi [33] developed a relationship between entanglement entropy of the boundary CFT and an area-term in the bulk of AdS, inspired by this similarity between entanglement entropy and thermodynamical entropy. Specifically, they proposed that the entanglement entropy  $S$  of a part  $A$  of the boundary CFT can be calculated (to first order) by

$$S[A] = \frac{\text{Area}(\gamma_A)}{4G_N}, \quad (119)$$

where  $\gamma_A$  is the minimal surface in AdS, spanned up by the edges of the CFT region  $A$ .

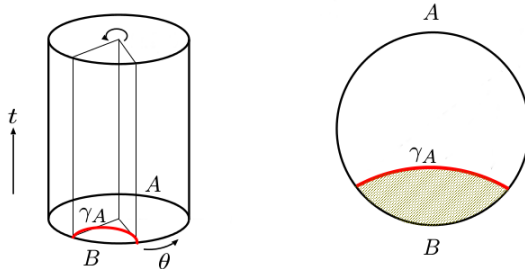


Figure 24: Two graphical representations [33] of the holographic calculation of entanglement entropy on the boundary in the AdS/CFT correspondence. It has been proposed [142] that bulk operators in the bulk spacetime inside  $\gamma_A$  can be reconstructed on  $A$ .

##### 4.4.1 Validity in $\text{AdS}_3/\text{CFT}_2$

Because the Ryu-Takayanagi formula will be central to the rest of this dissertation, its validity in the  $\text{AdS}_3/\text{CFT}_2$  case is checked here, at least qualitatively.

To do this, the calculation of the area of the minimal surface is compared to conformal field theory results. According to the Brown-Henneaux relationship [143], an early predecessor of AdS/CFT, the central charge  $c$  of the CFT<sub>2</sub> is

$$c = \frac{3R_{AdS}}{2G}. \quad (120)$$

For a two-dimensional CFT living on an infinitely long line, the entanglement entropy of subsystem A of length  $L$  is given [104] by

$$S[A] = \frac{c}{3} \log \left( \frac{L}{a} \right), \quad (121)$$

where  $a$  is a UV cut-off (recall the lattice spacing of the previous chapter) that deals with the ever-present UV divergence of entanglement entropy in a quantum field theory. In the Poincaré patch of empty AdS<sub>3</sub>, the geodesic equation [90] can be used [104, 144] to prove that  $\gamma_A$  is parametrized by

$$(z, x) = \frac{R_{AdS}}{2} (\sin(s), \cos(s)) \quad \text{with} \quad \epsilon < s < \pi - \epsilon, \quad (122)$$

where  $\epsilon = 2a/L$  incorporates the CFT UV cut-off into the calculation. The area of  $\gamma_A$ , which in this dimensionality is nothing more than a length, is given by

$$\text{Area}(\gamma_A) = 2R_{AdS} \int_{\epsilon}^{\pi/2} \frac{ds}{\sin(s)} = \left[ -\log \left( \cot \left( \frac{s}{2} \right) \right) \right]_{\epsilon}^{\pi/2} = 2R_{AdS} \log \left( \frac{L}{a} \right), \quad (123)$$

up to first order [104]. Using the Brown-Henneaux relationship, equation (120), in equation (121) then shows that the Ryu-Takayanagi formula is valid in AdS<sub>3</sub>/CFT<sub>2</sub>.

#### 4.4.2 Higher Dimensions, Heuristically

Extension to other dimensionalities and spacetimes is possible [33, 129, 141] but in general, direct proofs of Ryu-Takayanagi are limited by the need to calculate entanglement entropy in strongly coupled CFT's. A heuristic approach is possible [104, 141, 144] and will be briefly discussed here, but first, a bit more background on entanglement entropy calculations using euclidean path integrals has to be provided.

The calculation of the entanglement entropy in a two-dimensional CFT, like the one on the conformal boundary of AdS<sub>3</sub>, is most conveniently achieved using the so-called replica trick [104, 144]. The replica trick consists of formal differentiation [43, 104, 141] with respect to an integer  $n$ ,

$$S[A] = -\text{tr}_A (\rho_A \ln(\rho_A)) = \lim_{n \rightarrow 1} \frac{1}{1-n} \ln (\text{tr}_A (\rho_A^n)) = -\frac{\partial}{\partial n} [\text{tr}_A (\rho_A^n)] |_{n=1}. \quad (124)$$

In the Euclidean path integral formalism, the terms  $\text{Tr}(\rho_A^n)$  (a.k.a. Rényi entropies) can be calculated by integrating over  $n$  replicas of the two-dimensional CFT. The ground state wave-functional of the CFT is defined by [104],

$$|\varrho[\phi_0(x)]\rangle = \int_{t=-\infty}^{t=0} \mathcal{D}\phi e^{-S} |_{\phi(t=0,x)=\phi_0(x)} . \quad (125)$$

where  $\phi(t, x)$  is the field that defines the the 2D CFT. The corresponding bra,  $\langle \varrho[\phi'_0(x)] |$ , is found by integrating over the CFT from  $t = +\infty$  to  $t = 0$ . The boundary conditions  $\phi_0(x)$  and  $\phi'_0(x)$  depend on  $x$  and here,  $\phi_0(x)$  is the value of the CFT fields at  $t = 0$  as observed from  $t = \infty$  and  $\phi'_0(x)$  is the value of the fields at  $t = 0$  as seen from  $t = -\infty$ .

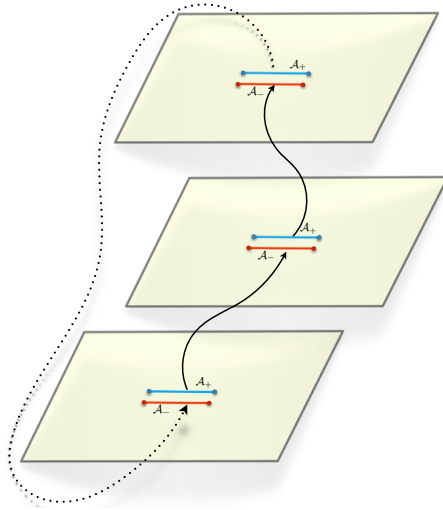


Figure 25: A graphical representation from Rangamani and Takayanagi's upcoming book on "Holographic Entanglement Entropy" [141]. This visualization show how to calculate the entanglement entropy of a region  $A$  of a two-dimensional CFT in Euclidean signature. The region  $A$  has different boundary conditions at the top and at the bottom. Here, these are indicated here by  $A^+$  and  $A^-$ . Each time an integral passes through a side of the  $A$  region, it goes to another sheet of the Riemann surface.

The reduced density matrix  $\rho_A(\phi_0(x), \phi'_0(x))$  is obtained [141, 144] by putting  $\phi'_0(x) = \phi_0(x)$  outside the region  $A$ , and integrating, i.e. taking the trace, over the CFT with boundary condition  $\phi_1(x)$  just above the region  $A$ , and  $\phi_2(x)$  just below it. This situation is shown on each of the sheets of figure 25. The trick [104, 141] to calculate the Rényi entropies  $\text{tr}_A(\rho_A^n)$ , is then to see that this expression is obtained by integrating described above, but with  $n$  copies of the CFT cyclically linked to one-another at the boundary conditions. The resulting geometry, an  $n$ -sheeted Riemann surface, is shown in figure 25.

The situation created here is thus essentially [43, 141, 144] that of an  $n$ -sheeted Euclidean Riemann surface where the different boundary conditions let the path integral cycle through the different sheets of the manifold. For a two-dimensional

CFT, it has been shown that this approach does indeed give the Rényi entropies and it is generally expected to work for higher dimensions. According to the AdS/CFT correspondence, and as mentioned before, there is an equivalence [28, 86, 104, 144] between the generating functionals of the CFT and the (super)gravity theory.

Similarly [104, 144], the path integral that calculates  $\text{tr}_A(\rho_A^n)$  should be equal to the generating path integral for the gravity theory with a boundary geometry equal to the multi-sheeted Riemann surface of the replica trick. In general, this calculation is highly non-trivial [104, 144, 145] but it has been shown [144, 146] that, in the  $n \rightarrow 1$  limit at which  $\text{tr}_A(\rho_A^n)$  is evaluated, equation (124) reduces to the area of an extremal surface in the original AdS spacetime. This proves, at least heuristically, the validity of Ryu-Takayanagi in higher dimensions.

#### 4.5 HOLOGRAPHIC TENSOR NETWORKS

To advance the study of numerical simulations of emergence in strongly-interacting situations, condensed matter physicists [55, 56, 147] developed computationally efficient representations of the entanglement structures of quantum many-body systems. These representations, called tensor networks [57, 147], are typically hierarchical arrays, or other data structures, with tailor-made algorithms defined on them. This dissertation will make extensive use of these quantum informational research tools because they provide a tangible model of holographic emergence of gravity in AdS/CFT.

Recall from the lattice toy model in the previous chapter, that some kind of renormalization flow was needed to describe how the variables of the coarse-grained model scaled with the lattice distance. To obtain a computationally efficient renormalization flow for quantum systems, entanglement renormalization [148–150] was invented. The key idea [58, 148–150] in entanglement renormalization is that the removal of local entanglement is essential to describe certain approximations of ground-state wave-functions of quantum many-body systems.

The two ideas described above, tensor networks and entanglement renormalization, were combined to formulate [148–152] the Multiscale Entanglement Renormalization Ansatz (MERA). MERA is a set of tensor networks, built to model long-range entanglement in certain scale-invariant ground states while aiming to efficiently approximate the corresponding wave functions. The main idea behind MERA [58, 148–150] is to leverage hierarchical structure of the tensor network to represent entanglement at different length scales, as shown in figure 26.

It has been pointed out [58] that a MERA network resembles the emergence of gravity in AdS/CFT, at the very least on a superficial level. Here the set-up would be that the quantum entanglement in the boundary theory acts as the input for the network which would then reproduce some of the physics in the emergent direction. The question then is whether concrete tensor network models can be found that reproduce holography in a meaningful way.

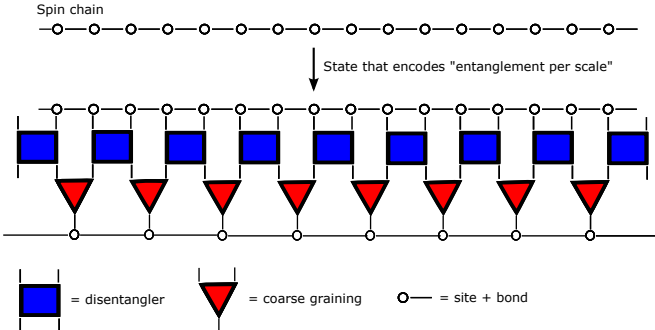


Figure 26: A graphical representation [58] of MERA. Without going into technical detail, it can be remarked [58] that the disentanglers, a (unitary) type of tensors shown as blue squares, are used to remove local entropy. The red triangles are coarse-grainers, isometric tensors, that compress the unentangled degrees of the ground state. In this picture the ground state is a spin chain.

#### 4.5.1 Perfect Tensors

What a good tensor network model for holography should be able to do is a matter of debate and a large number of different proposals [57–59, 61, 62, 153, 154] exist. In this dissertation, the so-called HaPPY tensor networks [57] will be studied. Next to being exactly solvable these tensor networks have the upside of being uniform in the bulk: each HaPPY tensor network is structured upon a uniform hyperbolic tiling, known as a hyperbolic tessellation [57, 62], which incorporates the hyperbolic nature of an AdS-slice. An important remark here is that a single hyperbolic tile is of approximately AdS-radius size.

The building block of a HaPPY tensor network is the perfect tensor [57, 154], a special case of the isometric tensor. To define [57] the isometric tensor, take two Hilbert spaces  $H_A$  and  $H_B$  (with  $\dim(H_A) \leq \dim(H_B)$ ) and isometric mapping  $T$  between them. The map  $T$  can be written as a two-index tensor according to

$$T : |a\rangle \rightarrow \sum_b |b\rangle T_{ba}, \quad (126)$$

where  $\{|a\rangle\}$  and  $\{|b\rangle\}$  are the complete orthonormal basis for  $H_A$  and  $H_B$  respectively. Because the map  $T$  is isometric,

$$\sum_b T_{a'b}^\dagger T_{ba} = \delta_{a'a}. \quad (127)$$

A tensor  $T_{ab}$  with this property, is known as an isometric tensor. Perfect tensors, themselves, are defined [57] as even-indexed tensors that are (proportional to) an isometric tensor from a set of its indices to the complementary set indices as long as the complementary set is not smaller than the initial set.

Isometric, and thus perfect, tensors have the property [57] that an operator  $O$  acting on a tensor leg related to  $H_A$ , can be replaced by an operator  $O'$  acting on a tensor leg that is related to  $H_B$ . These two legs are known as the incoming

$$\begin{array}{c}
 \boxed{O} \quad \boxed{T} \quad = \quad \boxed{T} \quad \boxed{O'} \\
 \boxed{O'} \quad \equiv \quad \boxed{T^\dagger} \quad \boxed{O} \quad \boxed{T}
 \end{array}$$

Figure 27: A graphical representation [57] of the crucial property of an isometric tensor: the "pushing of an operator". This property, explained in equation (128), will allow for an implementation of the HaPPY tensor network code.

and the outgoing leg. This operation is known as "pushing an operator through a tensor". The proof of this property is straightforward,

$$TO = TOT^\dagger T = (TOT^\dagger)T \doteq O'T. \quad (128)$$

#### 4.5.2 HaPPY Tensor Networks

A network of perfect tensors can be used [57] to describe a pure state of a set of maximally entangled degrees of freedom. It can also be used as an encoding map of a quantum error correcting code. These two approaches will be used to construct two different HaPPY tensors networks, one that acts as a code and models the quantum error correcting properties [45] of holographic emergence and one that forms a state and carries an algorithmic version of the Ryu-Takayanagi formula [33].

*HaPPY [57] is a peculiar acronym of the names: Harlow, Pastawski, Preskill and Yoshida.*

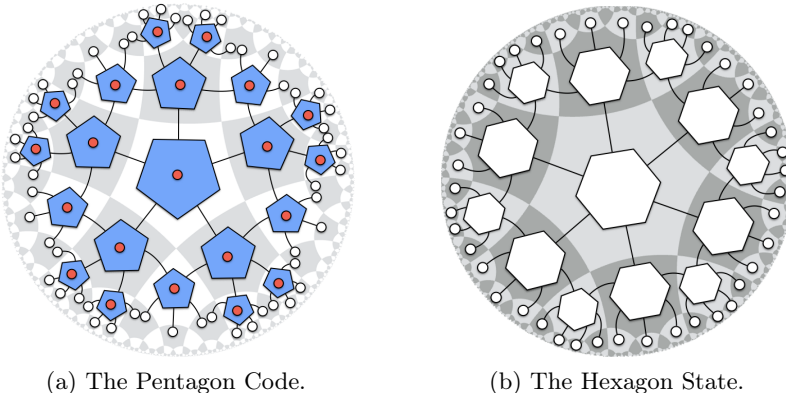


Figure 28: Graphical representations [57] of the HaPPY tensor networks. In the background the tessellation of the two-dimensional hyperbolic space that is an  $\text{AdS}_3$  time-slice is shown. In both the code and the state each single tile, which is of  $\text{AdS}$ -radius size, contains exactly one tensor. The pentagon code has a free bulk leg at each tensor, shown by a red dot.

For a tensor network with quantum error correcting properties [45, 57], consider a uniform tiling of an  $\text{AdS}_3$  time-slice by pentagons, as can be seen in figure 28a. Then place a perfect tensor with six legs at the center of each pentagon so that

the legs are connected to (exactly) the middle of the sides of each pentagon. In this set-up, each tensor has one open leg in the bulk, the other five are contracted with legs of neighboring tensors. The degrees of freedom of the free legs, i.e. those at the boundary and the uncontracted bulk legs, are identified [57, 58] with spins. The boundary can thus be seen as a complicated spin chain.

Each of the tensors in this tessellation [62], acts as a linear and isometric map encoding the information of one bulk spin into the five spins or contracted legs. This way, a quantum error correcting code can be formed. Because each bulk spin is encoded into the remaining block of five legs (contracted or not), it is protected [57, 135] against the erasure of any two spins related to those five legs of that tensor. The AdS-Rindler reconstruction can be achieved [45, 57] here, by pushing any local bulk operator to the boundary, via equation (128). Once more, this kind of reconstruction on the boundary is not unique.

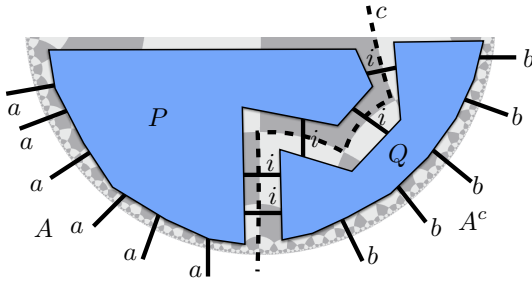


Figure 29: A graphical representation [57] of the cut  $c$  and accompanying decomposition into two tensors,  $P$  and  $Q$ . The boundary legs  $a$  and  $b$  determine the degrees of freedom in the region  $A$  and the complementary region  $A^c$ . The  $i$ 's indicate the legs that are cut.

To obtain a tensor network which can carry a discrete version of Ryu-Takayanagi [33, 57], the two-dimensional AdS-slice is tessellated with hexagons and six-legged perfect tensors are placed at the center of each hexagon. In this set-up, all internal legs of the perfect tensors are contracted with the neighboring tensors at (exactly) the middle of the edges of the hexagons and no free bulk legs remain. The collection of spins at the outer-edge forms a state, which is known [57] as the holographic hexagon state.

Because HAPPY tensor networks [57] are defined upon two-dimensional slices of AdS, the area of  $\gamma_A$  is just a length. The validity of the Ryu-Takayanagi formula has been discussed explicitly in this dimensionality, earlier in this chapter. In the discrete setting of tensor networks [57], this length is interpreted as the number of contracted legs that are "cut" by  $\gamma_A$ . Due to this cut, the tensor network can be deconstructed into two large tensors,  $P$  and  $Q$  as shown in figure (29).

The two tensors are contracted along the cut  $c$ ; the number of legs contracted between them, denoted as  $|c|$ , is the formal definition [57] of the length of the cut. If the cut is the Ryu-Takayanagi geodesic  $\gamma_A$ , then the connected boundary region  $A$  of the hexagonal tensor network can be identified as the set of boundary legs of  $P$ . The other set of boundary legs then forms the complementary region

of  $A$ . Due to this decomposition [57] into  $P$  and  $Q$ , the holographic state  $|\psi\rangle$  defined by the hexagonal HaPPY tensor network may be re-expressed as

$$|\psi\rangle = \sum_{a,b,i} |ab\rangle P_{ai} Q_{bi} \doteq \sum_i |P_i\rangle_A \otimes |Q_i\rangle_{A^c}, \quad (129)$$

where  $a$  and  $b$  run, respectively, over the entire bases for  $A$  and  $A^c$ , and where  $i$  can take all possible values of the legs that were cut by  $c$ . The corresponding density matrix on  $A$  is thus given [34, 57] by

$$\rho_A = \sum_{i,i'} \langle Q_{i'} | Q_i \rangle |P_i\rangle \langle P_{i'}|. \quad (130)$$

The rank of  $\rho_A$  is no more than the number of terms that the sum over  $i$  contains. Now, it is also known [34, 57] that density matrices of maximally entangled systems, like the Bell pair in equation (109), are proportional to the identity and have an entanglement entropy equal to the log of its rank, so that an upper bound on the entanglement entropy can be given by

$$S[A] \leq \log(v)|c|, \quad (131)$$

where  $v$  is the number of values each individual index, i.e. a tensor leg, can take and where  $c$  is used to obtain the lowest of upper bounds. In general, it is not necessary nor certain that  $|P_i\rangle$  and  $|Q_i\rangle$  are orthogonal sets. However, if the tensors  $P$  and  $Q$  are isometric tensors from  $i$  to  $a$  and  $b$  respectively, then  $P$  and  $Q$  form a maximally entangled state and the above formula, equation 131, reverts to an equality, i.e.

$$S[A] = \log(v)|c|, \quad (132)$$

which would be a discrete lattice version of the Ryu-Takayanagi formula up to normalization. The remaining question is whether or not the tensors  $P$  and  $Q$  in the hexagonal HaPPY tensor network are indeed isometric. It turns out [57] that for a non-positively curved, simply-connected planar tensor network of perfect tensors it can be shown, using graph theory and quantum circuit techniques [57, 155, 156], that  $P$  and  $Q$  are isometric. The discrete Ryu-Takayanagi formula, equation (132), is thus valid [33, 57] for the hexagonal HaPPY tensor network.

#### 4.5.3 The Greedy Algorithm

The axiomatization of the discrete Ryu-Takayanagi formula [33, 57] can be expanded even further on the hexagonal tensor network. An algorithm [57, 155, 156] has been devised that determines a discrete geodesic,  $\gamma_A^*$ , called the greedy geodesic, that fulfills the role of  $\gamma_A$  up to the resolution of the tensor network. The only input of the algorithm, which is fittingly called the greedy algorithm [57, 157, 158], is the boundary region  $A$  of interest. The algorithm starts from the region  $A$  and

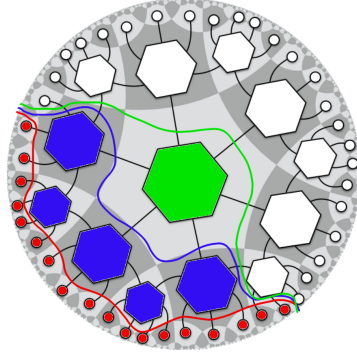


Figure 30: An adapted graphical representation [57] of the greedy algorithm in action. The first layer, shown in red, is nothing more than the given boundary region. The second and third layer, shown respectively in blue and green, are obtained by including all tensors which have at least half of their legs contracted with a tensor inside the previously defined region.

aims to expand this region by including all perfect tensors which have at least half of their legs contracted with a tensor inside the previously defined region.

For the hexagonal tensor network, a.k.a. the holographic hexagon state, any tensor that has three legs or more connected to the region "inside" the greedy algorithm, is absorbed into that region. The algorithm keeps repeating this process iteratively, until no further inclusions can be made. It has been proven [33, 57, 155, 157] that in this setting, the edge of the region absorbed by greedy algorithm, i.e.  $\gamma_A^*$ , is indeed the correct cut for the discrete Ryu-Takayanagi formula on the boundary region  $A$ . Practically, this means that the number of cuts made by  $\gamma_A^*$  can be counted to obtain the entanglement entropy  $S[A]$ .

#### 4.6 CONCLUSION

From the origin of information theory in Shannon's mathematical theory of communication, to the development of the discrete Ryu-Takayanagi formula on tensor networks, this chapter has been covering the applications of quantum information to holography. Special interest was given to quantum error correction and entanglement entropy but it is important to note that the literature has (recently) advanced beyond the discussions here, both in scope and complication.

Within the literature, advanced ideas about quantum error correction properties, specifically close to the boundary, have been developed. Nonetheless, the main conclusions made here remain valid. The AdS-Rindler reconstruction in different wedges still produces different operators with the same action on a low energy subspace that is increasingly better protected against boundary erasures as it moves deeper into the bulk. The situation close to the boundary can, however, be better described by an algebra [45, 135, 159] of quantum error correcting operators.

The direction further developed in this dissertation is that of entanglement entropy and its connection to tensor networks. In principle it should be possible to expand the discussion in this chapter to higher-dimensional situations [57, 141, 144, 145]. In this dissertation the  $\text{AdS}_3/\text{CFT}_2$  case will be studied. The underlying reason for this choice is that there are convenient ways in 2+1-dimensional gravity to study other spacetimes [41, 42, 51] than pure AdS. A challenge of current interest in this regard is to expand the HaPPY tensor networks to these less trivial spacetimes.

Additionally, gravity in three dimensions is relatively less complicated [50–52] than higher-dimensional gravity and hence more attention can be given to the quantum informational aspects. It has, for instance, been shown that there are non-minimal but extremal curves, which probe regions of spacetimes in 2+1-dimensional gravity [41, 42] that cannot be accessed via Ryu-Takayanagi. The length of these curves correspond [42, 43] to a new quantum information quantity, called entwinement. It is an open question whether or not this situation can be translated to the HaPPY tensor networks. The aim of the following two chapters is to bring entwinement to the HaPPY tensor networks.



III

## BLACK HOLES, ORBIFOLDS AND TENSOR NETWORKS



### 5.1 INTRODUCTION

CFT data can be used to probe the bulk spacetime of AdS/CFT, as seen in the previous chapters. Specifically, the spatial entanglement entropy of a boundary region is known to give rise to a minimal surface in the bulk via the Ryu-Takayanagi formula. One could hence hope to reconstruct the local geometry in the bulk using boundary field theory information. For this approach to work completely however, the union of all minimal surfaces that can be obtained via Ryu-Takayanagi must cover all of the bulk spacetime.

It turns out [41] that in the case of empty AdS, the spacetime can be entirely covered by Ryu-Takayanagi minimal surfaces. However, the biggest possible minimal surfaces, those that are anchored on the endpoints of a boundary interval half the size of the boundary, must be included or otherwise the central region of empty AdS would not be covered. Through study of  $2 + 1$ -dimensional gravity [50, 51] a systematic set of examples [41, 42] in which it is not possible to find a full covering with Ryu-Takayanagi minimal surfaces can be obtained.

The central region of these spacetimes that cannot be probed is known as the entanglement shadow [41]. In recent developments, a novel holographic quantum informational measure on the boundary has been introduced that corresponds to non-minimal but extremal bulk curves. This quantity, called entwinement [41, 43], probes the entanglement shadow via these new curves.

*Quantum corrections to Ryu-Takayanagi are not considered here.*

### 5.2 $2 + 1$ -DIMENSIONAL GRAVITY

Three-dimensional general relativity, a.k.a.  $2 + 1$ -dimensional gravity, has significantly simpler dynamics [50, 51, 160] than the four-dimensional case [89, 90] due to the complete lack of local degrees of freedom in this theory. Yet three-dimensional gravity is an interesting gravitational model to investigate various aspects of holography. For instance, black hole solutions can be found [53, 161, 162] in three-dimensional gravity if given a negative cosmological constant. This allows for the study of comparatively simple black hole solutions in the AdS/CFT correspondence.

*For ease of notation, three-dimensional gravity is the preferred term in this thesis.*

The conjecture of the AdS/CFT correspondence facilitates the formulation of  $\text{AdS}_3$  quantum gravity in terms of its corresponding two-dimensional conformal field theory at the boundary. However, a strong relationship between  $\text{AdS}_3$  and  $\text{CFT}_2$  had already been found before the birth of the holographic correspondence. Brown and Henneaux [143], showed that the asymptotic sym-

metry group of asymptotically  $\text{AdS}_3$  spacetimes is generated by the algebra of local two-dimensional conformal transformations. This insight yielded the Brown-Henneaux relationship that was used in the previous chapter, equation (120), and which might be seen [51] as a precursor of the AdS/CFT correspondence. Therefore,  $\text{AdS}_3/\text{CFT}_2$  is seen as a natural and useful laboratory to test holography.

### 5.2.1 Negatively Curved Gravity in Three Dimensions

To understand entwinement in  $\text{AdS}_3/\text{CFT}_2$  it is sensible to first (very) briefly study three-dimensional gravity. The three-dimensional Einstein-Hilbert action, in accordance with the GR discussion from the first chapter, is given [51] by

$$S = \int d^3x \sqrt{|det(g)|} \left( \frac{1}{2\kappa^2} (R - 2\Lambda) \right), \quad (133)$$

where  $\Lambda$  is the cosmological constant which here is chosen to be  $\Lambda = -R_{\text{AdS}}^{-2}$ . The equations of motion following from this action (after variation with respect to the metric) are the vacuum Einstein's equations with a negative cosmological constant,

$$R_{\mu\nu} - \frac{1}{2}g_{\mu\nu}R - \Lambda g_{\mu\nu} = 0. \quad (134)$$

It can be shown [50, 51, 160] that any three-dimensional solution of the above equation with  $\Lambda < 0$  is locally  $\text{AdS}_3$ .

### 5.2.2 Gravity as a Topological Theory

To support the claim that three-dimensional gravity lacks any dynamical degrees of freedom, a simple counting exercise is useful [51]. The metric tensor  $g_{\mu\nu}$  of  $D$  dimensional spacetime has  $D(D+1)/2$  components.  $D$  of those components can always be removed due diffeomorphism invariance [51, 162]. In addition, another  $D$  components of the metric tensor act as Lagrange multipliers [51, 162] in the Einstein-Hilbert action, e.g. equation (133), so that they do not count as degrees of freedom. The total remaining number of degrees of freedom in a  $D$ -dimensional Einstein gravity is thus

$$\frac{D(D+1)}{2} - 2D = \frac{(D^2 - 3D)}{2}. \quad (135)$$

In the case of three-dimensional gravity, the amount of dynamical degrees of freedom is thus zero. At a first glance, this complete absence of local degrees of freedom might seem to indicate [50, 51] that three-dimensional gravity is essentially sterile as there are no gravitational waves and hence no graviton in this theory of gravity. This apparent lack of complexity stands in stark contrast with the earlier claim that a black hole can be contained in negatively curved three-dimensional gravity.

The reason that three-dimensional gravity still harbors interesting physics, even though each of its solution is locally equivalent to a maximally symmetric spacetime with constant curvature, is that [50, 51, 162] different solutions of three-dimensional gravity with a negative cosmological constant differ from each other by global properties. This opens up the possibility [50, 51] of having non-trivial causal structures and thus allows for the existence of black hole solutions. To show that the theory of three-dimensional gravity is purely topological, it can be reformulated as a Chern-Simons gauge theory [50, 163]. This is shown explicitly in the appendices.

### 5.2.3 BTZ Black Holes

As claimed earlier, three-dimensional gravity contains black hole solutions. In the early 1990's, Bañados, Teitelboim and Zanelli (BTZ) showed [161] that 2 + 1-dimensional gravity can describe a black hole that seems to be somewhat physically similar to a Kerr black hole. The metric [51, 161] of a BTZ black hole of mass  $M$  and angular momentum  $J$  is

$$ds^2 = (N(r))^2 dt^2 - (N(r))^{-2} dr^2 - r^2 (d\varphi + N^\varphi(r)dt)^2, \quad (136)$$

with

$$N(r) = \sqrt{-8GM + \frac{r^2}{R_{\text{AdS}}^2} + \frac{16G^2J^2}{r^2}} \quad \& \quad N^\varphi(r) = -\frac{4GJ}{r^2}. \quad (137)$$

Clearly, this solution of three-dimensional gravity is purely dependent on the parameters  $M$  and  $J$  which means [164] that, just like the Kerr black hole, it has no hair. Furthermore, it was shown in the literature that a BTZ black hole can arise from gravitational collapse. Two important differences [53] with a Kerr black hole are however, that the BTZ black hole is asymptotically AdS instead of being asymptotically flat and that it has no coordinate singularity at the origin. Nevertheless, the BTZ black hole has a causal structure [53, 164] with an inner and an outer horizon just like the Kerr black hole. When  $0 \leq |J| < MR_{\text{AdS}}$ , the inner and outer horizon are located at  $r_-$  and  $r_+$  which are defined [51] by

$$r_\pm^2 = 4GMR_{\text{AdS}}^2 \left( 1 \pm \sqrt{1 - \left( \frac{J}{MR_{\text{AdS}}} \right)^2} \right). \quad (138)$$

Outside this parameter domain [51], i.e. when  $|J| > MR_{\text{AdS}}$  or  $M < 0$ , both the horizons are removed and the spacetime describes a conical defect (or excess) with a naked conical singularity. When  $J = 0$  and  $M = -1/(8G)$  the singularity also disappears, leaving a spacetime which is exactly  $\text{AdS}_3$ . The overview [51] of the spectrum of the BTZ metric in function of  $J$  and  $M$  is shown in figure 31.

BTZ black holes have been studied extensively [51, 164, 165] and show up in many domains of modern theoretical physics. In this dissertation however, mainly

*The Kerr black hole solution is an uncharged, rotating black-hole.*

*There is however a causal singularity at the BTZ-BH origin.*

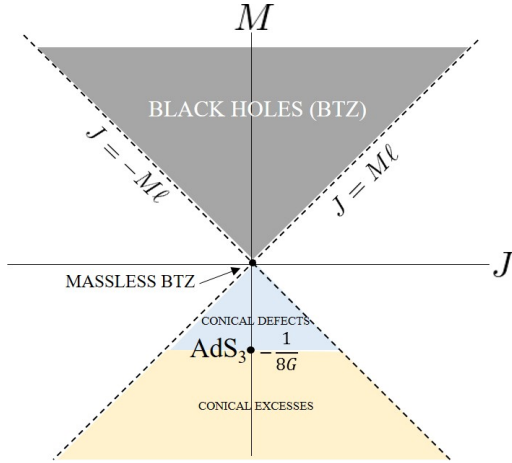


Figure 31: Visual representation [51] of the spectrum of the BTZ metric. BTZ black holes (grey) exist for  $M \geq 0$ ,  $|J| \leq MR_{\text{AdS}}$ . The vacuum state, i.e.  $\text{AdS}_3$ , resides at  $M = -1/(8G)$ ,  $J = 0$ . The other colored regions denote conical defects (blue) and conical excesses (orange).

the orbifold aspect of BTZ black holes will be necessary. Finally, for future use it is noted that the mass and angular momentum of a BTZ black hole can be described [51, 164] in function of  $r_{\pm}$ ,

$$M = \frac{r_+^2 + r_-^2}{8GR_{\text{AdS}}^2} \quad \& \quad J = \frac{r_+ r_-}{4GR_{\text{AdS}}} . \quad (139)$$

#### 5.2.4 Orbifolds

As discussed before, any solution of gravity with negative curvature in three dimensions is locally Anti-de Sitter spacetime. So every patch of a spacetime in the BTZ metric spectrum, like the BTZ black hole, is isometric to some part of  $\text{AdS}_3$ . Specifically [164, 166], any (vacuum) spacetime with negative curvature in three-dimensional gravity can be constructed by patching together bits and pieces of (empty) anti-de-Sitter spacetime by identification under  $\text{SO}(2,2)$ , the isometry group of  $\text{AdS}_3$ , or equivalently  $(\text{SL}(2, \mathbb{R}) \times \text{SL}(2, \mathbb{R})) / \mathbb{Z}_2$ .

The fact that  $\text{SO}(2,2)$  is the isometry group of  $\text{AdS}_3$  can be distilled [166] from the definition of  $\text{AdS}_3$  [61, 62] in four-dimensional flat space with two time directions

$$-x_0^2 - x_1^2 + x_2^2 + x_3^2 = R_{\text{AdS}}^2 . \quad (140)$$

This four-dimensional hyperbole is conserved under  $\text{SO}(2,2)$  rotations.

Henneaux, Bañados, Teitelboim and Zanelli [53] made a thorough, explicit and systematic overview of the isometries of  $\text{AdS}_3$  that are used to obtain the different spacetimes of the BTZ spectrum. For the purposes of this dissertation, the analysis of isometries is more convenient in the  $\text{SL}(2, \mathbb{R})$  group.

It turns out [53, 166, 167] that  $\text{SL}(2, \mathbb{R})$  contains three different types of elements  $g$ : the hyperbolic ( $\text{Tr}(g) > 2$ ) elements which act as squeeze mappings, the

elliptic ( $\text{Tr}(g) < 2$ ) elements which act as rotations and the parabolic ( $\text{Tr}(g) = 2$ ) elements which act as shear mappings. In addition, it can be shown [51, 53, 166] that each spacetime in the BTZ spectrum is a quotient space obtained by making identifications of regions in  $\text{AdS}_3$ , which in this construction is known as the covering space, under the orbit of the action of these elements of  $\text{SL}(2, \mathbb{R})$ .

The elements  $g$  in the hyperbolic conjugacy class provide the identifications [53] of  $\text{AdS}_3$  regions that give a massive BTZ black hole. Elliptic elements give identifications [53, 166] which yield the conical defects (or excesses) and the parabolic elements lead to massless BTZ black holes. Massless BTZ black holes are a limiting case [169] of both the elliptic and hyperbolic identifications but the limits taken from hyperbolic and the elliptic conjugacy classes are different. Because these spacetimes are all quotient spaces of the covering spacetime, they are known as orbifolds [167, 170].

*This classification is known as the Iwasawa decomposition [168] of  $\text{SL}(2, \mathbb{R})$ .*

### 5.3 ENTWINEMENT OF ORBIFOLDS

The orbifold spacetimes that follow from empty  $\text{AdS}_3$  by a non-trivial group action contain an entanglement shadow [41]. For instance, it has been shown [41–43, 171], see figure 32, that spatial slices of BTZ black holes have an entanglement shadow with a thickness of approximately AdS scale surrounding its (outer) horizon. Not only does this area of shadow hinder the attempt to reconstruct the geometry from the boundary, it also reflects the obscure nature [12, 13, 63] of the AdS/CFT correspondence in bulk regions of less than AdS-size.

As briefly explained in the introduction of this dissertation,  $N^2$  conformal field degrees of freedom at the boundary are encoded into the bulk physics of a region of AdS-size via the AdS/CFT correspondence. The way in which these  $N^2$  degrees of freedom capture quantum gravity in these regions is yet unknown [12, 13, 63]. Probing the entanglement shadow might also be an advance in the attempt to understand sub-AdS locality. In the next chapter, the question of whether or not there is an actual link between sub-AdS locality and entwinement will be explored.

*The exact challenge of sub-AdS locality will be discussed in more detail in the next chapter.*

This all motivates the idea that a measure [42, 43] of the entanglement of internal degrees of freedom of the boundary CFT might correspond to a bulk curve, or surface in higher dimensions, that probes the entanglement shadow. In addition, internal degrees of freedom are known to have comparatively small energy gaps and are thus expected [41, 42] to capture the deep IR behavior of the (boundary) field theory. Via AdS/CFT, the IR physics of the boundary CFT is associated to the deep interior of the bulk spacetime, exactly where the entanglement shadow lives.

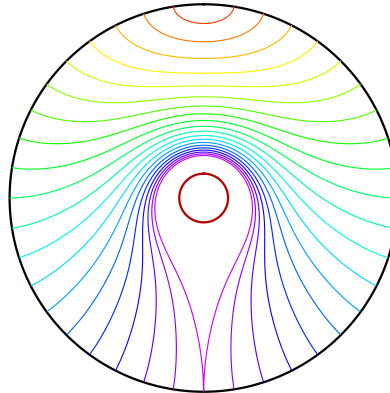


Figure 32: Visual representation [171] of a family of geodesics around a BTZ black hole. The horizon of the BTZ black hole (thick, dark red) is shown at the center of the picture. The other (rainbow) colored lines, show how a geodesic, i.e. the minimal surface on two-dimensional disk, gets deformed as its anchor-points on the boundary are moved further and further along the boundary. If this process were to be repeated for every spatial interval on the boundary, a bulk region of AdS-size thickness along the horizon would remain that is never probed by the geodesics. This region is the entanglement shadow of a spatial slice of a BTZ black hole. Note that for aesthetic visualization reasons, the radial coordinate is compactified to  $\rho = \tan^{-1}(r)$ .

### 5.3.1 Introducing Entwinement

The arguments in the previous section and the success of the Ryu-Takayanagi formula strongly suggest that to probe inside the entanglement shadows some form of entanglement measure for internal degrees of freedom of the CFT has to be developed. Naively, one could try to calculate the reduced density matrix for a fraction of the Hilbert space of the CFT [42] and then obtain the entanglement entropy in the usual way. The problem with this approach is that the subset of the Hilbert space may not, in general [172–174], be gauge invariant. A straightforward solution [42] to this technical issue is to embed the Hilbert space into a larger theory, compute entanglement entropy in that theory and then sum over different gauge copies to get a gauge invariant quantity. This newly obtained quantum informational variable is known in the literature as entwinement.

Just like spatial entanglement entropy can be related to minimal bulk surfaces via Ryu-Takayanagi [33], entwinement turns out to have an interpretation [42] in the bulk theory in terms of extremal (but non-minimal) surfaces. For instance, it has been shown [42, 43] that entwinement in a two-dimensional conformal field theory is dual to the length of non-minimal curves in a slice of a conical defect. Specifically, the covering space  $\text{AdS}_3$  and its boundary CFT were used to play the role of embedding theory. Here, entwinement is defined as the quantity equal to the length of the Ryu-Takayanagi geodesics originating from the covering space

$\text{AdS}_3$ , after the application of the orbifold identifications that produce the conical defect.

### 5.3.2 Winding around Conical Defects

A conical defect can be obtained [42] from (global)  $\text{AdS}_3$  by identification under  $\mathbb{Z}_n$ . Recall that the global  $\text{AdS}_3$  coordinates (in the mostly minus signature) are

$$ds^2 = \left(1 + \frac{\tilde{r}^2}{R_{\text{AdS}}^2}\right) d\tilde{t}^2 - \left(1 + \frac{\tilde{r}^2}{R_{\text{AdS}}^2}\right)^{-1} d\tilde{r}^2 - \tilde{r}^2 d\tilde{\theta}^2. \quad (141)$$

The effect of the  $\mathbb{Z}_n$  identification is remarkably simple; the metric is retained but the angular coordinate  $\tilde{\theta}$  is prescribed to become periodic under  $2\pi/n$ . To obtain [42] a coordinate system where the angular coordinate runs from 0 to  $2\pi$ , the previous metric can be rescaled by

$$\theta = n\tilde{\theta} \quad \& \quad r = \tilde{r}/n \quad \& \quad t = n\tilde{t}, \quad (142)$$

so that the new metric,

$$ds^2 = \left(\frac{1}{n^2} - \frac{r^2}{R_{\text{AdS}}^2}\right) dt^2 - \left(\frac{1}{n^2} - \frac{r^2}{R_{\text{AdS}}^2}\right)^{-1} dr^2 - r^2 d\theta^2, \quad (143)$$

has a spacetime singularity at  $r = 0$ . Geodesics on a conical defect time-slice can be found by taking geodesics in  $\text{AdS}_3$ , which given by

$$\tan^2(\tilde{\theta}) = \frac{\tilde{r}^2 \tan^2(\tilde{\alpha}) - R_{\text{AdS}}^2}{\tilde{r}^2 + R_{\text{AdS}}^2} \quad (144)$$

where  $\alpha$  is the opening angle, and making the relevant  $\mathbb{Z}_n$  identification so that according to equation (142),

$$\tan^2\left(\frac{\theta}{n}\right) = \frac{n^2 r^2 \tan^2\left(\frac{\alpha}{n}\right) - R_{\text{AdS}}^2}{n^2 r^2 + R_{\text{AdS}}^2}. \quad (145)$$

Most of the resulting geodesics wind [42] around the central singularity of the conical defect, as can be seen in figure 33, and are thus extremal but non-minimal curves. These curves are called "long" geodesics, the conventional geodesics, which do not take the long way around the conical defect, are called the "short" geodesics.

The length  $\mathcal{L}(\alpha, \ell)$  of the geodesics (both long and short) in a conical defect is given [42] by

$$\mathcal{L}(\alpha, \ell) = 2R_{\text{AdS}} \log \left[ \frac{2R_{\text{AdS}}}{\epsilon_{UV}} \sin\left(\frac{\alpha + 2\pi\ell}{2n}\right) \right], \quad (146)$$

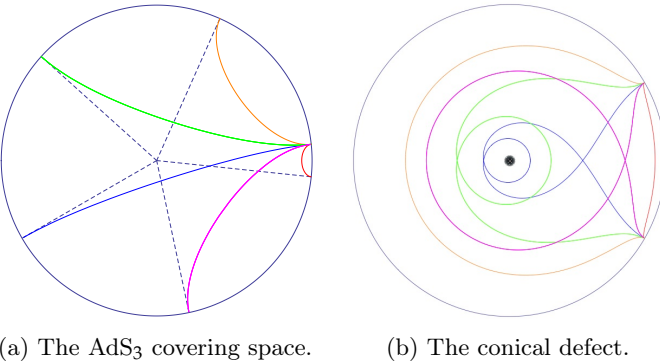
(a) The  $\text{AdS}_3$  covering space. (b) The conical defect.

Figure 33: Graphical representation [42] of geodesics on the conical defect. The time-slice of the  $\text{AdS}_3$  covering space picture is shown on the left, the conical defect  $\text{AdS}_3/\mathbb{Z}_n$  is shown on the right. In this case  $n = 5$ . The geometry of spatial geodesics in the conical defect descends from geodesics in the covering space as shown on the left. The covering space picture also shows the different sections of the  $\text{AdS}_3$  time-slice that are identified under  $\mathbb{Z}_5$ .

where  $\alpha$  is the opening angle of the corresponding geodesic on the covering space and where  $\ell$  counts the number of windings. The factor  $\epsilon_{UV}$  is a gravitational IR cut-off [33], reminiscent of the UV cut-off in spatial entanglement entropy [34] and which deals with the tails of the geodesics which would otherwise be of infinite length as they near the boundary.

As can be inferred from figure 33, there are  $n$  different geodesics between each two (different) boundary points of the conical defect space. One of them is minimal and does not wind around the singularity. It is this minimal geodesic that calculates the spatial entanglement entropy of the boundary interval, upon which it is anchored, by use of the [33] the Ryu-Takayanagi formula. The other geodesics have windings and/or penetrate the entanglement shadow and their length is postulated to calculate this new holographic boundary quantity called entwinement [42].

### 5.3.3 A Covering Space Picture for Massive BTZ's

An obvious question in this story is whether or not the above described approach can be extended to the BTZ black holes. A massless BTZ can be obtained [43, 166, 169] (to some extent) by taking  $n \rightarrow \infty$  in the conical defect metric. As a consequence [42] the massless BTZ spacetime contains spatial geodesics that wrap around the black hole horizon infinitely many times, which does not happen around the conical defect singularity.

Massive BTZ black holes, which are obtained from orbifolding  $\text{AdS}_3$  by a hyperbolic element of  $\text{SL}(2, \mathbb{R})$ , present a more serious challenge for entwinement. The reason for this is that necessary hyperbolic identifications of the covering space  $\text{AdS}_3$  are equivalent [42, 61, 62] to Lorentz boosts in the flat embedding space-

The central copy of the BTZ black hole geometry, to which all other copies are eventually brought back, is called the fundamental domain.

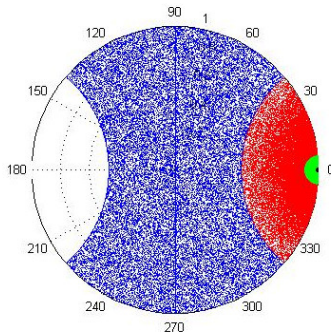


Figure 34: A numerical simulation of the effect of boosts on points on a time-slice of the  $\text{AdS}_3$  covering space. In blue, a uniform random distribution of points onto the fundamental domain is shown. In red, the effect of one single boost on the points in the fundamental domain is shown. In green the effect of two successive boosts is shown. Without the limitations of time and computer memory, this process could be repeated indefinitely. Obviously, the boost could also have happened in the other direction, this would provide the same picture as above but mirrored with respect to the vertical axis. The code listing for this figure can be found in the appendices.

time with two time dimensions (see equation 140). In general, a Lorentz boost mixes space and time non-trivially, so that a constant time-slice in the BTZ black hole geometry does not necessarily correspond [42] to a constant time-slice of the covering  $\text{AdS}_3$  spacetime.

This means that for generic, massive BTZ black hole state, it is impossible to apply the covering space definition of entwinement on spatial slices. Even though there is a subclass of massive BTZs in which the covering space approach can be applied, as will be shown later on in this chapter, there is still another challenge present. The action of a boost on the flat embedding spacetime of  $\text{AdS}_3$  has a non-compact orbit [42]. This implies that the  $\text{AdS}_3$  geometry contains infinitely many copies of the massive BTZ geometry.

This dissertation shows the existence of a covering space picture of entwinement for non-rotating but massive BTZ black holes. The reason for this is that the action of Lorentz boosts on a  $t = 0$  time-slice of  $\text{AdS}_3$  (embedded in that four-dimensional flat spacetime) can be used to map all points of  $\text{AdS}_3$  into a fundamental domain that is purely spatial [61, 62] and entirely part of that original time-slice of  $\text{AdS}_3$ . A numerical simulation of the effect of these Lorentz boosts on a random sets of points in a slice of  $\text{AdS}_3$  is shown in figure 34.

To see why  $t = 0$  time-slices of  $\text{AdS}_3$  are preserved under orbifolding in the case of a massive but non-rotating BTZ black hole geometry, it is convenient to start from the metric for a non-rotating, massive BTZ black hole in the Euclidean

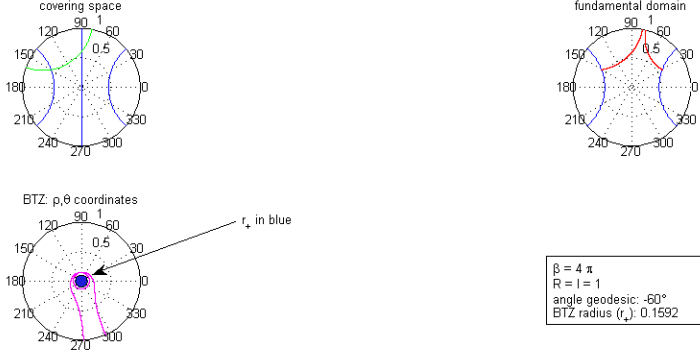


Figure 35: A numerical visualization of the covering space picture for a time-slice of a massive BTZ black hole is shown on the left. On the right, the effect of the successive combination of reflections is shown, i.e. all curves are brought back to the fundamental domain. On the bottom left, the resulting curves are shown on BTZ black hole time-slice. For the covering space picture, the coordinates  $(y_1, y_2)$  were used. The black hole horizon is shown in solid blue on lower left picture. The code listing for this picture can be found in the appendices.

signature (after multiplying it with a factor  $-1$  so that a negative definite metric is evaded) which conform [62] to equation (136) is

$$ds^2 = \frac{(r^2 - r_+^2)}{R_{\text{AdS}}^2} dt^2 + \frac{R_{\text{AdS}}^2}{(r^2 - r_+^2)} dr^2 + r^2 d\theta^2. \quad (147)$$

Note that equation (139) was used to write the metric in function of  $r_+$  and  $r_-$ . Applying the following coordinate transformations [175],

$$w^\pm = \left( \frac{r^2 - r_+^2}{r^2} \right)^{1/2} \exp \left( \frac{r_+(\theta \pm t)}{2R_{\text{AdS}}} \right), \quad z = \left( \frac{r^2 - r_+^2}{r^2} \right)^{1/2} \exp \left( \frac{r_+(t)}{2R_{\text{AdS}}} \right), \quad (148)$$

to the Euclidean metric of the massive non-rotating BTZ black hole, reduces the metric to

$$ds^2 = \frac{R_{\text{AdS}}^2}{z^2} (dw^+ dw^- + dz^2), \quad (149)$$

where due to the periodicity of  $\theta$ ,

$$w^\pm \cong \exp \left( \frac{4\pi^2}{\beta} \right) w^\pm, \quad z \cong \exp \left( \frac{4\pi^2}{\beta} \right) z, \quad (150)$$

with  $\beta$  the inverse temperature of the black hole. This relatively simple expression for the non-rotating, massive BTZ can be translated [62] to the four-dimensional embedding of  $\text{AdS}_3$  via the following set of transformations,

$$x_0 = -\frac{z}{2} \left( 1 + \frac{R_{\text{AdS}}^2 + w^+ w^-}{z^2} \right) \quad \& \quad x_1 = \frac{R_{\text{AdS}}}{2z} (w^+ + w^-), \quad (151)$$

$$x_2 = \frac{z}{2} \left( 1 - \frac{(R_{\text{AdS}}^2 - w^+ w^-)}{z^2} \right) \quad \& \quad x_3 = -\frac{R_{\text{AdS}}}{2iz} (w^+ - w^-). \quad (152)$$

In this embedding space, the hyperbolic elements of  $\text{SL}(2, \mathbb{R})$  are equivalent to Lorentz boosts. For the non-rotating, massive BTZ geometry, the identifications of  $\text{AdS}_3$  are achieved [61, 62] by Lorentz boosts in the  $x_0$ - $x_2$ -plane of the embedding space given by

$$x'_0 = x_0 \cosh(\eta) + x_2 \sinh(\eta) \quad \& \quad x'_2 = x_2 \cosh(\eta) + x_0 \sinh(\eta), \quad (153)$$

where  $\eta = 4\pi^2/\beta$ . Because the rest of this dissertation will focus on the  $t = 0$  time-slice of  $\text{AdS}_3$  (which in this case remains a time-slice after orbifolding),  $x_3 = 0$  can be assumed for the remainder of this text.

As it happens [61, 62], the Lorentz boosts in the flat four-dimensional embedding space can be reconstructed by a sequence of successive reflections under hyperplanes  $P_1$  and  $P_2$  with corresponding normals  $n_1 = (0, 0, 1, 0)$  and  $n_2 = (\cosh(\frac{\eta}{2}), 0, \sinh(\frac{\eta}{2}), 0)$ . To see this recall from elementary mathematics that the effect [176, 177] of the reflection of a point  $X = (x_0, x_1, x_2, x_3)$  with respect to a hyperplane with normal  $n$  is

$$X' = X - 2(n \cdot X)n, \quad (154)$$

where the dot indicates in the inner product (in this case in the flat four-dimensional embedding space). The transformation induced by the combined reflections under  $P_1$  and  $P_2$  is simply a Lorentz boost along the  $x_0 - x_2$ -plane, i.e.

$$\begin{cases} x'_0 = x_0 \cosh(\eta) + x_2 \sinh(\eta), \\ x'_2 = x_2 \cosh(\eta) + x_0 \sinh(\eta). \end{cases} \quad (155)$$

Knowing that the orbifold transformations needed to obtain a massive, non-rotating BTZ black hole from the covering space, are given by reflecting across two hyperplanes  $P_1$  and  $P_2$  in the embedding space of  $\text{AdS}_3$ , allows for a covering space picture of  $M \neq 0, J = 0$  BTZ black hole entwinement. Once more, the approach is to take a geodesic on the  $t = 0$   $\text{AdS}_3$  time-slice and select the parts of the curve that lie outside the fundamental domain.

These sections then get mirrored across  $P_1$  and  $P_2$  until all parts of the geodesic would lie in the fundamental domain. A caveat here is that due to the fact that the orbit of the Lorentz boosts is, in fact, not finite, the amount of reflections used in this process is not bounded from above.

Practically, it is most convenient to introduce the Poincare unit disk coordinates  $(y_1, y_2)$ , which conformal coordinates subject to  $y_1^2 + y_2^2 \leq 1$ . The Poincare disk coordinates are obtained from the embedding space via

$$y_1 = \frac{x_2}{1+x_0} \quad \& \quad y_2 = \frac{x_1}{1+x_0}. \quad (156)$$

These coordinates are most useful to determine whether or not a part of a geodesic lies inside or outside of the fundamental domain. Calculating the reflections, happens most naturally in the embedding coordinates. An example of the effects of the hyperbolic identifications of  $\text{AdS}_3$  on a geodesic, obtained in this way, is shown in figure 35. It shows that geodesics that have parts that lie outside the fundamental domain produce curves that are wound up around the BTZ singularity after the orbifold identifications.

#### 5.4 ENTWINEMENT OF DISCRETELY GAUGED THEORIES

Even though the previous sections provided a conceptual and geometrical notion of what entwinement is, exactly defining entwinement has turned out to be a challenging question. Currently, a complete mathematical understanding of entwinement in terms of a Von Neumann entropy, is still lacking. Recently however [43] progress has been made in this endeavor; for instance, Balasubramanian, Bernamonti, Craps, De Jonckheere and Galli have developed an exact expression for the entwinement of discrete gauge theories.

In their approach [43], the replica trick is applied to define entwinement in symmetric product orbifold CFTs [178]. As an explicit example, the D<sub>1</sub>-D<sub>5</sub> CFT was used by them to calculate entwinement and compare it to the length of winding geodesics in conical defects and massless BTZ black holes. In this section, the concepts of symmetric product orbifold CFTs, entwinement, the replica trick and the D<sub>1</sub>-D<sub>5</sub> CFT is explored.

##### 5.4.1 Defining Entwinement

To understand entwinement in discretely gauged theories, recall that in the replica trick (Euclidean) path integrals are taken over multi-sheeted Riemann surfaces to calculate the entanglement entropy of the CFT region that links together the different sheets. Equivalently [43, 179], states formed by Euclidean path integrals can be calculated via correlation functions of so-called twist operators. By definition, these twist operators link together the different copies of the CFT that normally arise in the replica trick. For discretely gauged theories entwinement is defined in terms of correlation functions of these twist operators.

To apply this approach concretely, consider a CFT [43, 178] with as its target space  $M^N/S_N$ . This CFT contains  $N$  groups of fields, where each group of fields is a coordinate set on one of the  $N$  copies of the smooth manifold  $M$ . In this kind of CFT, known as a symmetric product orbifold CFT, each possible configuration of the fields is identified under the  $S_N$  permutations of these  $N$  sets of fields. By gauge fixing the  $S_N$  identification, the fields can be interpreted as changing continuously from point to point so that [43], a continuous (closed) string, not to be confused with a string from string theory, lives in each  $M$  of  $M^N$ .

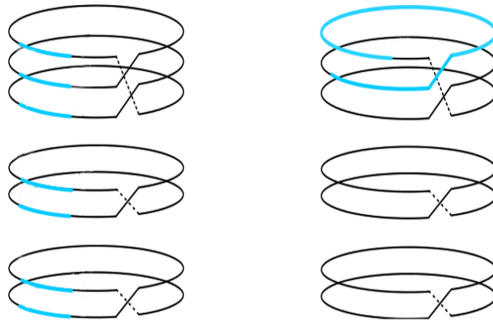


Figure 36: A visual representation [43] of the strings in a symmetric product orbifold CFT [178]. Here, the same twisted sector is shown twice. The number of strands shown here is seven, there are two strings that have two windings and one string that three windings. On the left, the sections of the strands that would correspond to the spatial region of conventional entanglement entropy are shown in blue. On the right, the region of the strands of the entwinement of one and half strings is shown. In the latter case, a symmetrization under  $S_N$  is still necessary to correctly define entwinement.

A symmetric product orbifold CFT contains [43] "twisted sectors" in which the embedded strings are periodic up to permutations. Inspired by the group structure of  $S_N$ , each twisted sector is labeled by a conjugacy class. Each of these conjugacy classes is characterized by the lengths of its permutation cycles. The lengths  $m$  of the permutation cycles, of which there are  $N_m$ , must fulfill [43] the requirement that  $\sum_m N_m m = N$ . Visually, each of these cycles can be seen as a long string winding  $m$  times. Each of these windings can be imagined to be a shorter piece of string, which for clarity [43] is referred to as a "strand".

Intuitively [42, 43], entwinement captures the entanglement of intervals that extend over some but not all strands. The conventional spatial entanglement entropy is equal to the entwinement of a union of identical intervals on every strand. Due to the identification under  $S_N$ , the entwinement of an interval of a specific individual string cannot be defined, but it is well defined to consider the entwinement of a specific number of strings as long as they themselves are unspecified.

Recall from the previous chapter that the entanglement entropy of an interval  $A$ , as defined in equation (124), can easily be expressed in function of the Rényi entropies  $S_n$ , as

$$S_A = \lim_{n \rightarrow 1} S_n, \quad (157)$$

where the Rényi entropies are defined by

$$S_n \doteq \frac{1}{1-n} \text{Tr}(\rho_A^n). \quad (158)$$

*2D CFT's have holomorphic and anti-holomorphic coordinates.*

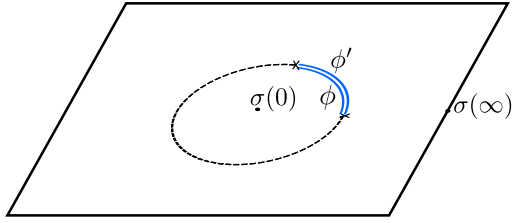


Figure 37: A visual representation [43] of the calculation of a reduced density matrix  $\rho(\phi, \phi')$  of a two-dimensional CFT in the framework of radial quantization. The path integral is taken from the origin (which corresponds to  $t = -\infty$ ) to radial infinity. The boundary conditions at the inside and the outside of the unit circle are respectively  $\phi$  and  $\phi'$ . Outside of the interval arc  $[0, \alpha]$  (shown in blue) these boundary conditions are put equal to one another.

For ease of notation, only the holomorphic CFT coordinate is used here.

Furthermore, it is convenient here [43] to work in the framework of radial quantization, where, in two-dimensional case, equal-time slices are circles of fixed radius. A pure state can be created in this kind of theory by acting with an operator  $\sigma$  at the origin. The corresponding density matrix  $\rho(\phi, \phi')$  is then obtained [43, 180] by inserting  $\sigma$  at the origin and at infinity and imposing boundary conditions  $\phi$  and  $\phi'$  at the inside and the outside of the unit circle.

The reduced density matrix  $\rho_A$  for an interval arc  $A = [0, \alpha]$  on the unit circle is calculated [43] by tracing over, i.e. taking the path integral from 0 to (radial) infinity, the remainder of the circle. To calculate [179, 181] terms of the form  $\text{Tr}(\rho_A^n)$ , which are essential to calculate Rényi entropies, the two-dimensional CFT plane (and the state it is in) are replicated and glued together at the cut  $[0, \alpha]$ .

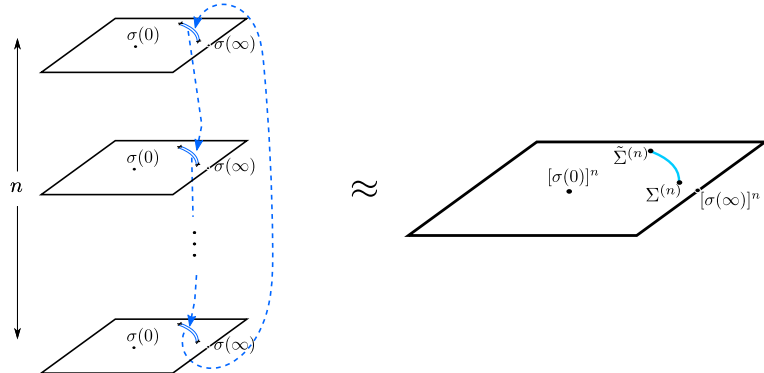


Figure 38: A visual representation [43] of the replica trick for a two-dimensional CFT in the framework of radial quantization. On the left, approach with the  $n$ -sheeted Riemann surface is shown. On the right the alternative but equivalent approach using Rényi twist operators is shown. Once more, the radial interval  $[0, \alpha]$  on the unit circle is shown in blue.

Just as in the regular case, the geometry resulting from the replica trick in radial quantization is an  $n$ -sheeted Riemann surface. To obtain the Rényi entropy,

a Euclidean path integral is taken over this surface as was explained in the previous paragraph. Equivalently [43, 179], see figure 38, the  $\text{Tr}(\rho_A^n)$  terms can be calculated on a single sheet of the cyclic orbifold of the two-dimensional CFT, as the correlation function of Rényi twist operators  $\Sigma^{(n)}$ . A Rényi twist operator [43, 179] grafts together  $n$  copies of the CFT (cyclically) so that when a path integral moves in between two Rényi twist, it enters the next copy of the CFT.

Recall that the kind of CFTs regarded here, called symmetric product orbifold CFTs, are of the form  $M^N/S_N$  and contain twisted sectors. To deal with these twisted sectors, the Rényi twist operators can be written [43] in function of elementary twists  $\Sigma_i^{(n)}$  by

$$\Sigma^{(n)} = \prod_1^N \Sigma_i^{(n)}. \quad (159)$$

Each of these elementary twists  $\Sigma_i^{(n)}$  is defined so that it only glues together the  $n$ -replicas of the  $i$ -th strand. Each of the elementary twists is chosen [43] in the fundamental representation of  $S_N$  so that the action of  $g \in S_N$  on them is given by

$$g \left[ \Sigma_i^{(n)} \right] = \Sigma_{g(i)}^{(n)}. \quad (160)$$

Finally, the entwinement of interval  $[0, \alpha + 2\pi\ell]$ , where  $\ell \neq 0$  indicates that the interval is taken over more than one strand, can be defined [43] as a bi-local, gauge-invariant quantity in terms of the elementary twists  $\Sigma_i^{(n)}$  as

$$E(\alpha, \ell) = \lim_{n \rightarrow 1} \frac{1}{1-n} \log \left[ \langle \psi | \frac{1}{|S_N|} \sum_{g \in S_N} \tilde{\Sigma}_{g(i)}^{(n)}(1) \Sigma_{g(i)}^{(n)}(e^{i(\alpha+2\pi\ell)}) | \psi \rangle \right], \quad (161)$$

where as usual only the holomorphic coordinate is used. The operator  $\tilde{\Sigma}_i^{(n)}$  is defined [43] so that its action is opposite to that of  $\Sigma_i^{(n)}$ . When  $\ell$  is larger than the number of strands in a long string it means [43] that the entwinement calculates the entanglement between the entirety of the long string and the rest of the system.

## 5.5 A LIGHTNING INTRODUCTION TO THE D1-D5 CFT

As a practical example of a symmetric orbifold CFT [178] and entwinement [43], the long strings in the D1-D5 CFT [179, 182] will be discussed. To obtain [42, 182] this CFT, start from type IIB (super)string theory and compactify the theory on a  $S^1 \times T^4$  spacetime, where the  $T$  denotes a torus. Then, regard  $N_1$  D1-branes wrapping around  $S^1$  and  $N_5$  D5-branes wrapping around  $S^1 \times T^4$ . The low energy limit description of this theory is known as the D1-D5 CFT. In the strong coupling regime the D1-D5 CFT is exactly dual [42, 43] to Type IIB supergravity on  $\text{AdS}_3 \times S^3 \times T^4$ .

In the fully decoupled regime of the D1-D5 CFT, at its so-called orbifold point, the dynamics of the theory reduces [42, 43] to that of a free (supersymmetric) sigma model with  $(T^4)^N/S_N$  as target space. For this regime of the D1-D5 CFT [43],  $N \doteq N_1 N_5$  and central charge  $c$  is equal to  $6N$ . The D1-D5 CFT is thus a symmetric orbifold CFT on  $N$  copies of  $M = T^4$  which are permuted by  $S_N$ .

### 5.5.1 Conical Defects, Once More

In the strong coupling regime of the D1-D5 CFT [42, 43, 183], there exist large  $N$  states in the D1-D5 CFT that are dual to conical defects and massless BTZ black holes in the bulk. For instance [43], the CFT state dual to the  $\mathbb{Z}_m$  conical defects is

$$|\psi\rangle = [\sigma_m(0)]^{\frac{N_m}{m}} |0\rangle , \quad (162)$$

where each  $\sigma_m(0)$  acts on a different subset of the  $N$  different set of CFT fields. By inserting this state into equation (161), and working out the significantly non-trivial correlation function that follows from it, it can be shown [43, 182], using equation (146) for  $\mathcal{L}(\alpha, \ell)$ , that

$$E(\alpha, \ell) = 2 \log \left[ \frac{2R_{\text{AdS}}}{\epsilon_{UV}} \sin \left( \frac{\alpha + 2\pi\ell}{2m} \right) \right] = \frac{\mathcal{L}(\alpha, \ell)}{R_{\text{AdS}}} . \quad (163)$$

So it turns out [43] that entwinement, as defined in equation (161), which can only be calculated at the orbifold point of the D1-D5 CFT, corresponds to the gravitational covering space interpretation of entwinement which is valid at strong coupling. This is somewhat surprising, but it is known [43] from the literature [184, 185] that certain "protected" quantities in the D1-D5 CFT are the same when calculated at strong and weak coupling. Whether or not entwinement is similarly protected under renormalization flow is unclear.

### 5.5.2 Relationship with Entanglement Entropy

For self-consistency [43], the entwinement of the same interval  $[0, \alpha]$  on all the different strands of a CFT, as shown in figure 36, should be equal to the conventional spatial entanglement entropy of the region  $[0, \alpha]$ . According to the Ryu-Takayanagi formula [33, 43], the entwinement of this situation should simply be equal to the length of geodesics in  $\text{AdS}_3$ . In the case of the D1-D5 CFT, it was shown that [43] that the entwinement of single interval on all the strands corresponds to  $\ell = 0$  in equation (163).

### 5.5.3 Massless BTZ Black Holes

For BTZ black holes, the situation is significantly more subtle [43]. On one hand, massless BTZ black hole geometry act as the  $m \rightarrow \infty$  case of a  $\mathbb{Z}_m$  conical

defect and could naively be expected to be some similar limit in the dual CFT. However, according to the literature [183], the average number of  $m$ -cycles  $\langle N_m \rangle$  in the D1-D5 CFT is

$$\langle N_m \rangle = \frac{8}{\sinh\left(\sqrt{\frac{2\pi^2}{N}}m\right)}. \quad (164)$$

In the large  $N$  limit, typical states [43] have a number of  $m$ -cycles that is very close to this average. Therefore, this average can be used to construct the corresponding CFT state. In this case, it has, once more, been shown [43] that the (regularized) length of non-minimal geodesics that penetrate the entanglement shadow is given by entwinement of the boundary CFT.

## 5.6 CONCLUSION

At the beginning of this chapter, three-dimensional gravity was introduced. Even though Einstein gravity in 2+1 dimension has no propagating degrees of freedom, it is most certainly not a sterile theory. Starting from empty  $\text{AdS}_3$ , non-trivial spacetimes like conical defects and the BTZ black hole can be obtained. To do this, identifications of the points of  $\text{AdS}_3$  are made under elements of the isometry group  $\text{SO}(2, 2)$  in a process known as orbifolding.

It turns out that the spacetimes obtained by orbifolding  $\text{AdS}_3$  have regions that cannot be probed by minimal surfaces related to Ryu-Takayanagi. This kind of regions are known as the entanglement shadow. To probe the shadow, a new holographic quantum information quantity, called entwinement, has recently been developed. Entwinement aims to link the entanglement of internal degrees of freedom of a boundary CFT to quantities in the bulk, specifically non-minimal bulk curves. The two main ways to describe entwinement – the covering space picture and the entwinement definition for discretely gauged theories – have been discussed in this chapter.

This chapter has also shown that the possibility of a covering space picture for massive, non-rotating BTZ black holes exists. This is an expansion on the previously known covering space pictures for conical defects and massless BTZ black holes. According to the literature, the D1-D5 CFT, which was briefly discussed in this chapter, can be used to explicitly calculate the entwinement dual to the geometries of conical defects and massless BTZs. It is however yet unknown how to expand this approach to massive BTZs. Motivated by both the success and challenges of entwinement, the next chapter will show how to introduce entwinement to tensor networks.



### 6.1 INTRODUCTION

In the past five chapters, the link between quantum information and holography has been discussed. So far, a lot of attention has been given to tensor networks, entanglement entropy, entwinement and the Ryu-Takayangi formula. In this final corpus chapter these ingredients will be combined to show that there exists a hitherto unknown conceptual link between CFT entwinement and the bulk physics within an AdS-sized region of conical defects or the massless BTZ black hole. Along the way, the concept of entwinement is introduced to tensor networks, which leads to new (stacked) holographic tensor networks on conical defects and massive, non-rotating BTZ black holes.

### 6.2 ENTANGLEMENT SHADOWS

It was mentioned in the previous chapters that certain spacetimes like the conical defect and the BTZ black hole have an area in the bulk that cannot be probed [41–43] by minimal surfaces or geodesics. This region is known as the entanglement shadow. As shown in that chapter, there is a novel quantum informational quantity called entwinement [42, 43] that corresponds to non-minimal but extremal curves that can probe the entanglement shadow. To understand how entwinement can be used in combination with tensor networks, it would first be interesting to gauge if the entanglement shadow also exists in tensor networks. This would provide significant motivation for the development entwinement in tensor networks.

#### 6.2.1 Why are there Shadows?

In AdS/CFT, an entanglement shadows show up [41, 186] when a boundary region that is continuously increased in size, suddenly changes from being anchored on one bulk surfaces to another. To be more specific, when a boundary region is increased and the corresponding bulk surface is pulled inwards [41] until it suddenly switches to another bulk surface, there will be a region in the middle of the time-slice of the asymptotically AdS in question whose geometry not probed by spatial entanglement entropy.

The conical defect is a simple yet important example [41, 42] of how this sudden switch between surfaces (in this case geodesics) can happen. Recall from last

*Think of a soap bubble snapping [186] and then quickly reforming as a different surface.*

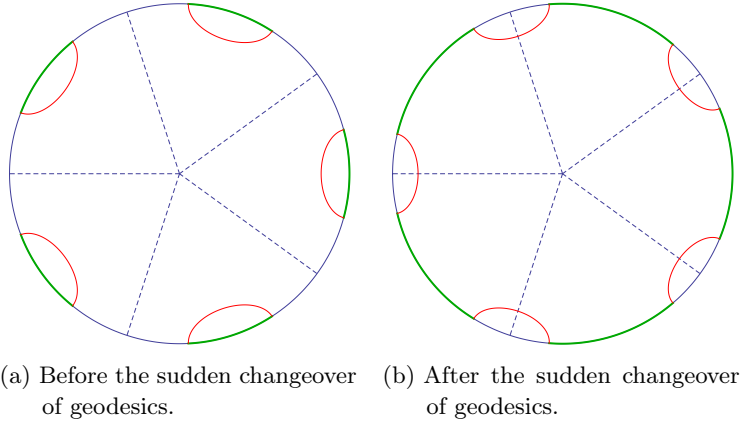


Figure 39: A graphical representation [42] of the "flip" between geodesics that occurs in spacetimes that have an entanglement shadow. In this case the spacetime is a conical defect obtained by  $\mathbb{Z}_5$  identifications of  $\text{AdS}_3$ . The geodesics are shown in red, the boundary intervals are shown in green.

chapter that conical defects do indeed have an entanglement shadow and that they can be obtained from  $\text{AdS}_3$  under identification by  $\mathbb{Z}_m$ . The reason that there is a sudden "flip" between which geodesics correspond to the boundary interval, is that Ryu-Takayanagi links boundary intervals with globally minimal surfaces [33, 41, 186] or curves. This means that curves have to be minimal under the  $\mathbb{Z}_m$  identification.

From figure 39, it can be observed that when a boundary interval is big enough, the lengths of the corresponding curves are minimized by passing through the edges of the boundary intervals in the different copies of the conical defect geometry. The question now is, can this sudden transition be translated to HAPPY tensor networks? To check this, the hexagon tensor network, which produces the holographic state [57], and its discrete Ryu-Takayangi description, the greedy algorithm, will be studied under  $\mathbb{Z}_m$  identification.

### 6.2.2 A Tensor Network for the Conical Defect.

Recall from chapter 4 that in the hexagon tensor network, there is an algorithm called the greedy algorithm which produces a cut through the tensor network whose length, defined by the number bonds that are cut, is the discrete equivalent of the length of a Ryu-Takayangi geodesic. By identifying the hexagon tensor network under  $\mathbb{Z}_m$  and using the greedy algorithm, it is possible to check if and when a "flip" occurs in the tensor network equivalent of conical defect geometry.

To work out how the tensor network behaves under  $\mathbb{Z}_m$  identifications, it is necessary to work out how many tensors each layer of the hexagon tensor network contains. A subtlety here is that once the central tensor is chosen, the tensor network turns out to have two kinds of tensors, a tensor with one leg connected

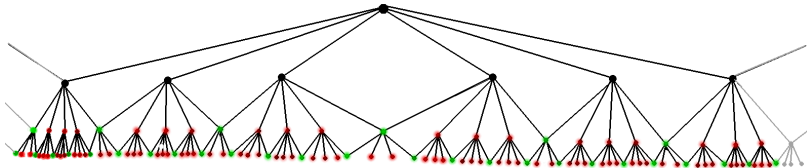


Figure 40: A visual representation of the open-folded hexagonal HaPPY tensor network.

Two layers (representing layer  $n$  and layer  $n+1$ ) are colored in. The red tensors are type  $f$ , the green tensors are type  $g$ . The number of the layer increases with depth, so layer  $n$  is drawn above layer  $n+1$ . With this figure, the discussion on the recursive relation can be checked.

to the previous layer and a tensor with two legs connected to the previous layer, these tensor are denoted by  $f$  and  $g$ , respectively.

In the appendices of the HaPPY tensor network paper [57], a recursive relationship for the number of  $f$  and  $g$  tensors in a layer of the pentagon code was developed. Accordingly, as part of the research in thesis, a similar recursive relationship for the hexagonal tensor network was developed. From inspection of the tensor network, it was inferred that the recursive relationship is

$$\begin{pmatrix} f_{n+1} \\ g_{n+1} \end{pmatrix} = \begin{pmatrix} 3 & 2 \\ 1 & 1 \end{pmatrix} \begin{pmatrix} f_n \\ g_n \end{pmatrix}. \quad (165)$$

To understand this recursive relation, look at figure 40, and realize that each  $f_n$  type tensor gives rise to three  $f_{n+1}$  tensors and two  $g_{n+1}$  tensors. Similarly, it can be seen from that figure that each  $g_n$  tensor will produce two  $f_{n+1}$  tensors and two  $g_{n+1}$  tensors. To get the total amount of tensors in layer  $n+1$ , one must realize that all the  $g_{n+1}$  tensor are shared by two tensors in layer  $n$ . Therefore, the amount of  $g_{n+1}$  tensors that naively follow from  $f_n$  and  $g_n$  must be divided by two. The result of this counting exercise is thus exactly that  $f_{n+1} = 3f_n + 2g_n$  and that  $g_{n+1} = f_n + g_n$ , as is denoted in equation (165).

The recursive relation described in equation (165), is only valid from the third layer on, which has 18 type  $f$  tensors and 6 type  $g$  tensors so that

$$\begin{pmatrix} f_n \\ g_n \end{pmatrix} = \begin{pmatrix} 3 & 2 \\ 1 & 1 \end{pmatrix}^n \begin{pmatrix} 18 \\ 6 \end{pmatrix}. \quad (166)$$

where  $n - 3$  was relabeled to  $n$ . Continuing to expand the ideas first presented in the HaPPY paper to the hexagonal tensor network, it can be shown that at large  $n$ ,

$$f_n + g_n = 24 \left(2 + \sqrt{3}\right)^n \left[1 + \mathcal{O}\left(\left(\frac{2 - \sqrt{3}}{2 + \sqrt{3}}\right)^n\right)\right]. \quad (167)$$

Because this kind of calculations are parnumber to this chapter, it is worthwhile to take a brief look at the technicalities. To obtain the above expression, start from equation (166), and diagonalize

$$M = \begin{pmatrix} 3 & 2 \\ 1 & 1 \end{pmatrix} \quad (168)$$

which can be done via  $M = SDS^{-1}$  where the coordinate transformation matrices are,

$$S = \begin{pmatrix} 1 - \sqrt{3} & 1 + \sqrt{3} \\ 1 & 1 \end{pmatrix} \quad \& \quad S^{-1} = \begin{pmatrix} \frac{-1}{2\sqrt{3}} & \frac{3+\sqrt{3}}{6} \\ \frac{1}{2\sqrt{3}} & \frac{3-\sqrt{3}}{6} \end{pmatrix}, \quad (169)$$

and where the diagonalized matrix is

$$D = \begin{pmatrix} 2 - \sqrt{3} & 0 \\ 0 & 2 + \sqrt{3} \end{pmatrix}. \quad (170)$$

The resulting reformulation of equation (166) is thus

$$\begin{pmatrix} f_n \\ g_n \end{pmatrix} = 6 \begin{pmatrix} 1 - \sqrt{3} & 1 + \sqrt{3} \\ 1 & 1 \end{pmatrix} \begin{pmatrix} 2 - \sqrt{3} & 0 \\ 0 & 2 + \sqrt{3} \end{pmatrix}^n \begin{pmatrix} \frac{-1}{2\sqrt{3}} \\ \frac{1}{2\sqrt{3}} \end{pmatrix}, \quad (171)$$

Working out this expression gives that

$$\begin{pmatrix} f_n \\ g_n \end{pmatrix} = 6 \begin{pmatrix} 3 \\ 1 \end{pmatrix} \left[ 1 + \mathcal{O} \left( \left( \frac{2 - \sqrt{3}}{2 + \sqrt{3}} \right)^n \right) \right] (2 + \sqrt{3})^n, \quad (172)$$

which immediately yields equation (167). Similarly, calculations for the hexagonal tensor network under  $\mathbb{Z}_3$  were developed in this dissertation. Specifically, it can be calculated at which number of boundary tensor, the "flip" of the geodesics happens. To do this however, it must be realized that after the "flip" the "outside" of the geodesic is covered by the greedy algorithm instead of the "inside". Because at first instance, this might seem to be counter-intuitive, a simple example is shown in figure 41.

To determine when the sudden transition between geodesics happens, it suffices to calculate the minimal number of tensors needed to have the greedy algorithm reach the central tensor. When the central tensor is included, it is certain that the greedy algorithm covers the inside of the tensor network, and hence the "flip" has happened. To determine the minimal number of tensors for the greedy algorithm to reach the central tensor, it is necessary to go to a layer of the hexagonal tensor network which has an number of tensors divisible by the  $m$  of the  $\mathbb{Z}_m$  of interest. In that layer, the minimal region of tensors that cause the greedy algorithm to reach the central tensor can be determined by trial-and-error. Once this minimal region of the layer is determined, a recursive formula reminiscent of

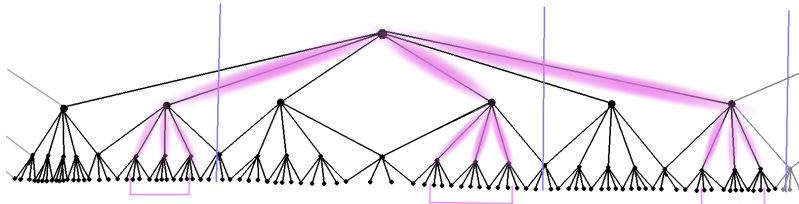


Figure 41: A visual representation of the open-folded hexagonal HaPPY tensor network for a  $\mathbb{Z}_3$  conical defect. In purple everything inside the greedy algorithm. It is obvious that the geodesic is on the inside of the purple region. So the greedy algorithm is outside the entanglement wedge. The blue lines indicate the  $\mathbb{Z}_3$  identifications. The grey areas are copies of the black areas on the other side. This indicates the that the tensor network is closed.

Table 1: An overview of the results of the calculations of the minimal and maximal fractions of the boundary regions needed to respectively include or bar the central tensor in/from the greedy algorithm as run on the  $\mathbb{Z}_n$  identified hexagonal HaPPY tensor network.

$\text{ADS}_3$	IDENTIFICATION	MINIMAL FRACTION	MAXIMAL FRACTION
$\mathbb{Z}_2$		$1/3$	$2/3$
$\mathbb{Z}_3$		0,27	$1/2$
$\mathbb{Z}_6$		0,27	0,80

the one used above to determine the number of each kind of tensor in each layer can be developed. Practically, these recursion relations are once more obtained as a tensor type counting exercise. Technical details, including the explicit form of the recursion relationships for several conical defect hexagonal HaPPY tensor networks, can be found in the appendix on tensor network calculations.

Having obtained the correct recursion relations for the amount of tensors that is needed in each layer (deeper than the one on which the trial-and-error was used) it is again possible to diagonalize and work out an equation for  $f'_n + g'_n$  of the same form that equation (172) has. Here,  $f'_n$  and  $g'_n$  are the  $f$  and  $g$  type tensors in layer  $n$  that are needed to obtain the "flip". For each of the considered conical defects, the leading order terms of this  $f'_n + g'_n$  expression can also be found in the appendix on tensor network calculations. This will turn out to be useful later on. One remark in this context is that these expressions are only valid for large  $n$ .

From the above described procedure, it is known how many tensors are needed for a flip in each layer. To compare this calculation to the continuum case, it has to be worked out what fraction of tensors at the boundary is necessary for

the greedy algorithm to reach the central tensor. To calculate this fraction, the expression for the minimal amount of tensors in layer  $n$  needed for the "flip" is divided by the total amount of tensors in that layer. Because the nominator in this expression is derived from recursion relations with initial conditions determined in a single wedge of the conical defect, the denominator of this expression has to be obtained by taking equation (167) and dividing it by the amount wedges in the covering space of the conical defect.

Finally, to obtain the explicit value of this fraction tensors at the boundary, the limit  $n \rightarrow \infty$  has to be applied to the above described calculation. As a result of this limit, only the dominant terms in both the nominator and the denominator remain (the sub-dominant terms turn out to converge to zero). Practically, one could look up the dominant term of  $f'_n + g'_n$  in the appendix (or calculate it as shown in the beginning of this section), divide it by the dominant term in equation (167), i.e.  $24(2 + \sqrt{3})^n$ , multiply the entire expression by the amount of wedges before taking the limit  $n \rightarrow \infty$ . The result is the (globally) minimal fraction of boundary tensors needed in the greedy algorithm to produce the "flip".

An important remark here is that because tensor networks are discrete, there might be some off-set in the above described calculation depending on where (angularly speaking) in the tensor network the initial minimal region is chosen. In the above prescription, the recursion relations is determined starting from the absolute minimal amount of tensors needed for the "flip". However, to obtain a better gauge of when the sudden transition happens, it also useful to look at local minima. Specifically, it is worthwhile to regard the maximum of all local minima. This region can also be determined by observation and trial-and-error and the same procedure obtain a fraction at the boundary as used previously, can be used. Once more, recursion relations for these regions and the resulting dominant terms in  $f'_n + g'_n$  can be found in the appendix on tensor network calculations.

The results for the boundary fractions for both minimum of all minima and the maximum of all minima in the cases of the  $\mathbb{Z}_2, \mathbb{Z}_3 \& \mathbb{Z}_6$  conical defect are shown in table 1. From these results it can be realized that the continuum value always lies in between the minimal and maximal fraction, which provides confidence in the fact that the greedy algorithm behaves (roughly) like Ryu-Takayanagi geodesics are known to do in the AdS/CFT correspondence, even in non-trivial spacetimes. This motivates the study of entwinement in tensor networks. One major question is whether or not a covering space picture can be developed for the hexagon HaPPY tensor network. Similarly, one may wonder if the long string model for entwinement can be linked to the tensor networks.

### 6.3 A COVERING SPACE PICTURE FOR TENSOR NETWORKS

In the previous chapter, the covering space picture for entwinement was discussed and, at least partially, expanded to a massive but non-rotating BTZ black hole.

In essence the idea was to take a covering space, typically  $\text{AdS}_3$ , and orbifold it to obtain a more complex spacetime upon which the geodesics become extremal but non-minimal curves. The idea is then that these curves correspond to the entwinement of the boundary CFT.

Because entwinement is expected [42, 43] to capture some kind of measure for the entanglement of the internal degrees of freedom of the CFT, it would be expected that a tensor network capable of simulating entwinement has some kind of internal structure on the boundary and is capable of forming more extremal but non-minimal curves via an algorithm akin to the greedy algorithm. In this dissertation it is shown that these aims can be achieved by orbifolding the hexagonal HaPPY tensor network.

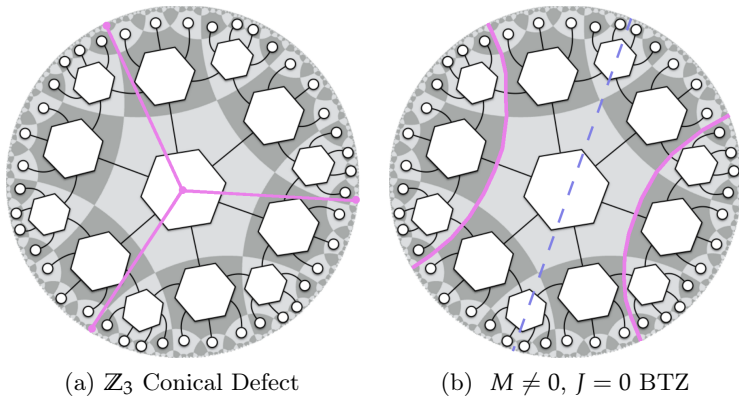


Figure 42: Graphical representation of two examples of orbifolded tensor networks. The pink lines show the edges of the fundamental domain. The dotted blue line show the extra reflective surface used in the massive non-rotating BTZ.

In the case of the conical defect, the orbifolding is relatively simple. If the tensor network is deep enough, there will be a layer whose number of tensors is divisible by the  $n \in \mathbb{N}$  that determines  $\mathbb{Z}_n$ . In this case the conical defect is found by taking the  $n$  copies of the conical defect geometry with their tensor network and superimposing them all on top of each other. This is distinctly different from other proposals for holographic tensor networks.

To obtain the winding geodesics expected from the covering space picture of conical defects, the greedy algorithm can be run on the covering  $\text{AdS}_3$  time-slice and the resulting discrete geodesic can be orbifolded. No qualitative differences compared to the continuum case show up. This set-up can be interpreted as having a network with tensors with  $6n$  legs, which gives it some sub-structure. The only subtlety here is in the central tensor, which has only 6 legs, each of them connected to one layer of sub-structure.

### 6.3.1 A Tensor Network for a Massive BTZ black hole

In the previous paragraphs, the multi-layered variant of the hexagonal HaPPY tensor network for the conical defect and its entwinement applications were briefly discussed. It is however not clear whether it is generically possible obtain a (multi-layered) hexagonal HaPPY tensor network, with an entwinement description, for a generic (orbifold) spacetime. In this dissertation it is shown that at least for a massive but non-rotating BTZ there exists cases in which it can be done via orbifold transformations on the hexagonal HaPPY tensor network on the  $t = 0$  time-slice of  $\text{AdS}_3$ .

Recall from the extensive discussion on the massive, non-rotating BTZ black hole as an orbifold of  $\text{AdS}_3$  that was held in the previous chapter, that the necessary orbifold transformations, for the regarded BTZ, can be obtained via a combination of reflections over geodesics in the  $t = 0$  time-slice of  $\text{AdS}_3$ . While extending this orbifold procedure to a tensor network setting, it is important to respect the tensor network structure. To make sure that this happens, the geodesics must be chosen so that they only cut through the middle of contracted tensor legs.

The above requirement on the geodesics clearly strongly limits the number of orbifold transformations that can be applied to a tensor network. To get a better or more intuitive understanding of which geodesics are still allowed, an alternative, more practical, formulation of the requirement on the geodesics must be considered [61, 62]. To do this, the tessellations of hyperbolic spaces that are related to tensor networks like the hexagonal HaPPY tensor network are needed. As explained in chapter four, the HaPPY tensor networks were constructed by tiling a time-slice of  $\text{AdS}_3$  and placing a tensor in the middle of each tile. The legs of the tensors meet at the middle of the edges of the tiles. In this way there is a (reciprocal) relationship between the tessellation of an  $\text{AdS}_3$  time-slice and the tensor network that is defined upon that time-slice.

In the language of hyperbolic tessellations of the  $t = 0$   $\text{AdS}_3$  time-slice, the above discussed requirement on the choice of geodesics in the orbifolding procedure is translated to the demand that the geodesics (over which must be reflected during the orbifolding) must lie entirely on edges of tiles of the tessellation. An example of geodesics fulfilling this requirement is shown in figure 42b, where it can clearly be seen that the geodesics (which are drawn in pink) run along the edges of tessellation tiles. From that figure it can also be deduced, considering the geometry of the Poincare disk, that those contracted tensor legs that are cut by the geodesic, are indeed cut right in the middle.

The fundamental domain of the BTZ shown in figure 42b, is the region in between the two geodesics. The tensor network in the fundamental domain can be read off from figure 42b. As in the beginning of this chapter, it is practical to develop a tensor network visualization that is not related to the underlying tessellation. The resulting visualization of the tensor network in the fundamental domain of the BTZ, can be seen in figure 43.

One aspect of the tensor network for a massive but non-rotating BTZ that can be seen in figure 43, is that it has open legs on the sides (shown in figure 43 with green dots). These open legs are caused by the cut made by the geodesics that demarcate the edges fundamental domain, which are exactly the geodesics that are used to reflect over in the orbifold transformation.

To close, i.e. contract, these legs there are two options, either glue them together [61, 62] as shown by the gray dotted lines and keep a single layer of tensor network or create a stack of tensor networks each of them each connected to neighboring layers via these legs on the side. In this second situation, the massive but non-rotating BTZ tensor network model is similar to the model for tensor network entwinement on conical defects discussed in the previous section. By applying the greedy algorithm to this BTZ tensor network setup with many layers of tensors, the greedy algorithm equivalent of winding geodesics can be obtained. Hence, once more, it is expected that entwinement of tensor networks requires some layers, or internal structure, of tensors.

### 6.3.2 The Coxeter group

In the above discussion it was postulated that the geodesics used in the orbifold transformation for massive but non-rotating BTZs must lie on the edges of the tessellation tiles of the tensor network, if the tensor network structure has to be respected. In this way, a hyperbolic tessellation determines which geodesics, and hence orbifold transformations, are allowed. Even though requirement that the geodesic must lie on the edges of the tiles of the tensor network can be understood on an intuitive level, i.e the tensor legs are cut in half, it is worthwhile to take a somewhat more mathematical look at the matter.

To gain a more general understanding why the above described geodesics must lie on the edges of the tessellation tiles of the tensor network of  $\text{AdS}_3$ , one must consider the how tessellations of the hyperbolic plane are constructed. Typically, a (regular) tessellation is constructed by placing a polygon, like for instance a hexagon or a pentagon, in the center of the hyperbolic space. This polygon is the first tile of the tessellation and the rest of the tiling is obtained by iteratively reflecting the polygon over its own edges. It is clear that exactly these reflections over the edges retain the tessellation structure and hence the tensor structure. So the reflections that do not break the tensor network structure are made of reflections over the edges of tiles, explaining the requirement on the geodesics.

The reflections over the edges of the tiles of a hyperbolic tessellation from a (formal) symmetry group known as the Coxeter group [176, 187, 188]. The Coxeter group has been used in the literature [61, 62] to discuss holographic tensors networks of other tessellations than those used in the HaPPY paper. It is currently not entirely clear if the greedy algorithm and/or the orbifold procedure described here can be expanded on those other holographic tensors networks.

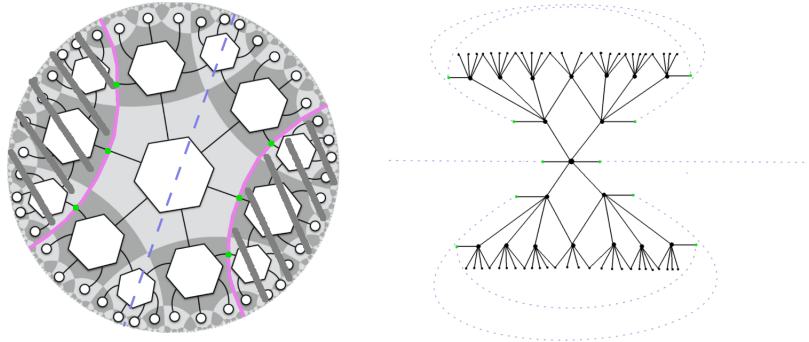


Figure 43: The hexagonal HaPPY tensor network for the fundamental domain of the massive non-rotating BTZ with  $\beta = 4\pi$ . On the left the corresponding fundamental domain is shown. The grey lines there, indicate the part of the tensor network that lies outside the fundamental domain. One option to deal with a tensor network like this is to glue together the edges, as shown here by green points and grey dotted lines (right figure). In the model proposed in this dissertation, the (infinite number of) copies of the fundamental domain are stacked upon each other creating a tensor network with sub-structure in the tensors.

#### 6.4 THE PATH TO SUB-ADS LOCALITY

As the situation stands, there is a tensor network model for entwinement, which probes the entanglement shadow, in terms of stacked tensors. An important comment here, is that there is now more than one tensor on each AdS-sized patch of bulk spacetime. As mentioned in the introduction, it is still unknown how the boundary CFT encodes the information of the gravitational physics within one AdS-sized bulk region. Ab initio, there are no concrete reason to suspect that entwinement, which was developed to probe a central bulk region, would play a significant role in answering the questions about sub-AdS locality which is present throughout the bulk, except maybe for the fact that the entanglement shadow around a BTZ black hole is of AdS size.

##### 6.4.1 Matrix Degrees of Freedom

To understand how entwinement is related to sub-AdS locality it is more than worthwhile to have a detailed discussion on the exact nature of the problem. Conceptually, it is known that there exists a so-called UV/IR-correspondence [12, 13] within the AdS/CFT correspondence. More concretely [47], an ultraviolet cut-off of the boundary CFT at a certain wavelength  $\delta$  is equivalent, in dimensionless units, to a radial cutoff at  $r = 1 - \delta$ . The question of sub-AdS locality is essentially one of how the information of the (quantum) gravitational physics within the radial cutoff is stored in a CFT subject to a UV cut-off.

Practically [13, 47], it is most convenient to study the sub-AdS locality conundrum in the  $\text{AdS}_5/\text{CFT}_4$  correspondence. Consider a 3-sphere in the boundary CFT, filled with UV cut-off cells of coordinate size  $\delta$ . The total number of cells needed to fill the ball is  $\mathcal{O}(\delta^{-3})$ . To facilitate a counting exercise, it is assumed [12, 13, 47] that each independent quantum field degree of freedom on the boundary corresponds to a single degree of freedom in each of the cut-off cells.

Recall from the second and third chapter of this dissertation that in AdS/CFT, the boundary physics governed by a supersymmetric  $SU(N)$  theory. The number of field degrees of freedoms in a  $U(N)$  theory is thus of order  $N^2$ . Therefore [12, 13], the number of boundary degrees of freedom  $N_{d.o.f.}$  inside the 3-sphere is of order,

$$N_{d.o.f.} \sim \mathcal{O}\left(\frac{N^2}{\delta^3}\right). \quad (173)$$

Taking this idea to its most extreme, i.e.  $\delta = 1$ , means looking at a bulk sphere of dimensionless volume 1. This kind of sphere has a proper radius [47] of  $R_{\text{AdS}}$  and a surface area of  $R_{\text{AdS}}^3$ . This thus means that an AdS-sized region of the bulk is described by  $\mathcal{O}(N^2)$  degrees of freedom. The great challenge of sub-AdS locality [47] is in understanding how these  $N^2$  (matrix) degrees of freedom encode the gravitational bulk physics within an AdS-sized sphere.

As a sanity check for the above counting exercise, it can easily be show that the degrees of freedom scale with the area of the sphere, as would be expected from the holographic principle. To do this [47] first realize, using for instance equation (53), that the area  $A$  of the considered 3-sphere times the compactified  $S^5$  is

$$A = \frac{R_{\text{AdS}}^8}{\delta^3}. \quad (174)$$

Then recall from the discussions below equation (50) and the discussion above equation (69) that  $R_{\text{AdS}}^4 = 4\pi g_s N l_s^4$  and  $2G = \pi^4 g_s^4 l_s^8$  so that it can be inferred that

$$\frac{A}{G} \sim \mathcal{O}\left(\frac{N^2}{\delta^3}\right). \quad (175)$$

Combining the two above equations with equation (173) gives that  $N_{d.o.f.} \sim A/G$ , so that the degrees of freedom do indeed [47] scale with area of the sphere. This verification of the above counting argument indicates that, at least in AdS/CFT, a region of AdS-size in the bulk can be described holographically by  $N^2$  boundary degrees of freedom, like for instance the entries of an  $N \times N$  matrix, but that the exact description is unknown.

#### 6.4.2 Long Strings to the Rescue

In the case of the  $\text{AdS}_3/\text{CFT}_2$  correspondence, specifically the conical defect, the number of tiles that are placed on one AdS-sized region is dependent on the choice

of  $n$  in  $\mathbb{Z}_n$ . Ideally, one would want to have a stack of  $N$  or  $N^2$  tensors on each tile (or one tensor valued tensor) and a (quantum information) bulk property related to those tensors. To achieve thi, the definition of entwinement as developed in the setting of the D1-D5 CFT has to be recalled. There, entwinement was seen as the entanglement entropy of sections of different windings, known as strands, of a set of closed, long strings, which describe the D1-D5 CFT. To introduce tensor networks to this setting, each long string is identified with the border of a tensor network. The windings of the long strings are achieved in the tensor network by making  $\mathbb{Z}_n$  identifications.

According to the earlier discussion on entwinement in D1-D5 CFT, the long string state for a  $\mathbb{Z}_m$  conical defect spacetime that is dual to the D1-D5 CFT has  $m$  windings in each long string. The number of long strings is  $N$ . The newly proposed holographic tensor network state dual to the  $\mathbb{Z}_m$  conical defect spacetime thus consists of  $N$  layers of tensors, where each group of  $m$  tensor layers is connected (cyclically) to itself at the angular boundary.

For massless BTZs, the same model can be applied as long as the procedure from the earlier discussion on entwinement in the continuum case is followed. In that setting, the canonical description was used in which the total number of strands were allowed to fluctuate. Because  $N$  is taken to be large,

$$\langle N_m \rangle = \frac{8}{\sinh\left(\sqrt{\frac{2\pi^2}{N}}m\right)}. \quad (176)$$

will be the dominant contribution. Again identification under  $\mathbb{Z}_m$  is used. Adding in the symmetrization under  $S_n$  gives the prescription of the holographic tensor network state dual to massless BTZs.

The above described novel tensor network model links entwinement with the sub-AdS locality problem. Currently the connection is mainly conceptual but one can hope on further expansion of this newly proposed holographic tensor network. In that regard, there are two subtleties to take into account. First off, each kind of dual spacetime would correspond to a different tensor network state. This makes general analysis challenging. The second subtlety is that the central tile is not covered by  $N$  tensors but by  $N/n$  tensors. In the case of a conical defect, for instance, the central tile is only covered by  $N/n$ .

#### 6.4.3 On Pluperfect Tensors and sub-AdS locality

Recently, an alternative tensor model that claims to capture some aspects of sub-AdS locality has been published [154]. Instead of using perfect tensors, that paper proposes to use plu-perfect tensors. Plu-perfect tensors are a generalization of perfect tensors obtained by imposing the so-called plu-perfection conditions. The goal of these conditions is to create a network called the bi-directional holographic code. Aside from trying to unify the holographic code and the holographic state into a single network, it tries to create a code with sub-AdS resolution.

Contrary to the approach taken in this dissertation, where most of the attention is given to the holographic HaPPY state, the authors of the paper about plu-perfect tensors focused on the holographic HaPPY code. In the holographic code, when trying to increase the number of tensors in each AdS-sized region of the bulk, the bulk Hilbert space becomes larger than dimension of boundary Hilbert space. By use of the plu-perfect conditions, the bi-directional holographic code creates a so-called "physical" bulk Hilbert space which would have a fitting size. Instead of stacking tensors on top of one-another as was proposed in this dissertation, the bi-directional holographic code is obtained by relaxing [154] the requirement to have a uniform tessellation of the Poincare disk. Due to the use of a non-uniform tessellation, it is possible to put more than one tensor on an AdS-sized region, introducing sub-AdS resolution to the tensor network. It is however, not clear if and how this tensor network can be used to shed light on the previously discussed encoding of the bulk degrees of freedom that lies at the heart of the sub-AdS locality.

## 6.5 CONCLUSION

In this chapter, the introduction of entwinement to tensor networks was presented. First it was shown that the sudden changeovers that characterize entanglement shadows are also present in the hexagonal HaPPY tensor network, specifically in the geometry of the  $\mathbb{Z}_2$ ,  $\mathbb{Z}_3$  and  $\mathbb{Z}_6$  conical defect. By using the covering space picture, exploiting the Coxeter group and using the greedy algorithm, winding geodesics can be obtained in tensor networks. In this approach tensor networks are formed that have multiple layers of tensors on each AdS-sized bulk patch.

An sich, there is no reason to expect that entwinement, which focuses on creating a link between boundary information, is linked to sub-Ads locality which is present throughout the bulk. To make the connection ever stronger, the long string model for entwinement in the D1-D5 CFT was extrapolated to the hexagonal HaPPY tensor network. The resulting holographic state contains a tensor network for each long string, which is orbifolded like a  $\mathbb{Z}_m$  conical defect where  $m$  indicates the number of windings in the string.

The resulting situation, has up to  $N$  tensors on each AdS-sized patch. These internal degrees of freedom are expected to describe an AdS-sized bulk region. An alternative model which gives up on the uniform tiling of the hyperbolic space, has recently been proposed in the literature. In that model, which uses a different kind of tensors, some form of sub-AdS resolution is achieved, so maybe the road to sub-AdS locality is indeed paved by tensors. More research on the similarities between the two described models and their relationship to sub-AdS locality is therefore necessary.



IV

## CONCLUSION AND OUTLOOK



### 7.1 QUANTUM INFORMATION, HOLOGRAPHY AND ENTWINEMENT

In the continuous attempt to unify all aspects of physics, the concept of holography has come to prominence. The AdS/CFT correspondence, the most common of holographic realizations, asserts that quantum gravity (UV completed by string theory) is equivalent to a lower-dimensional non-gravitational conformal field theory. Recently it has been discovered that holography, specifically AdS/CFT, has a connection with quantum information theory. In this dissertation that link was further explored.

The AdS/CFT correspondence is often conceived to be a relationship between a  $D + 1$ -dimensional quantum gravity theory in an asymptotically Anti de-Sitter spacetime and  $D$ -dimensional conformal field theory living on its boundary. Continuing this train of thought, it can be shown that bulk physics within particular minimal surfaces is reconstructible from the spatial entanglement entropy on the boundary of AdS. In certain (three-dimensional) cases however, there are certain central regions, known as the entanglement shadow, that cannot be accessed using boundary spatial entanglement entropy.

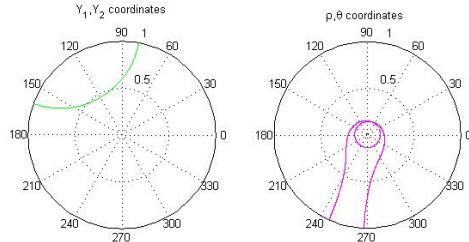


Figure 44: The effect of the orbifold transformation of a massive but non-rotating BTZ black hole. On the left side the  $t = 0$  time-slice of empty  $\text{AdS}_3$  with a geodesic. On the right the corresponding  $t = 0$  time-slice of the massive but non-rotating BTZ black hole. The geodesic has become a winding curves, that does no penetrate the black hole horizon. This is an example of how entwinement cannot be used to probe inside the horizon of a black hole.

To probe these regions, recent literature proposes the introduction of a new quantum informational measure on the boundary. This newly proposed quantum informational quantity – called entwinement – agrees with the lengths of non-minimal bulk curves and measures the internal entanglement of parts of the

boundary CFT. This is strongly reminiscent of how globally minimal bulk curves, i.e. geodesics, are known to correspond to the spatial entanglement entropy of the boundary region upon which their end-points are anchored.

Another region that cannot be probed by the entanglement entropy of the boundary CFT is the interior of a black hole. Because non-minimal bulk curves, related to entwinement, probe the entanglement shadow around a black hole horizon, one could wonder whether or not these curves also penetrate the black hole horizon. From the literature, it is known that single Ryu-Takayanagi surfaces in static spacetimes cannot probe beyond the horizon. It has been observed that the horizon of massless black holes in three-dimensional negatively curved spacetimes, i.e. massless BTZ black holes, cannot be probed by these non-minimal curves. In this dissertation, the same was seen for massive but non-rotating BTZ black holes.

In addition, it is unknown how bulk physics inside an AdS-sized region is encoded into the boundary CFT. This seeming lack of resolution is commonly known as the problem of sub-AdS locality. More specifically, sub-AdS locality is the question of how  $N^2$  boundary degrees of freedom describe the bulk physics within a 3-sphere of AdS-scale. The central result of this dissertation is that entwinement, a measure of the internal structure of the CFT, can be linked to sub-AdS locality via tensor networks. To understand this relationship, this dissertation had to expand the ideas of entwinement to orbifolded holographic tensor networks.

## 7.2 ORBIFOLDING HOLOGRAPHIC TENSOR NETWORKS

Tensor networks, which originate from condensed matter physics, are mathematical models that exploit the (entanglement) structure of a strongly coupled system to create a numerical simulation of that system. It has been proposed in the holography community that a tensor network could capture some aspects of AdS/CFT and make them tangible.

Harlow, Pastawski, Preskill and Yoshida (HaPPY) have shown that there are tensor networks which have a discrete analogy, called the greedy algorithm, of the geodesics described in the previous section. The same group of researchers showed that a tensor network exists that emulates certain quantum error correcting properties of AdS/CFT. Inspired by their success, this dissertation aspired to expand these tensor networks so that they could include some algorithmic version of entwinement.

A first way to describe entwinement, which is particularly useful for time-slices of three-dimensional spacetimes, is to start from empty AdS and then transform it so that both boundary and bulk consist of more than one layer. This approach creates some internal structure in the boundary CFT, the entanglement of which is captured by entwinement. It has been shown in the literature that by orbifolding  $\text{AdS}_3$ , i.e. taking identifications under its isometries, the geodesics of

the original  $\text{AdS}_3$  time-slice are turned into the extremal but non-minimal curves. Their length is the entwinement of the spacetimes obtained by orbifolding, e.g. conical defect, massless BTZ.

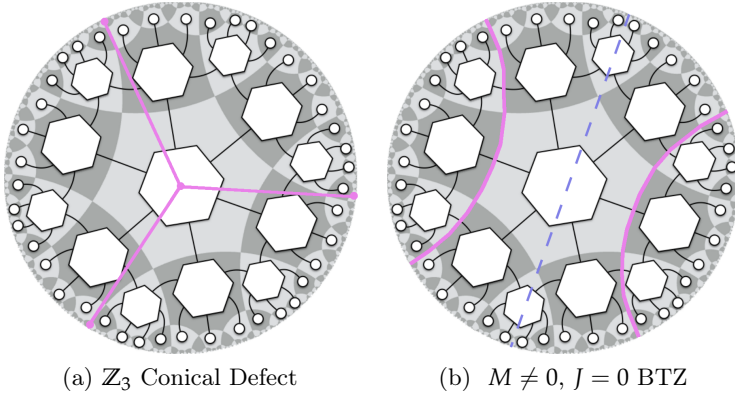


Figure 45: Graphical representation of two examples of how to orbifolded the hexagonal HaPPY tensor network. The pink lines show the edges of the fundamental domain. Throughout this thesis, these lines are referred to as the angular boundary. The dotted blue line show the extra reflective surface used in the massive non-rotating BTZ.

The reason that it is challenging to translate the above described covering space pictures to tensor networks, which impose some sort of hyperbolic tessellation, is that tensor networks do not retain all of the isometries of the underlying  $\text{AdS}_3$  time-slice. So depending on the choice of tensor network, the amount of possible orbifold transformations is limited. Nonetheless, it was shown in this dissertation that the hexagonal HaPPY tensor network and accompanying greedy algorithm can be transformed into a tensor network for conical defects and certain massive but non-rotating BTZ black holes. The main observation resulting from this endeavor, is that a system of stacked tensors is necessary to describe the non-minimal curves expected from entwinement.

### 7.3 SUB-ADS LOCALITY IN TERMS OF LONG STRINGS

A second, but seemingly equivalent, notion of entwinement can be found in the long string picture for discretely gauged theories like the D1-D5 CFT. In this model, entwinement is defined as the spatial entanglement entropy between different parts of the strands of the long strings. Recall that a strand is defined as a single winding of the long string. According to the literature, this kind of entanglement entropy can be calculated in the case of full decoupling – at the orbifold point – and it turns out to be equivalent to the length of the winding curves in the three-dimensional spacetimes dual to the strongly coupled regime of the D1-D5 CFT.

An important aspect of the above described model is that the number of windings of the long strings is  $N = N_1 N_5$  where  $N_1$  and  $N_5$  are the number of  $D1$ -branes and  $D5$ -branes. Following 't Hooft's argument  $N$  is taken to be large. The result is thus a system with a large number of strands. The boundary of a tensor network, which is essentially a spin chain, resembles a long string. In the previous section, it was explained that tensor networks can be folded up and hence it is possible to devise a set-up in which each long string is identified with a tensor network and where each winding is implemented as an orbifold of the tensor network.

Remarkably, this situation bridges the gap between the challenges of sub-AdS locality and the concept of entwinement. By folding the tensor networks and superimposing them, up to  $N$  tensors are placed upon each tile of the hyperbolic tessellation. The critical point here is that each polytope of the hexagonal HaPPY tensor network is AdS-sized. This shows that the tensor network model of entwinement according to the long string picture provides a natural way to introduce substructure to sub-AdS bulk physics. This insight is the first, albeit mainly conceptual, link between sub-AdS locality, tensor networks and entwinement.

#### 7.4 OUTLOOK

Even though an interesting conceptual relationship with entwinement was discovered, a solution for the problem of sub-AdS locality is still missing. A stricter or more concrete understanding of how the entwinement of the boundary CFT is related to the internal (entanglement) structure of a AdS sized region in the bulk might shed some light on the problem. There is at least one additional significant question regarding the  $D1$ - $D5$  tensor network model for entwinement that is directly related to the work presented in this dissertation.

As explained in the sixth chapter, there exists a recent and alternative approach to linking sub-AdS locality and tensor networks that makes use of plu-perfect tensors. There the idea is to push several tensor onto a single AdS sized area of the Poincare disk by using a non-uniform tessellation of the hyperbolic plane. Whether or not this model can be translated, in part or in whole, to the long string tensor model developed in this dissertation remains an open question.

Concerning the concept of entwinement itself there are many open questions. A central challenge for entwinement is that a definition in terms of a Neumann entropy is still missing. Another question is whether or not the definition for discrete gauge theories can be expanded to other kinds of theories. Furthermore, one can wonder whether or not that approach can be expanded to massive and rotating BTZ black holes. Currently, it is not clear how to construct the appropriate states nor is it generally known how to calculate the correlation function that follows from it.

Pertaining to two of the practical results developed in this dissertation, the covering space picture of massive but non-rotating BTZ black holes and the

(entwinement oriented) tensor network models of the same BTZ black holes and of the conical defects, it must be said that it is likely that there are significant challenges in expanding them. It is, for example, not clear how to deal with the non-trivial combination of time and space that would result from the orbifold transformations needed to obtain any kind of rotating BTZ.

Another challenge is to figure out how to take the  $n \rightarrow \infty$  limit of the  $\mathbb{Z}_n$  identifications made in the conical defect tensor network. The motivation for this is that the resulting tensor network would describe the geometry of a massless BTZ black hole, whose entwinement is understood in both the covering space picture and as a dual to the discretely gauge theories as discussed in chapter five. Similarly, it is unclear if a tensor network picture for massless BTZs can be obtained as the limit of either conical defect or massive non-rotating BTZ black hole.

Finally, it was realized during this dissertation that developing a solid notion of time-evolution for holographic tensor networks is a profound and pressing challenge. Not only is this development necessary to obtain tensor networks for rotating BTZs, it could also be useful to understand time-evolution of entwinement and the quantum error-correcting properties of AdS/CFT.

## 7.5 FURTHER READING

Even though the interplay of holography and quantum information is a young field of research, there are some excellent and extensive review papers available. A pedagogical overview of the quantum physics of black holes and holography, can be found in Daniel Harlow's "Jerusalem Lectures on Black Holes and Quantum Information" [189]. Extensive and insightful discussions (and diagrams) on the relationship between spacetime, entanglement and gravitation can be found in Mark Van Raamsdonk's "Lectures on Gravity and Entanglement" [144].

Takayanagi and Rangamani are currently writing a book on holography and quantum information and have published the early chapters [141] as an advanced review paper of the topic. Neither this paper nor the others mentioned in this section contain discussions on either entwinement or holographic tensor networks. In that last regard the original papers by Swingle [58] and the HaPPY collective [57] are strongly recommended. Most of the currently published aspects of entwinement in holography can be found in the two founding papers [42, 43] by Vijay Balasubramanian and his collaborators.

## 7.6 ONE MORE THING

And then finally, there is one more pressing open question, the first ever question asked in this dissertation; are we holographers or holographists? Neither the Cambridge nor the Oxford Advanced dictionary have any clear opinion on the matter. On-line use of the word 'holographer' is however common with regard

to the appropriate researchers in the field of photonics. Whether or not this colloquial use can be expanded to high-energy physics researchers is a matter of taste upon which the author of this dissertation has no further opinion to offer.

V

## TECHNICAL APPENDICES



# A

## NOTATION, CONVENTIONS AND SOME DIFFERENTIAL GEOMETRY

---

This appendix provides an overview of several notations and conventions as used in this dissertation. At the end some notions of differential geometry are recapped.

### A.1 NOTATION

- A. Spacetime indices are typically denoted by Greek letters at the end of the alphabet, i.e.  $\mu, \nu, \rho$ .
- B. Spinor indices are typically denoted by Greek letters at the beginning of the alphabet, i.e.  $\alpha, \beta, \gamma$ .
- C. Symmetry indices are typically denoted by capital Latin letters, i.e.  $A, B, C$ .

### A.2 CONVENTIONS

- A. The metric tensor used here is the "Mostly Minus" or "West Coast" metric, i.e.

$$\eta = \text{diag}(+, -, \dots, -).$$

- B. The Levi-Civita tensor is defined here according to

$$\epsilon_{0123} = 1 \quad \& \quad \epsilon^{0123} = -1.$$

- C. Anti-symmetrization is always taken with weight one, i.e.

$$A_{[ab]} = \frac{1}{2} (A_{ab} - A_{ba}).$$

- D. The gamma matrices are defined by

$$2g_{\mu\nu} = \gamma_\mu \gamma_\nu + \gamma_\nu \gamma_\mu,$$

$$(\gamma^\mu)^\dagger = \gamma^0 \gamma_\nu \gamma^0,$$

$$\gamma_{\mu\nu} = \gamma_{[\mu} \gamma_{\nu]}, \quad \gamma_{\mu\nu\rho} = \gamma_{[\mu} \gamma_{\nu} \gamma_{\rho]} \dots$$

## A.3 DIFFERENTIAL GEOMETRY

Throughout this dissertation, standard notions from differential geometry are used. In the interest of thoroughness, some of them are briefly recapped here.

- A. Of the different concepts that can be defined within differential geometry, totally anti-symmetric tensors have received special attention. They are known as  $p$ -forms and are defined, in function of the coordinate differentials  $dx^\mu$ , as

$$\omega^{(p)} = \frac{1}{p!} \omega_{\mu_1 \mu_2 \dots \mu_p} dx_1^\mu \wedge dx_2^\mu \wedge \dots \wedge dx_p^\mu.$$

- B. The wedge product  $\wedge$  used in the above expression is defined as

$$\omega^{(p)} \wedge v^{(q)} = (p+q)! \omega_{[\mu_1 \mu_2 \dots \mu_p} v_{\mu_{p+1} \mu_{p+2} \dots \mu_{p+q}]}$$

- C. The exterior derivative is defined as completely antisymmetric by

$$d\omega^{(p)} = \frac{1}{p!} \partial_\mu \omega_{\mu_1 \mu_2 \dots \mu_p} dx^\mu \wedge dx_1^\mu \wedge dx_2^\mu \wedge \dots \wedge dx_p^\mu.$$

- D. On a  $D$ -dimensional manifold, any  $D$ -form can be chosen as an integral defining volume form  $\omega$ ,

$$I = \int \omega.$$

In essence, this integral is thus nothing more than a map from an  $D$ -form (field) to the real numbers. The canonical volume form  $dx^D$  is defined by

$$dx^D = dx^0 \wedge dx^1 \wedge \dots \wedge dx^{D-1},$$

which due to the definition of the wedge product is indeed a  $D$ -form. Recall that the Levi-Civita tensor is defined by  $\epsilon_{\mu\nu\dots\rho} = \sqrt{|\det(g)|} \bar{\epsilon}_{\mu\nu\dots\rho}$  where  $\bar{\epsilon}$  is the Levi-Civita symbol. Choosing

$$\omega = \frac{1}{D!} \epsilon_{\mu\nu\dots\rho} dx^\mu \wedge dx^\nu \wedge \dots \wedge dx^\rho$$

allows the volume elements  $\omega$  and  $dx^D$  to be related to one-another because,

$$\frac{1}{D!} \epsilon_{\mu\nu\dots\rho} dx^\mu \wedge dx^\nu \wedge \dots \wedge dx^\rho = \frac{1}{D!} \sqrt{|\det(g)|} \bar{\epsilon}_{\mu\nu\dots\rho} dx^\mu \wedge dx^\nu \wedge \dots \wedge dx^\rho,$$

so that

$$\omega = \frac{1}{D!} \sqrt{|\det(g)|} \bar{\epsilon}_{\mu\nu\dots\rho} dx^\mu \wedge dx^\nu \wedge \dots \wedge dx^\rho = \sqrt{|\det(g)|} dx^D,$$

so that integral over a scalar function  $\phi(x)$  (like a Lagrangian density) on a  $D$ -dimensional manifold is given by,

$$I = \int \phi(x) \sqrt{|\det(g)|} dx^D.$$

# B

## THREE-DIMENSIONAL GRAVITY AS A CHERN-SIMONS THEORY

---

### B.1 CHERN-SIMONS THEORIES

It was shown in the second chapter of this dissertation that gravity can be expressed in terms similar to that of a gauge theory. In the case of three-dimensional gravity, the theory can be expressed [50, 51] exactly as gauge theory, more specifically as a Chern-Simons type of gauge theory. Chern-Simons theories [50, 163] are topological theories; which means that they can be written purely in terms of a gauge field, without the requirement of an involvement of a metric tensor.

For a compact symmetry group  $G$  with a gauge field  $A = A_\mu dx^\mu$ , a Chern-Simons gauge theory is of the form [50, 163]

$$S_{\text{C.S.}} = \int d^D x \text{Tr} \left[ A \wedge dA + \frac{2}{3} A \wedge A \wedge A \right], \quad (177)$$

where the wedge product  $\wedge$  and the exterior derivative  $d$  are defined as discussed in the appendix on differential geometry. The variation of the action with respect to  $A$  gives [51], via integration by parts, that

$$\delta S_{\text{C.S.}} = \int d^D x \text{Tr} [2\delta A \wedge (dA + A \wedge A)] - \int_{\partial} d^{D-1} x \text{Tr} [A \wedge \delta A]. \quad (178)$$

Assuming that the variation of the gauge field,  $\delta A$ , vanishes at the boundary, the second integral term can be dropped. Then the equation motions require that the field strength

$$F \doteq (dA + A \wedge A), \quad (179)$$

must vanish. Locally, this implies that  $A = g^{-1}dg$  with  $g \in G$  so that  $A$  is purely a gauge term which explains why the Chern-Simons theory [50, 163] has no propagating, i.e. dynamical, degrees of freedom.

### B.2 NEGATIVELY CURVED THREE-DIMENSIONAL GRAVITY

To obtain [51] a Chern-Simons theory for three-dimensional gravity with  $\Lambda < 0$ , take the symmetry group  $G = \text{SL}(2, \mathbb{R})$ . This particular choice will be motivated later on. Starting from the frame field,  $e^a = e_\mu^a dx^\mu$ , and the spin connection  $\omega^a = \frac{1}{2}\epsilon^{abc}\omega_{\mu bc}dx^\mu$ , two gauge fields can be defined as,

$$A^{(\pm)a} = \omega^a \pm \frac{1}{R_{\text{AdS}}}e^a. \quad (180)$$

In the mostly minus-sign metric, the corresponding generators  $T^a$  are given [164] by

$$T^0 = \begin{pmatrix} 0 & 1/2 \\ -1/2 & 0 \end{pmatrix}, \quad T^1 = \begin{pmatrix} 1/2 & 0 \\ 0 & -1/2 \end{pmatrix}, \quad T^2 = \begin{pmatrix} 0 & 1/2 \\ 1/2 & 0 \end{pmatrix}. \quad (181)$$

Now, inspired by the Lie algebra isomorphism  $SO(2, 2) = SL(2, \mathbb{R}) + SL(2, \mathbb{R})$  it is postulated [51, 164] that the Chern-Simons theory for three-dimensional gravity is a combination of the Chern-Simons theories for  $A^+$  and  $A^-$ , specifically

$$S_{\text{C.S.}} = S_{\text{C.S.}}(A^+) - S_{\text{C.S.}}(A^-), \quad (182)$$

is proposed. Indeed, the above expression can be worked out [51, 164] and rewritten [51] to read,

$$S_{\text{C.S.}} = \int \left( 2e^a \wedge d\omega_a + \frac{1}{2}\epsilon_{abc}\omega^b \wedge \omega^c + \frac{1}{3R_{\text{AdS}}^2}\epsilon_{abc} e^a \wedge e^b \wedge e^c \right), \quad (183)$$

which is the frame-field equivalent of equation (133). Three-dimensional gravity is thus a Chern-Simons gauge theory which are always purely topological theories. To assure [51] that the variation of the Chern-Simons action is well-defined, boundary conditions have to be imposed.

# C

## TENSOR NETWORK CALCULATIONS

---

### C.1 GENERAL APPROACH

As explained in the sixth chapter, to calculate when the "flip" happens in  $\mathbb{Z}_m$  orbifolded tensor networks, certain recursive formulas for the  $f$  and  $g$  type tensors in the minimal regions have to be developed. There, the remark was made that there are different locally minimal regions of a layer of a tensor network. With minimal, it is meant that the amount of tensors in that regions just suffice for the greedy algorithm to include the central tensor. In this appendix the recursion relations are given for both the absolute minimum regions and the maximum of the locally minimal regions. The only qualatively new feature here, arises in the case of the absolute minimal regions. This feature is that there recursive formula's are of the form,

$$\begin{pmatrix} f'_{n+1} \\ g'_{n+1} \end{pmatrix} = M \begin{pmatrix} f'_n \\ g'_n \end{pmatrix} + P,$$

where  $M$  is  $2 \times 2$ -matrix and where  $P$  is an extra vector. The reason for this extra vector is that each tensor will produce more than three tensors in the next layer and the greedy algorithm only needs three legs. The vector  $P$  will remove the superficial legs from the minimal counting. To obtain the  $n \rightarrow \infty$  limit of these cases, almost the same procedure as explained in chapter six can be used to work out the above expressions in function of some initial conditions. Specifically, equations of the form

$$\begin{pmatrix} f'_n \\ g'_n \end{pmatrix} = M^n \begin{pmatrix} f'_{i.c.} \\ g'_{i.c.} \end{pmatrix} + \sum_{k=0}^{n-k} M^k P.$$

will be used. Notice that there is an extra term dealing with the vector  $P$ . When trying to determine  $f'_n + g'_n$ , this term is dealt with by use of the formula

$$\sum_{k=0}^n z^k = \frac{1 - z^{n+1}}{1 - z}. \quad (184)$$

To determine the initial conditions for each different conical defect, the tensor network must be drawn up to a layer where the total amount of tensors is divisible by  $m$ . There, the minimal/maximal section of tensors must be determined by observation. Notice also, that the recursive formulas are only valid from that layer on. By repeating the diagonalization procedure used in chapter six, the  $n \rightarrow \infty$  limit of the resulting expression for the amount of tensors needed for the

flip can be obtained. The recursive formulas for the different kind of  $\mathbb{Z}_m$  orbifolds are given in this appendix. In addition the relevant – being the dominant – parts of the expressions for the amount of  $g_n + f_n$  tensors for large  $n$  resulting from the recursive relationships are shown.

### C.2 CASE 1: $\mathbb{Z}_2$

#### A. Minimal section

$$\begin{pmatrix} f'_{n+1} \\ g'_{n+1} \end{pmatrix} = \begin{pmatrix} 3 & 2 \\ 1 & 1 \end{pmatrix} \begin{pmatrix} f'_n \\ g'_n \end{pmatrix} + \begin{pmatrix} -2 \\ -1 \end{pmatrix} \quad \& \quad \text{I.C. } \begin{pmatrix} 4 \\ 1 \end{pmatrix},$$

$$f'_n + g'_n \approx \frac{(2 + \sqrt{3})^2 (2 + \sqrt{3})^n}{\sqrt{3}}.$$

#### B. Maximal section

$$\begin{pmatrix} f'_{n+1} \\ g'_{n+1} \end{pmatrix} = \begin{pmatrix} 3 & 2 \\ 1 & 1 \end{pmatrix} \begin{pmatrix} f'_n \\ g'_n \end{pmatrix} + \begin{pmatrix} 0 \\ 0 \end{pmatrix} \quad \& \quad \text{I.C. } \begin{pmatrix} 6 \\ 2 \end{pmatrix},$$

$$f'_n + g'_n \approx \frac{(2 + \sqrt{3})^2 (2 + \sqrt{3})^n}{2\sqrt{3}}.$$

### C.3 CASE 2: $\mathbb{Z}_3$

#### A. Minimal section

$$\begin{pmatrix} f'_{n+1} \\ g'_{n+1} \end{pmatrix} = \begin{pmatrix} 3 & 2 \\ 1 & 1 \end{pmatrix} \begin{pmatrix} f'_n \\ g'_n \end{pmatrix} + \begin{pmatrix} -2 \\ -1 \end{pmatrix} \quad \& \quad \text{I.C. } \begin{pmatrix} 3 \\ 0 \end{pmatrix},$$

$$f'_n + g'_n \approx \frac{(2 + \sqrt{3})(2 + \sqrt{3})^n}{\sqrt{3}}.$$

#### B. Maximal section

$$\begin{pmatrix} f'_{n+1} \\ g'_{n+1} \end{pmatrix} = \begin{pmatrix} 3 & 2 \\ 1 & 1 \end{pmatrix} \begin{pmatrix} f'_n \\ g'_n \end{pmatrix} + \begin{pmatrix} 0 \\ 0 \end{pmatrix} \quad \& \quad \text{I.C. } \begin{pmatrix} 3 \\ 1 \end{pmatrix},$$

$$f'_n + g'_n \approx \frac{(2 + \sqrt{3})^2 (2 + \sqrt{3})^n}{2\sqrt{3}}.$$

### C.4 CASE 3: $\mathbb{Z}_6$

#### A. Minimal section

$$\begin{pmatrix} f'_{n+1} \\ g'_{n+1} \end{pmatrix} = \begin{pmatrix} 3 & 2 \\ 1 & 1 \end{pmatrix} \begin{pmatrix} f'_n \\ g'_n \end{pmatrix} + \begin{pmatrix} -2 \\ -1 \end{pmatrix} \quad \& \quad \text{I.C. } \begin{pmatrix} 4 \\ 1 \end{pmatrix},$$

$$f'_n + g'_n \approx \frac{(2 + \sqrt{3})(2 + \sqrt{3})^n}{2\sqrt{3}}.$$

B. Maximal section

$$\begin{pmatrix} f'_{n+1} \\ g'_{n+1} \end{pmatrix} = \begin{pmatrix} 3 & 2 \\ 1 & 1 \end{pmatrix} \begin{pmatrix} f'_n \\ g'_n \end{pmatrix} + \begin{pmatrix} 0 \\ 0 \end{pmatrix} \quad \& \quad \text{I.C. } \begin{pmatrix} 3 \\ 0 \end{pmatrix} \text{ or } \begin{pmatrix} 2 \\ 1 \end{pmatrix}.$$

$$f'_n + g'_n \approx \frac{3(2 + \sqrt{3})(2 + \sqrt{3})^n}{2\sqrt{3}}.$$



# D

## CODE LISTING OF SELECTED GRAPHS

---

### D.1 FIGURE 34

```
1 %% preamble
close all
R = 1;
eta = -1;
X_00 = cosh(eta)*R:0.00001:10;
6 X_01 = 10:0.1:1000;
X_0 = [X_00 X_01];
phi = (-35)*pi/180;
figure

11 %% geodesic 1 & 2
eta = 1;
Y1_1 = (X_0.*tanh(eta))./(1 + X_0);
Y2_1 = sqrt(X_0.*X_0 - (cosh(eta)*R)^2)./(cosh(eta).*(1 + X_0));

16 [theta,rho] = cart2pol(Y1_1,Y2_1);
polar(theta,rho, 'b')
hold all
[theta,rho] = cart2pol(Y1_1,-Y2_1);
polar(theta,rho, 'b')

21 Y1_2 = (X_0.*tanh(-eta))./(1 + X_0);
Y2_2 = sqrt(X_0.*X_0 - (cosh(eta)*R)^2)./(cosh(-eta).*(1 + X_0));

26 [theta,rho] = cart2pol(Y1_2,Y2_2);
polar(theta,rho, 'b')
[theta,rho] = cart2pol(Y1_2,-Y2_2);
polar(theta,rho, 'b')

31 %% geodesic 3
eta = 0;
Y1_3 = 0;
X_0_3 = cosh(eta):100;
Y2_3 = sqrt(X_0_3.*X_0_3 - (cosh(eta)*R)^2)./(cosh(eta).*(1 + X_0_3));
36 [theta,rho] = cart2pol(Y1_3,Y2_3);
polar(theta,rho, 'b')
[theta,rho] = cart2pol(Y1_3,-Y2_3);
polar(theta,rho, 'b')
```

```

41
%% geodesic 4
eta = -1;
Y1_4 = (X_0.*tanh(eta))./(1 + X_0);
Y2_4 = sqrt(X_0.*X_0 - (cosh(eta)*R)^2)./(cosh(eta).*(1 + X_0));
46
[theta,rho] = cart2pol(Y1_4,Y2_4);
theta = theta + phi;
[Y1n,Y2n]= pol2cart(theta,rho);
polar(theta,rho, 'g')
51 [theta,rho] = cart2pol(Y1_4,-Y2_4);
theta = theta + phi;
[Y1nn,Y2nn]= pol2cart(theta,rho);
polar(theta,rho, 'g')

56 %% mirrors
Y1_full = [Y1nn Y1n];
Y2_full = [Y2nn Y2n];
Y1s_cover = Y1_full;
Y2s_cover = Y2_full;
61 Y1_final = [];
Y2_final = [];

while length(Y1s_cover) ~= 0
    [Y1_fund,Y2_fund,Y1s_cover,Y2s_cover] = mirror(Y1s_cover,Y2s_cover);
66    length(Y1_fund)
    Y1_final = [Y1_final Y1_fund];
    Y2_final = [Y2_final Y2_fund];
end
[theta,rho] = cart2pol(Y1_final,Y2_final);
71 h = polar(theta,rho, '.r');
set(h, 'markersize',3)
[theta,rho] = cart2pol(Y1s_cover,Y2s_cover);
polar(theta,rho, 'm');

```

## D.2 FIGURE 35

```

1 %% param
Beta = 4*pi*pi;
phi = (-60)*pi/180;

%% preamble
6 close all
R = 1;
l = R;
T = 1/Beta;
eta = Beta/(4*pi*pi);
11 r_plus = (eta*l)/(2*pi);

```

```

X_00 = cosh(eta)*R:0.00001:10;
X_01 = 10:0.1:1000;
X_0 = [X_00 X_01];
16
%% COV FIG

figure
subplot(2,2,1) % first plot in 1 x 3 grid
21
%% geodesic 1 & 2
Y1_1 = (X_0.*tanh(eta))./(1 + X_0);
Y2_1 = sqrt(X_0.*X_0 - (cosh(eta)*R)^2)./(cosh(eta).* (1 + X_0));
26 [theta,rho] = cart2pol(Y1_1,Y2_1);
polar(theta,rho,'b')
hold all
[theta,rho] = cart2pol(Y1_1,-Y2_1);
polar(theta,rho,'b')
31 Y1_2 = (X_0.*tanh(-eta))./(1 + X_0);
Y2_2 = sqrt(X_0.*X_0 - (cosh(eta)*R)^2)./(cosh(-eta).* (1 + X_0));
[theta,rho] = cart2pol(Y1_2,Y2_2);
36 polar(theta,rho,'b')
[theta,rho] = cart2pol(Y1_2,-Y2_2);
polar(theta,rho,'b')

%% geodesic 3
41 eta_3 = 0;
Y1_3 = 0;
X_0_3 = cosh(eta_3):100;
Y2_3 = sqrt(X_0_3.*X_0_3 - (cosh(eta_3)*R)^2)./(cosh(eta_3).* (1 + X_0_3));
46 [theta,rho] = cart2pol(Y1_3,Y2_3);
polar(theta,rho,'b')
[theta,rho] = cart2pol(Y1_3,-Y2_3);
polar(theta,rho,'b')
51 %% geodesic 4
eta_4 = -1;
Y1_4 = (X_0.*tanh(eta_4))./(1 + X_0);
Y2_4 = sqrt(X_0.*X_0 - (cosh(eta_4)*R)^2)./(cosh(eta_4).* (1 + X_0));
56 [theta,rho] = cart2pol(Y1_4,Y2_4);
theta = theta + phi;
[Y1n,Y2n]= pol2cart(theta,rho);
polar(theta,rho,'g')
[theta,rho] = cart2pol(Y1_4,-Y2_4);
61 theta = theta + phi;

```

```

[Y1nn,Y2nn]= pol2cart(theta,rho);
polar(theta,rho,'g')

title('covering space')
66
%% FUND FIG

subplot(2,2,2) % second plot in 1 x 3 grid

71 %% geodesic 1 & 2 (repeated)
Y1_1 = (X_0.*tanh(eta))./(1 + X_0);
Y2_1 = sqrt(X_0.*X_0 - (cosh(eta)*R)^2)./(cosh(eta).*(1 + X_0));

[theta,rho] = cart2pol(Y1_1,Y2_1);
76 polar(theta,rho,'b')
hold all
[theta,rho] = cart2pol(Y1_1,-Y2_1);
polar(theta,rho,'b')

81 Y1_2 = (X_0.*tanh(-eta))./(1 + X_0);
Y2_2 = sqrt(X_0.*X_0 - (cosh(eta)*R)^2)./(cosh(-eta).*(1 + X_0));

[theta,rho] = cart2pol(Y1_2,Y2_2);
polar(theta,rho,'b')
86 [theta,rho] = cart2pol(Y1_2,-Y2_2);
polar(theta,rho,'b')

%% mirrors
Y1_full = [Y1nn Y1n];
91 Y2_full = [Y2nn Y2n];
Y1s_cover = Y1_full;
Y2s_cover = Y2_full;
Y1_final = [];
Y2_final = [];
96
while length(Y1s_cover) ~= 0
    [Y1_fund,Y2_fund,Y1s_cover,Y2s_cover] = mirror2(Y1s_cover,Y2s_cover,
        eta);
    length(Y1_fund)
    Y1_final = [Y1_final Y1_fund];
101    Y2_final = [Y2_final Y2_fund];
end

[theta,rho] = cart2pol(Y1_final,Y2_final);
h = polar(theta,rho,'r');
106 set(h,'markersize',3)
[theta,rho] = cart2pol(Y1s_cover,Y2s_cover);
hold all
polar(theta,rho,'m');

```

```

111 title('fundamental domain')

%% BTZ

subplot(2,2,3) % third plot in 1 x 3 grid
116
Y1 = Y1_final;
Y2 = Y2_final;

X1 = 2.*Y2./(1 - Y1.^2 - Y2.^2);
121 X0 = (1 + Y1.^2 + Y2.^2)./(1 - Y1.^2 - Y2.^2);
X2 = 2.*Y1./(1 - Y1.^2 - Y2.^2);

r_plus = (eta*l)/(2*pi);
phi = l/(2*r_plus)*log(((X0-X2).*R)./(X0+X2));
126 r = r_plus*((X1./R).^2 + 1).^(1/2);

rho = atan(r);
rho = (2/pi)*rho;

131 h = polar(phi,rho,'.m')
set(h,'markersize',3)
rectangle('Position',[-(2/pi)*atan(r_plus),-(2/pi)*atan(r_plus),2*(2/pi)*
    atan(r_plus),2*(2/pi)*atan(r_plus)],'Curvature',[1 1],'FaceColor',[

0.12 0.12 0.85 ])
title('BTZ: \rho,\theta coordinates')

```



## BIBLIOGRAPHY

---

- [1] C. Kiefer. Conceptual Problems in Quantum Gravity and Quantum Cosmology. arXiv:gr-qc/0508120.
- [2] C. Kittel and H. Kroemer. *Thermal Physics*. W. H. Freeman, 1980. ISBN 9780716710882.
- [3] S. W. Hawking, J. M. Bardeen, and B. Carter. The four laws of black hole mechanics. *Communications in Mathematical Physics*, 31:161–170, June 1973. doi: 10.1007/BF01645742.
- [4] J. D. Bekenstein. Black Holes and Entropy. *Physical Review Letters D*, 7: 2333–2346, April 1973.
- [5] D. N. Page. Hawking radiation and black hole thermodynamics. *New Journal of Physics*, 7:203, September 2005. doi: 10.1088/1367-2630/7/1/203.
- [6] G. 't Hooft. Dimensional Reduction in Quantum Gravity. *ArXiv General Relativity and Quantum Cosmology e-prints*, October 1993. ArXiv:gr-qc/9310026.
- [7] L. Susskind. The world as a hologram. *Journal of Mathematical Physics*, 36: 6377–6396, November 1995. doi: 10.1063/1.531249. ArXiv:hep-th/9409089.
- [8] J. Maldacena. The Large-N Limit of Superconformal Field Theories and Supergravity. *International Journal of Theoretical Physics*, 38:1113–1133, 1999. Arxiv:hep-th/9711200.
- [9] S. S. Gubser, I. R. Klebanov, and A. M. Polyakov. Gauge theory correlators from non-critical string theory. *Physics Letters B*, 428:105–114, May 1998. doi: 10.1016/S0370-2693(98)00377-3. Arxiv:hep-th/9802109.
- [10] K. Becker, M. Becker, and J.H. Schwarz. *String Theory and M-Theory: A Modern Introduction*. Cambridge University Press, 2006. ISBN 9781139460484.
- [11] E. Witten. Anti-de Sitter space and holography. *Advances in Theoretical and Mathematical Physics*, 2:253–291, 1998. ArXiv:hep-th/9802150.
- [12] A. W. Peet and J. Polchinski. UV-IR relations in AdS dynamics. *ArXiv:hep-th/9809022*, 59(6):065011, March 1999. doi: 10.1103/PhysRevD.59.065011.
- [13] L. Susskind and E. Witten. The Holographic Bound in Anti-de Sitter Space. *ArXiv: hep-th/9805114*, May 1998.

- [14] Wikimedia Commons. Three-dimensional anti-de sitter space. <https://commons.wikimedia.org/w/index.php?curid=28910811>, . By Polytope24 - Own work, CC BY-SA 3.0, Accessed: 2017-01-26.
- [15] InspireHEP. Citation page for 'the large n limit of superconformal field theories and supergravity '. <http://inspirehep.net/record/451647/citations>. Accessed: 2017-01-26.
- [16] M. Harrison, T. Ludlam, and S. Ozaki. RHIC project overview. *Nuclear Instruments and Methods in Physics Research A*, 499:235–244, March 2003. doi: 10.1016/S0168-9002(02)01937-X.
- [17] M. Luzum and P. Romatschke. Conformal relativistic viscous hydrodynamics: Applications to RHIC results at  $s_{NN}=200$  GeV. *arXiv:nucl-th/0804.4015*, 78(3):034915, September 2008. doi: 10.1103/PhysRevC.78.034915.
- [18] Z. Merali. Collaborative physics: String theory finds a bench mate. *Nature*, 478:302–304, October 2011. doi: 10.1038/478302a.
- [19] W. A. Zajc. The Fluid Nature of Quark-Gluon Plasma. *Nuclear Physics A*, 805:283–294c, June 2008.
- [20] P. K. Kovtun, D. T. Son, and A. O. Starinets. Viscosity in Strongly Interacting Quantum Field Theories from Black Hole Physics. *Physical Review Letters*, 94(11):111601, March 2005. Arxiv:hep-th/0405231.
- [21] S. Sachdev. What can gauge-gravity duality teach us about condensed matter physics? *ArXiv e-prints: arXiv:1108.1197 [cond-mat.str-el]*, August 2011.
- [22] T. J. Osborne and M. A. Nielsen. Entanglement in a simple quantum phase transition. *Phys. Rev. A*, 66(3):032110, September 2002.
- [23] A. Osterloh, L. Amico, G. Falci, and R. Fazio. Scaling of entanglement close to a quantum phase transition. *Nature*, 416:608–610, April 2002.
- [24] R J Costa Farias and M C de Oliveira. Entanglement and the mott insulator–superfluid phase transition in bosonic atom chains. *Journal of Physics: Condensed Matter*, 22(24):245603, 2010.
- [25] S. Sachdev. Strange and Stringy. *Scientific American*, 308(1):44–51, December 2012. doi: 10.1038/scientificamericano113-44.
- [26] R. Islam, R. Ma, P. M. Preiss, M. Eric Tai, A. Lukin, M. Rispoli, and M. Greiner. Measuring entanglement entropy in a quantum many-body system. *Nature*, 528:77–83, December 2015.

- [27] A. Schmitt. *Introduction to Superfluidity: Field-theoretical Approach and Applications*. Springer International Publishing, 2014. ISBN 9783319079479.
- [28] M. Ammon and J. Erdmenger. *Gauge/Gravity Duality: Foundations and Applications*. Cambridge University Press, 2015. ISBN 9781316239728.
- [29] Clifford V. Johnson and Peter Steinberg. What black holes teach about strongly coupled particles. *Physics Today*, 63(5):29, 2010.
- [30] A. Buchleitner, C. Viviescas, and M. Tiersch. *Entanglement and Decoherence: Foundations and Modern Trends*. Lecture Notes in Physics. Springer Berlin Heidelberg, 2008.
- [31] C.E. Shannon and W. Weaver. *The Mathematical Theory of Communication*. University of Illinois Press, 1998. ISBN 9780252725463.
- [32] W.H. Zurek. *Complexity, Entropy, and the Physics of Information: The Proceedings of the 1988 Workshop on Complexity, Entropy, and the Physics of Information Held May-June, 1989, in Santa Fe, New Mexico*. Proceedings volume in the Santa Fe Institute studies in the sciences of complexity. Addison-Wesley, 1990. ISBN 9780201515060.
- [33] S. Ryu and T. Takayanagi. Holographic Derivation of Entanglement Entropy from the anti de Sitter Space/Conformal Field Theory Correspondence. *Physical Review Letters*, 96(18):181602, May 2006. doi: 10.1103/PhysRevLett.96.181602.
- [34] M.A. Nielsen and I.L. Chuang. *Quantum Computation and Quantum Information: 10th Anniversary Edition*. Cambridge University Press, 2010. ISBN 9781139495486.
- [35] Simons Foundation. 'about'page for 'it from qubit: Simons collaboration on quantum fields, gravity and information'. <https://www.simonsfoundation.org/mathematics-and-physical-science/>, note = Accessed: 2017-01-26.
- [36] M. van Raamsdonk. Building up spacetime with quantum entanglement. *General Relativity and Gravitation*, 42:2323–2329, October 2010. doi: 10.1007/s10714-010-1034-0. arXiv:hep-th/1005.3035.
- [37] E. Bianchi and R. C. Myers. On the Architecture of Spacetime Geometry. *ArXiv e-prints*, December 2012. arXiv:hep-th/1212.5183.
- [38] N. Lashkari, M. B. McDermott, and M. Van Raamsdonk. Gravitational dynamics from entanglement "thermodynamics". *Journal of High Energy Physics*, 4:195, April 2014. doi: 10.1007/JHEP04(2014)195. ArXiv: hep-th/1308.3716.

- [39] V. E. Hubeny and M. Rangamani. Causal holographic information. *Journal of High Energy Physics*, 6:114, June 2012. doi: 10.1007/JHEP06(2012)114. arXiv:hep-th/1204.1698.
- [40] John Preskill. Quantum information and spacetime. <http://www.theory.caltech.edu/~preskill/talks/QIP2017-tutorial-Preskill.pdf>. Accessed: 2017-01-26.
- [41] B. Freivogel, R. A. Jefferson, L. Kabir, B. Mosk, and I.-S. Yang. Casting shadows on holographic reconstruction. *Physical Review Letters*, 91(8):086013, April 2015. ArXiv:hep-th/1412.5175.
- [42] V. Balasubramanian, B. D. Chowdhury, B. Czech, and J. de Boer. Entwinement and the emergence of spacetime. *Journal of High Energy Physics*, arXiv:hep-th/1406.5859, 1:48, January 2015. doi: 10.1007/JHEP01(2015)048.
- [43] V. Balasubramanian, A. Bernamonti, B. Craps, T. De Jonckheere, and F. Galli. Entwinement in discretely gauged theories. *ArXiv e-prints*. arXiv hep-th/1609.03991.
- [44] R. Cleve, D. Gottesman, and H.-K. Lo. How to Share a Quantum Secret. *Physical Review Letters*, 83:648–651, July 1999.
- [45] A. Almheiri, X. Dong, and D. Harlow. Bulk locality and quantum error correction in AdS/CFT. *Journal of High Energy Physics*, 4:163, April 2015. doi: 10.1007/JHEP04(2015)163. arXiv:hep-th/1411.7041.
- [46] E. P. Verlinde. Emergent Gravity and the Dark Universe. *ArXiv e-prints*, November 2016. arXiv:hep-th/1611.02269.
- [47] L. Susskind. Holography in the flat space limit. In C. P. Burgess and R. C. Myers, editors, *General Relativity and Relativistic Astrophysics*, volume 493 of *American Institute of Physics Conference Series*, pages 98–112, November 1999.
- [48] J.J. Sakurai and J. Napolitano. *Modern Quantum Mechanics*. Pearson new international edition. Pearson, 2013.
- [49] V. Balasubramanian, M. B. McDermott, and M. Van Raamsdonk. Momentum-space entanglement and renormalization in quantum field theory. *Physical Review Letters*, 86(4):045014, August 2012. arXiv:1108.3568 [hep-th].
- [50] E. Witten.  $2+1$  dimensional gravity as an exactly soluble system. *Nuclear Physics B*, 311:46–78, December 1988.
- [51] L. Donnay. Asymptotic dynamics of three-dimensional gravity. *ArXiv e-prints:1602.09021 [hep-th]*, February 2016.

- [52] S. Deser and R. Jackiw. Three-dimensional cosmological gravity: dynamics of constant curvature. *Annals of Physics*, 153:405–416, 1984.
- [53] M. Bañados, M. Henneaux, C. Teitelboim, and J. Zanelli. Geometry of the 2+1 black hole. *Physical Review Letters D*, 48:1506–1525, August 1993. ArXiv/gr-qc/9302012.
- [54] G. Vidal. Efficient Classical Simulation of Slightly Entangled Quantum Computations. *Physical Review Letters*, 91(14):147902, October 2003.
- [55] F. Verstraete and J. I. Cirac. Renormalization algorithms for Quantum-Many Body Systems in two and higher dimensions. *arXiv:cond-mat/0407066*, July 2004.
- [56] F. Verstraete, V. Murg, and J. I. Cirac. Matrix product states, projected entangled pair states, and variational renormalization group methods for quantum spin systems. *Advances in Physics*, 57:143–224, March 2008.
- [57] F. Pastawski, B. Yoshida, D. Harlow, and J. Preskill. Holographic quantum error-correcting codes: toy models for the bulk/boundary correspondence. *Journal of High Energy Physics*, 6:149, June 2015.
- [58] B. Swingle. Constructing holographic spacetimes using entanglement renormalization. *ArXiv e-prints*. arXiv:1209.3304.
- [59] P. Hayden, S. Nezami, X.-L. Qi, N. Thomas, M. Walter, and Z. Yang. Holographic duality from random tensor networks. *Journal of High Energy Physics*, 11:9, November 2016.
- [60] P. W. Anderson. More Is Different. *Science*, 177:393–396, August 1972.
- [61] A. Peach and S. F. Ross. Tensor Network Models of Multiboundary Wormholes. *Classical and Quantum Gravity*, 34(10):105011.
- [62] A. Bhattacharyya, Z.-S. Gao, L.-Y. Hung, and S.-N. Liu. Exploring the tensor networks/AdS correspondence. *Journal of High Energy Physics*, 8:86, August 2016.
- [63] Y. Sekino and L. Susskind. Fast scramblers. *Journal of High Energy Physics*, 10:065, October 2008.
- [64] D.Z. Freedman and A. Van Proeyen. *Supergravity*. Cambridge University Press, 2012. ISBN 9780521194013.
- [65] F. Mandl and G. Shaw. *Quantum Field Theory*. A Wiley-Interscience publication. John Wiley & Sons, 2010. ISBN 9780471496830.
- [66] L.H. Ryder. *Quantum Field Theory*. Cambridge University Press, 1996.
- [67] M. Thomson. *Modern Particle Physics*. Cambridge University Press, 2013.

- [68] E. Noether and M. A. Tavel. Invariant variation problems. *Transport Theory and Statistical Physics*, 1:186–207, January 1971.
- [69] E. Noether. Invariante Variationsprobleme. *Nachr. D. König. Gesellsch. D. Wiss*, page 235–257, 1918.
- [70] T.W. Baumgarte and S.L. Shapiro. *Numerical Relativity: Solving Einstein's Equations on the Computer*. Cambridge University Press, 2010.
- [71] S. Carroll. *Spacetime and Geometry: An Introduction to General Relativity*. Always learning. Pearson Education, Limited, 2013. ISBN 9781292026633.
- [72] M.E. Peskin and D.V. Schroeder. *An Introduction to Quantum Field Theory*. Advanced book classics. Addison-Wesley Publishing Company, 1995. ISBN 9780201503975.
- [73] E. Zeidler. *Quantum Field Theory III: Gauge Theory: A Bridge between Mathematicians and Physicists*. Springer Berlin Heidelberg, 2011.
- [74] A. V. Gladyshev and D. I. Kazakov. Supersymmetry and lhc. 2006. doi: 10.1134/S1063778807090104. arXiv:hep-ph/0606288.
- [75] S. P. Martin. *A Supersymmetry Primer*, pages 1–98. World Scientific Publishing Co, 1998.
- [76] P. Higgs. Broken Symmetries and the Masses of Gauge Bosons. *Physical Review Letters*, 13, October 1964.
- [77] F. Englert and R. Brout. Broken Symmetry and the Mass of Gauge Vector Mesons. *Physical Review Letters*, 13, August 1964.
- [78] CMS Collaboration. Observation of a new boson at a mass of 125 GeV with the CMS experiment at the LHC. *Physics Letters B*, 716, September 2012.
- [79] R. Haag, J. T. Łopuszański, and M. Sohnius. All possible generators of supersymmetries of the S-matrix. *Nuclear Physics B*, 88:257–274, March 1975. doi: 10.1016/0550-3213(75)90279-5.
- [80] S. Coleman and J. Mandula. All Possible Symmetries of the S Matrix. *Physical Review*, 159:1251–1256, July 1967.
- [81] M. Gell-Mann. The interpretation of the new particles as displaced charge multiplets. *Il Nuovo Cimento (1955-1965)*, 4(2):848–866, 1956.
- [82] T.H. White. *The Once and Future King*. Penguin Publishing Group, 2011. ISBN 9781101657546.
- [83] M. Bertolini. Lectures on supersymmetry, April 2016.

- [84] Jonathan Bagger Julius Wess. *Supersymmetry and supergravity*. Princeton series in physics. Princeton University Press, 2nd ed., rev. and expanded edition, 1992. ISBN 9780691085562.
- [85] Varadarajan V.S. *Supersymmetry for mathematicians. An introduction*. Courant lecture notes in mathematics, 11. American Mathematical Society, 2004. ISBN 9780821835746.
- [86] A. V. Ramallo. Introduction to the AdS/CFT correspondence. *ArXiv e-prints: hep-th/1310.4319*, October 2013.
- [87] Wikimedia Commons. Conformal transformation of rectangular grid. <https://commons.wikimedia.org/w/index.php?curid=3440564>, . By Oleg Alexandrov - self-made with MATLAB, tweaked in Inkscape;, CC BY-SA 3.0, Accessed: 2017-01-26.
- [88] M. R. Gaberdiel. An introduction to conformal field theory. *Reports on Progress in Physics*, 63:607–667, April 2000. hep-th/9910156.
- [89] C.W. Misner, K.S. Thorne, and J.A. Wheeler. *Gravitation*. W. H. Freeman, 1973.
- [90] R.M. Wald. *General Relativity*. University of Chicago Press, 2010. ISBN 9780226870373.
- [91] C.J. Isham. *Modern Differential Geometry for Physicists*. Allied Publ., 2002.
- [92] G. W. Gibbons and S. W. Hawking. Action integrals and partition functions in quantum gravity. *Physical Review Letters D*, 15:2752–2756, May 1977.
- [93] D. Hilbert and S. W. Hawking. Die Grundlagen der Physik. *Konigl. Gesell. d. Wiss. Göttingen, Nachr. Math.-Phys.*, 1915.
- [94] N. J. Poplawski. Spacetime and fields. *ArXiv e-prints: arXiv:0911.0334 [gr-qc]*, November 2009.
- [95] E. Cartan. Sur la structure des groupes infinis de transformations. *Annales Scientifiques de l'École Normale Supérieure*, 1904.
- [96] W. Rarita and J. Schwinger. On a theory of particles with half-integral spin. *Phys. Rev.*, 60:61–61, Jul 1941.
- [97] E. Papantonopoulos. *From Gravity to Thermal Gauge Theories: The AdS/CFT Correspondence*. Lecture Notes in Physics. Springer Berlin Heidelberg, 2011.
- [98] N. Ambrosetti, J. Charbonneau, and S. Weinfurtner. The fluid/gravity correspondence. *Lectures notes from the 2008 Summer School on Particles, Fields, and Strings, UBC*, 2008.

- [99] J. M. Overduin and P. S. Wesson. Kaluza-Klein gravity. *Physical Reports*, 283:303–378, April 1997.
- [100] K. Becker, M. Becker, and J.H. Schwarz. *String Theory and M-Theory: A Modern Introduction*. Cambridge University Press, 2006.
- [101] J. Polchinski. *String Theory: Volume 1, An Introduction to the Bosonic String*. Cambridge Monographs on Mathematical Physics. Cambridge University Press, 1998.
- [102] J. Polchinski. *String Theory: Volume 2, Superstring Theory and Beyond*. Cambridge Monographs on Mathematical Physics. Cambridge University Press, 1998.
- [103] B. Zwiebach. *A First Course in String Theory*. Cambridge University Press, 2009.
- [104] H. Năstase. *Introduction to the AdS/CFT Correspondence*. Cambridge University Press, 2015.
- [105] A.S.T. Pires. *AdS/CFT Correspondence in Condensed Matter*. IOP Concise Physics: A Morgan & Claypool Publication. Morgan & Claypool Publishers, 2014.
- [106] M. Natsuume. *AdS/CFT Duality User Guide*. Lecture Notes in Physics. Springer Japan, 2015.
- [107] O. Aharony, S. S. Gubser, J. Maldacena, H. Ooguri, and Y. Oz. Large N field theories, string theory and gravity. *Physics Reports*, 323:183–386, January 2000.
- [108] G. 't Hooft. A planar diagram theory for strong interactions. *Nuclear Physics B.*, 1974.
- [109] R. P. Feynman and A. R. Hibbs. *Quantum Mechanics and Path Integrals*. New York: McGraw-Hill, 1965.
- [110] Wikimedia Commons. Particle paths. <https://commons.wikimedia.org/w/index.php?curid=409445>, . By Matt McIrvin - Own work, CC BY-SA 3.0, Accessed: 2017-04-23.
- [111] H. Kleinert. *Path Integrals in Quantum Mechanics, Statistics, Polymer Physics, and Financial Markets*. EBL-Schweitzer. World Scientific, 2009.
- [112] W. R. Hamilton. On a General Method in Dynamics. *Philosophical Transactions of the Royal Society*, 1834.
- [113] W. R. Hamilton. Second Essay on a General Method in Dynamics. *Philosophical Transactions of the Royal Society*, 1835.

- [114] K. Vogtmann, A. Weinstein, and V.I. Arnol'd. *Mathematical Methods of Classical Mechanics*. Graduate Texts in Mathematics. Springer New York, 2013.
- [115] T. Banks, M. R. Douglas, G. T. Horowitz, and E. Martinec. AdS Dynamics from Conformal Field Theory. *ArXiv High Energy Physics - Theory e-prints*, August 1998.
- [116] A. Hamilton, D. Kabat, G. Lifschytz, and D. A. Lowe. Holographic representation of local bulk operators. *Physical Review Letters D*, 74(6):066009, September 2006.
- [117] I. Heemskerk, D. Marolf, J. Polchinski, and J. Sully. Bulk and transhorizon measurements in AdS/CFT. *Journal of High Energy Physics*, 10:165, October 2012.
- [118] I. A. Morrison. Boundary-to-bulk maps for AdS causal wedges and the Reeh-Schlieder property in holography. *Journal of High Energy Physics*, 5: 53, May 2014.
- [119] K. Papadodimas and S. Raju. An infalling observer in AdS/CFT. *Journal of High Energy Physics*, 10:212, October 2013.
- [120] S. Roman. *Coding and Information Theory*. Graduate Texts in Mathematics. Springer New York, 1992.
- [121] R.B. Ash. *Information Theory*. Dover Books on Mathematics. Dover Publications, 2012.
- [122] J.R. Pierce. *An Introduction to Information Theory: Symbols, Signals and Noise*. Dover Books on Mathematics. Dover Publications, 2012.
- [123] R. Landauer. Irreversibility and heat generation in the computing process. *IBM Journal of Research and Development*, 5(3):183–191, July 1961.
- [124] C.H. Bennett. Notes on Landauer's principle, reversible computation, and Maxwell's demon". .
- [125] C.H. Bennett. The thermodynamics of computation—a review. .
- [126] A. Bérut, A. Arakelyan, A. Petrosyan, S. Ciliberto, R. Dillenschneider, and E. Lutz. Experimental verification of Landauer's principle linking information and thermodynamics. *Nature*, 483:187–189, March 2012.
- [127] Y. Jun, M. Gavrilov, and J. Bechhoefer. High-Precision Test of Landauer's Principle in a Feedback Trap. *Physical Review Letters*, 113(19):190601, November 2014.

- [128] J. Hong, B. Lambson, S. Dhuey, and J. Bokor. Experimental test of Landauers principle in single-bit operations on nanomagnetic memory bits. *Science Advances*, 2:e1501492–e1501492, March 2016.
- [129] Tatsuma Nishioka, Shinsei Ryu, and Tadashi Takayanagi. Holographic Entanglement Entropy: An Overview. *Journal of Physics*, 2009.
- [130] S. Barnett. *Quantum Information*. Oxford Master Series in Physics. OUP Oxford, 2009.
- [131] A. Zeilinger. *Dance of the Photons: From Einstein to Quantum Teleportation*. Farrar, Straus and Giroux, 2010.
- [132] D. P. Divincenzo. The Physical Implementation of Quantum Computation. *Fortschritte der Physik*, 48:771–783, 2000.
- [133] R. L. Rivest, A. Shamir, and L. Adleman. A Method for Obtaining Digital Signatures and Public-key Cryptosystems. *Commun. ACM*, 21(2):120–126, February 1978.
- [134] Bruce Schneier. *Applied Cryptography: Protocols, Algorithms and Source Code in C*. John Wiley & Sons, 2015.
- [135] D. Gottesman. An Introduction to Quantum Error Correction. *eprint arXiv:quant-ph/0004072*, April 2000.
- [136] W. K. Wootters and W. H. Zurek. A single quantum cannot be cloned. *Nature*, 10 1982.
- [137] D. Gottesman. *Stabilizer codes and quantum error correction*. PhD thesis, California Institute of Technology, 1997.
- [138] A. Einstein, B. Podolsky, and N. Rosen. Can Quantum-Mechanical Description of Physical Reality Be Considered Complete? *Physical Review*, 47:777–780, May 1935.
- [139] J. Bell. On the Einstein–Podolsky–Rosen paradox. *Physics*, 47:195–200, November 1964.
- [140] T. Buchert. Dark Energy from structure: a status report. *General Relativity and Gravitation*, 40:467–527, February 2008.
- [141] M. Rangamani and T. Takayanagi. Holographic Entanglement Entropy. *ArXiv e-prints:1609.0128*, September 2016.
- [142] X. Dong, D. Harlow, and A. C. Wall. Reconstruction of Bulk Operators within the Entanglement Wedge in Gauge-Gravity Duality. *Physical Review Letters*, 117(2):021601, July 2016.

- [143] J. D. Brown and M. Henneaux. Central Charges In The Canonical Realization Of Asymptotic Symmetries. *Commun. Math. Phys.*, 1986.
- [144] M. van Raamsdonk. Lectures on Gravity and Entanglement. In J. Polchinski and et al., editors, *New Frontiers in Fields and Strings (TASI 2015) - Proceedings of the 2015 Theoretical Advanced Study Institute in Elementary Particle Physics. Edited by POLCHINSKI JOSEPH ET AL. Published by World Scientific Publishing Co. Pte. Ltd., 2017. ISBN #9789813149441, pp. 297-351*, pages 297–351, 2017.
- [145] I. Cherednikov. Gauge-Invariant Gluon TMD and Evolution in the Coordinate Space. In *QCD Evolution 2015 (QCDEV2015)*, page 46, 2015.
- [146] A. Lewkowycz and J. Maldacena. Generalized gravitational entropy. *Journal of High Energy Physics*, 8:90, August 2013.
- [147] R. Orús. A practical introduction to tensor networks: Matrix product states and projected entangled pair states. *Annals of Physics*, 349:117–158, October 2014.
- [148] G. Vidal. Entanglement renormalization. *Phys. Rev. Lett.*, 99:220405, 2007.
- [149] G. Vidal. Class of quantum many-body states that can be efficiently simulated. *Phys. Rev. Lett.*, 101:110501, 2008.
- [150] G. Evenbly and G. Vidal. Entanglement renormalization in two spatial dimensions. *Phys. Rev. Lett.*, 102:180406, 2009.
- [151] G. Evenbly and G. Vidal. Algorithms for entanglement renormalization. *Phys. Rev. B*, 79:144108, 2009.
- [152] G. Evenbly and G. Vidal. Frustrated antiferromagnets with entanglement renormalization: Ground state of the spin- $1/2$  heisenberg model on a kagome lattice. *Phys. Rev. Lett.*, 104:187203, 2010.
- [153] B. Czech, L. Lamprou, S. McCandlish, and J. Sully. Tensor networks from kinematic space. *Journal of High Energy Physics*, 7:100, July 2016.
- [154] Z. Yang, P. Hayden, and X.-L. Qi. Bidirectional holographic codes and sub-AdS locality. *Journal of High Energy Physics*, 1:175, January 2016.
- [155] C. H. Papadimitriou and K. Steiglitz. Combinatorial Optimization: Algorithms and Complexity. *Courier Corporation*, 1998.
- [156] Y. Peres D. A. Levin and E. L. Wilmer. Markov Chains and Mixing Times. *American Mathematical Society*, 2008.
- [157] Charles E.; Rivest Ronald L. Cormen, Thomas H.; Leiserson. *Introduction to Algorithms*. MIT Press and McGraw-Hill, 1990.

- [158] J. Adler. Bootstrap percolation. *Physica A: Statistical Mechanics and its Applications*, 171:453–470, 1991.
- [159] D. Poulin D. W. Kribs, R. Laflamme and M. Lesosky. Operator quantum error correction. *Quant. Inf. Comp.*, 2006.
- [160] Edward Witten. Three-Dimensional Gravity Revisited. 2007. ArXiv: hep-th/0706.3359.
- [161] Maximo Banados, Claudio Teitelboim, and Jorge Zanelli. The Black hole in three-dimensional space-time. *Phys. Rev. Lett.*, 69:1849–1851, 1992.
- [162] Steven Carlip and Claudio Teitelboim. Aspects of black hole quantum mechanics and thermodynamics in (2+1)-dimensions. *Phys. Rev.*, D51:622–631, 1995.
- [163] Shiing-Shen Chern and James Simons. Characteristic forms and geometric invariants. *Annals of Mathematics*, 99(1):48–69, 1974.
- [164] S. Carlip. TOPICAL REVIEW: Conformal field theory, (2 + 1)-dimensional gravity and the BTZ black hole. *Classical and Quantum Gravity*, 22:R85–R123, June 2005.
- [165] S. Carlip. Lectures in (2+1)-Dimensional Gravity. *ArXiv General Relativity and Quantum Cosmology e-prints*, March 1995. ArXiv: gr-qc/9503024.
- [166] S. Carlip. Quantum Gravity in 2 + 1 Dimensions: The Case of a Closed Universe. *Living Reviews in Relativity*, 8:1, January 2005.
- [167] W.P. Thurston and S. Levy. *Three-Dimensional Geometry and Topology, Volume 1*. Princeton Mathematical Series. Princeton University Press, 2014. ISBN 9781400865321.
- [168] A.W. Knapp. *Lie Groups Beyond an Introduction*. Progress in Mathematics. Birkhäuser Boston, 2013.
- [169] S. Hemming, E. Keski-Vakkuri, and P. Kraus. Strings in the Extended BTZ Spacetime. *Journal of High Energy Physics*, 10:006, October 2002.
- [170] D. Cooper, C.D. Hodgson, and S. Kerckhoff. *Three-dimensional orbifolds and cone-manifolds*. Number v. 5. Mathematical Society of Japan, 2000.
- [171] V. E. Hubeny, H. Maxfield, M. Rangamani, and E. Tonni. Holographic entanglement plateaux. *Journal of High Energy Physics*, 8:92, August 2013.
- [172] H. Casini, M. Huerta, and J. A. Rosabal. Remarks on entanglement entropy for gauge fields. *Physical Review Letters D*, 89(8), April 2014.
- [173] W. Donnelly. Decomposition of entanglement entropy in lattice gauge theory. *Physical Review Letters D*, 85(8), April 2012.

- [174] P. V. Buividovich and M. I. Polikarpov. Entanglement entropy in gauge theories and the holographic principle for electric strings. *Physics Letters B*, 670, December 2008.
- [175] J. Maldacena and A. Strominger. AdS<sub>3</sub> black holes and a stringy exclusion principle. *Journal of High Energy Physics*, 12:005, December 1998. arXiv:hep-th/9804085.
- [176] H.S.M. Coxeter. *Introduction to Geometry*. Wiley Classics Library. Wiley, 1989. ISBN 9780471504580.
- [177] B. Iversen. *Hyperbolic Geometry*. London Mathematical Society St. Cambridge University Press, 1992. ISBN 9780521435284.
- [178] R. Dijkgraaf. Instanton strings and hyper-Kähler geometry. *Nuclear Physics B*, 543:545–571, March 1999.
- [179] C. T. Asplund and S. G. Avery. Evolution of entanglement entropy in the D1-D5 brane system. *Physical Review Letters D*, 84(12):124053, December 2011.
- [180] P. Ginsparg. Applied Conformal Field Theory. *ArXiv High Energy Physics - Theory e-prints*, November 1991.
- [181] T. Castellani and A. Cavagna. Spin-glass theory for pedestrians. *Journal of Statistical Mechanics: Theory and Experiment*, 5:05012, May 2005. ArXiv: cond-mat/0505032.
- [182] S. G. Avery. *Using the D1D5 CFT to understand black holes*. PhD thesis, The Ohio State University, 2010.
- [183] V. Balasubramanian, P. Kraus, and M. Shigemori. Massless black holes and black rings as effective geometries of the D1 D5 system. *Classical and Quantum Gravity, ArXiv e-prints:hep-th/0508110*, 22:4803–4837, November 2005.
- [184] V. Balasubramanian, J. de Boer, E. Keski-Vakkuri, and S. F. Ross. Supersymmetric conical defects: Towards a string theoretic description of black hole formation. *Physical Review Letters D*, 64(6), September 2001.
- [185] E. J. Martinec and W. McElgin. Exciting AdS Orbifolds. *Journal of High Energy Physics, ArXiv e-prints:hep-th/0206175*, 10:050, October 2002.
- [186] S. A. Hartnoll and R. Mahajan. Holographic mutual information and distinguishability of Wilson loop and defect operators. *Journal of High Energy Physics*, 2:100, February 2015.
- [187] J.E. Humphreys. *Reflection Groups and Coxeter Groups*. Cambridge Studies in Advanced Mathematics. Cambridge University Press, 1992.

- [188] H.S.M. Coxeter. *Regular Polytopes*. Dover Books on Mathematics. Dover Publications, 2012.
- [189] D. Harlow. Jerusalem Lectures on Black Holes and Quantum Information. *ArXiv e-prints:hep-th/1409.1231*, September 2014.

## INDEX

---

- AdS tessellation, 64, 97, 101
- AdS-Rindler bulk reconstruction, 47, 51, 64, 66
- AdS/CFT correspondence, 4, 5, 17, 24, 30, 32, 33, 37–40, 43, 45, 52, 55, 71, 100
- Anti-de-Sitter space, 4, 26, 30, 62
- Bi-directional holographic code, 101
- Black hole, 3, 52, 58, 71, 75
- Brout-Englert-Higgs particle, 21
- Brown-Henneaux relationship, 59, 71
- BTZ black hole, 73, 78, 81, 100
- Cartan structure equations, 27
- Causal wedge, 48
- Chern-Simons, 73, 115
- Condensed matter physics, 5, 41
- Conformal field theory, 4, 32, 43, 45, 48, 60
- Conical defect, 78, 86, 90, 92, 100
- Correlation function, 44, 45, 85, 86
- Cosmology, 3
- Coxeter Group, 97
- D1-D5 CFT, 86, 87, 100
- D3-branes, 30–32, 35, 37
- Dimensional reduction, 31, 43
- Einstein-Hilbert action, 27
- Emergent gravity, 7, 10
- Entanglement, 54, 61, 64
- Entanglement entropy, 6, 8, 9, 55, 58, 64, 66, 71, 75, 86
- Entanglement shadow, 7, 71, 75, 89
- Entropy, 3, 6, 52
- Entwinement, 9, 75, 82, 89, 94, 98, 100
- Frame fields, 27, 29
- Fundamental domain, 79, 82
- Gauge theories, 17, 82
- Gauge theory, 20, 21, 23, 24, 32, 40, 73, 115
- Gell-Mann’s totalitarian principle, 22
- General relativity, 3, 25, 27
- Generating functional, 44, 45
- Gravitinos, 29
- Graviton, 27
- Greedy algorithm, 64, 66, 92, 94
- HaPPY, 63, 64, 66, 67, 90, 94
- Heisenberg picture, 48
- Hierarchy problem, 21
- High energy physics, 3
- Holography, 3, 4, 7, 9, 10, 17, 33, 49
- Information theory, 6, 51
- Informational entropy, 52
- Isometric tensor, 62
- It from Bit, 6
- It from Qubit, 6
- Iwasawa decomposition, 74
- Landauer’s principle, 52
- Large N, 39, 86, 100
- Long strings, 9, 82, 100
- Lorentz transformations, 20, 27, 79, 81
- MERA, 61
- Minkowski spacetime, 17, 38
- Noether’s theorem, 18
- Orbifold, 71
- Orbifold point, 86

- Orbifolding, 9, 74, 79, 95
- Path integral, 43, 60, 82
- Perfect tensor, 62, 64, 66
- Plu-perfect tensors, 100
- Poincaré group, 19, 74
- Quantum error-correction, 7, 53, 57, 64, 66
- Quantum field theory, 3
- Quantum gravity, 3
- Quantum information theory, 6, 8, 10, 33, 51, 53, 54, 61, 78
- Quark-gluon plasma, 5
- Qutrit, 52, 57
- Rényi entropy, 60, 84
- Rényi twist operator, 85
- Relativistic Heavy Ion Collider, 5
- Renormalization, 41, 43, 46, 61, 86
- Replica trick, 60, 82, 85
- Ryu-Takayanagi formula, 6, 10, 52, 58, 61, 63, 64, 71, 78, 90
- Smearing function, 48
- Spin connection, 27
- String theory, 4, 33, 35–38, 40
- sub-AdS locality, 8, 11, 75, 98, 100
- Supergravity, 4, 17, 24, 27, 29, 32, 36, 40, 41, 45, 61
- Superstring theory, 36
- Supersymmetry, 17, 21, 22, 24, 29, 32, 37
- Symmetric product orbifold CFT, 83
- Symmetry, 17, 18, 20, 32, 74
- Tensor network, 8–10, 61, 63, 89, 95, 100
- The once and future king, 22
- Three-dimensional gravity, 9, 71, 115
- Type IIB supergravity, 30, 38, 86
- UV/IR correspondence, 4, 11, 41, 78, 98
- Von Neumann entropy, 8, 55
- Weyl scale factor, 24

## COLOPHON

This document was typeset using the typographical look-and-feel **classicthesis** developed by André Miede. The style was inspired by Robert Bringhurst's seminal book on typography "*The Elements of Typographic Style*". **classicthesis** is available for both L<sup>A</sup>T<sub>E</sub>X and LyX:

<https://bitbucket.org/amiede/classicthesis/>

The new color scheme and other visual elements added to the previously mentioned **classicthesis** package, are based on the style guide provided by the *Vrije Universiteit Brussel* as interpreted, to the best of his abilities, by the author. The style guide can be consulted on:

<http://huisstijl.vub.ac.be/>

